MULTIPLE LOCI OF INTRA- AND EXTRA-HYPOTHALAMIC LEPTIN RECEPTOR EXPRESSION AND ACTION IN THE MOUSE

by

Rebecca L. Leshan

A dissertation submitted in partial fulfillment
Of the requirements for the degree of
Doctor of Philosophy
(Molecular and Integrative Physiology)
in The University of Michigan
2009

Doctoral Committee:

Associate Professor Martin G. Myers, Jr., Chair
Professor Audrey F. Seasholtz
Professor Fred J. Karsch
Associate Professor Liangyou Rui
Assistant Professor Robert C. Thompson

Dedicated to my Family,

and to my mentor, Dr. Martin G. Myers, Jr.
and to the Myers Lab.

Acknowledgements

I would like to acknowledge the collaborations of Dr. Young-Hwan Jo (Albert Einstein College of Medicine), Dr. Heike Münzberg (Pennington Biomedical Research Center) and Dr. Christopher Rhodes (University of Chicago) to the studies described in this dissertation.

I would further like to acknowledge the contribution and support of Dr. Martin Myers, the Myers Laboratory, especially Gwendolyn Louis, Dr. Gina Leinninger and Darren Opland, as well as my thesis committee, and the department of Molecular & Integrative Physiology.

Table of Contents

Dedication……ii
Acknowledgements……iii
List of Tables…… v
List of Figures……vi
List of Neuroanatomical Abbreviations……viii
Abstract……ix
Chapter 1 Introduction……1
Chapter 2 Immunohistochemical Localization of LepRb-Expressing Cells in the CNS
2.1 Introduction……16
2.2 Methods……20
2.3 Results……22
2.4 Discussion……26
Chapter 3 LepRb in Midbrain Neurons
3.1 Introduction……30
3.2 Methods……33
3.3 Results……36
3.4 Discussion……38
Chapter 4 LepRb in Neurons of the Ventral Premammillary Nucleus of the Hypothalamus
4.1 Introduction……43
4.2 Methods……45
4.3 Results……51
4.4 Discussion……60
Chapter 5 LepRb deletion in cells expressing Nitric Oxide Synthase-1
5.1 Introduction……65
5.2 Methods……69
5.3 Results……73
5.4 Discussion……76
Chapter 6 Summary and Conclusions…… 79
Tables……86
Figures…… 90
References…… 118

List of Tables

1. Relative densities of labeled cells in $LepRb^{rosa\text{-}bgal}$ and $LepRb^{actin\text{-}bgal}$…….. 87
2. Relative densities of labeled cells in $LepRb^{EGFP}$ reporter mice……..88
3. Descriptions of utilized mouse lines……...89

List of Figures

1. The leptin receptor gene, "*lepr*", encodes several isoforms of leptin receptors (LepRa, b, c, d, e)…….. 91

2. *Lepr*^{cre} mice and cre-inducible systems to interrogate LepRb neurons……...92

3. Beta-gal labeling in *Rosa26*^{bgal} and *beta-Actin*^{bgal} mice……93

4. EGFP labelling in representative hypothalamic nuclei of LepRb^{EGFP} mice….94

5. LepRb^{EGFP} mice show EGFP-IR (A,C,E white; B,D,F green) in midbrain cells through several caudal-to-rostral sections……..95

6. Anterograde tracing from LepRb VTA neurons……...96

7. Anterograde tracing from LepRb VTA/RLi neurons……97

8. Retrograde tracing of inputs from LepRb VTA/RLi cells……98

9. Retrograde tracing of leptin-responsive inputs to VTA……..99

10. Summary of midbrain LepRb circuitry……100

11. NOS1 immunoreactivity (NOS1-IR) defines PMv boundaries……101

12. LepRb^{GFP} mice exhibit a substantial population of GFP-IR (green, cytoplasmic) cells in the PMv (A-C)……102

13. Regulation of LepRb PMv neuronal activity by leptin in LepRb^{GFP} mice…...103

14. PMv LepRb neurons are not activated by fasting……....104

15. Male or female odors increase Fos-IR in LepRb PMv cells of the opposite sex……...105

16. EGFP-IR projections from LepRb neurons to the POA and amygdala in LepRb^{EGFPf} mice……106

17. LepRb PMv projections in female mice……..…107

18. Retrograde tracing of inputs from LepRb PMv cells……..…108

19. Retrograde tracing of inputs to GnRH neurons from leptin-responsive PMv cells in BIG mice……109

20. Integration of sexual odorant and leptin signaling pathways in PMv LepRb neurons……..…110

21. The PMv contains Nos-1 expressing cells……..……111

22. Generation of *Nos1*^{cre};*lepr*$^{\Delta/flox}$ mice to delete LepRb in Nos1-expressing neurons……...112

23. Nos1^{Cre} expression is comparable to NOS1-IR, and is efficiently expressed in leptin-responsive PMv cells……..113

24. *Nos1*^{cre};lepr$^{\Delta/flox}$ study paradigm……...…114

25. *Nos1*^{cre};lepr$^{\Delta/flox}$ females have altered energy regulation……115

26. *Nos1*^{cre};lepr$^{\Delta/flox}$ females are euglycemic……...116

27. Onset of estrus is delayed in *Nos1*^{cre};lepr$^{\Delta/flox}$ females……...117

List of Neuroanatomical Abbreviations

ARC, arcuate nucleus of the hypothalamus
AvPv, anteroventricular periventricular nucleus
BLA, basolateral amygdala
CeA, central amygdala
DMH, dorsomedial nucleus of the hypothalamus
DpMe, deep mesencephalic nucleus
DR, dorsal raphe
IPAC, interstitial nucleus of the posterior limb of the anterior commissure
LHA, lateral hypothalamus
MeA, medial amygdala
NAc, nucleus accumbens
PAG, perriaqueductal grey
PBN, parabrachial nucleus
PMv, ventral premammillary nucleus of the hypothalamus
POA, preoptic area
PVN, paraventricular nucleus of the hypothalamus
RLi, linear raphe
SN, substantia nigra
VMH, ventromedial nucleus of the hypothalamus
VTA, ventral tegmental area

ABSTRACT

MULTIPLE LOCI OF INTRA- AND EXTRA-HYPOTHALAMIC LEPTIN RECEPTOR EXPRESSION AND ACTION IN THE MOUSE

by

Rebecca L. Leshan

Chair: Martin G. Myers, Jr.

The increasing incidence of obesity in developed nations represents an ever-growing challenge to health care by augmenting the collateral occurrences of diabetes, and other chronic conditions. The discovery of the satiety hormone, leptin, over a decade ago has facilitated the acquisition of new knowledge regarding the regulation of energy homeostasis. A great deal remains to be discovered regarding the specific actions of leptin at different regions within the brain, however. Our overarching goals were to develop a reliable method to detect long form leptin receptor (LepRb), to generate a comprehensive inventory of sites of LepRb-expressing cells in the brain and to characterize leptin action at two such sites. Here, we first define central sites of LepRb expression *in vivo* using "reporter" mice, in which LepRb- neurons express the fluorescent marker, enhanced green fluorescent protein (EGFP). We identified LepRb expression in neuronal populations both within and outside the hypothalamus and further

characterized two such LepRb populations, those within the midbrain ventral tegmental area and linear raphe (VTA/RLi), and LepRb cells within the ventral premammillary nucleus of the hypothalamus (PMv). We used a novel tract tracing system combined with standard techniques to determine regions innervated exclusively by LepRb VTA, LepRb RLi or LepRb PMv neurons, thus revealing LepRb VTA neuronal projections to regions of the amygdala, LepRb RLi projections to amygdala and nucleus accumbens (NAc), and LepRb PMv projections to the preoptic area (POA). We have further shown the retrograde accumulation in LepRb PMv neurons of a trans-synaptic tracer from GnRH neurons, revealing the direct innervation of gonadotropin releasing hormone (GnRH) neurons by many LepRb PMv neurons. Additionally, we demonstrate activation of this population by leptin and opposite-sex odors. Thus, LepRb VTA/RLi neurons are well positioned to couple energy balance cues with the mesolimbic dopamine reward circuit, while LepRb PMv neurons unite metabolic and sexual odorant cues and directly innervate GnRH neurons to regulate the reproductive axis. Finally, in preliminary studies representing future analyses of the functional roles of LepRb PMv cells we delete *Lepr* in nitric oxide synthase-1 containing cells and observe a delay in estrus onset as well as delayed onset obesity. Understanding the regulation and physiological function of these and other sites of central leptin action will be a crucial advancement in the quest to understand mechanisms of leptin action on physiology.

Chapter 1

Introduction

Obesity is a growing problem in many industrialized nations. Comorbid with increases in body weight are numerous chronic conditions including diabetes, cardiovascular disease and poor reproductive health (1). Inappropriate body weight regulation results when the normal effectors that regulate homeostasis are absent or impaired. One such effector, the hormone leptin, acts via its receptor (LepRb) on specific central nervous system (CNS) neurons to signal the adequacy of long-term energy stores, thereby instigating the appropriate adjustments in energy intake and expenditure to maintain health, as well as permitting the expenditure of resources on energy-intensive processes such as reproduction (2-7).

1.1 The ob and db genes

Though not termed “leptin” until much later, the hormone first appeared in the literature in the 1950s, when a spontaneous mutation arose in a non-inbred population of mice at The Jackson Laboratory which displayed obesity, linear growth retardation and infertility (8). Due to the overt obesity, the affected gene was termed *obese* or *ob*, and the homozygous animals, *ob/ob* mice. Studies further defined *ob* as a single autosomal gene and later localized it to

chromosome 6; the *ob/ob* mice carried a recessive nonsense mutation of the gene preventing production of *ob* mRNA or protein (9).

While the discovery of leptin's receptor similarly began with a spontaneously obese mouse at The Jackson Laboratory, the phenotypic feature unique to this mutant was its resemblance to diabetes mellitus (obesity, hyperglycemia, polyuria, glycosuria); thus the gene was termed "*diabetic*" or *db* (10). *Db* is an autosomal gene localized to chromosome 4 and the mutant allele is recessive (11,12).

At the time of *ob* and *db* discovery, the traditionally employed procedure to study circulating factors in animals was parabiosis. In this method, the vascular systems of two organisms are surgically joined allowing exchange of endocrine substances (13). In classic experiments, Coleman & Hummel joined wildtype, *ob/ob* and *db/db* in various pairings and concluded that a circulating factor controlling satiety was absent in *ob/ob* mice, and ineffective in *db/db* mice (14,15). Thus, *ob/ob* mice have an intact brain satiety center, but no circulating satiety factor, while *db/db* mice have a dysfunctional satiety center, but are able to produce the circulating satiety factor.

In 1994 Friedman, Leibel and colleagues revealed the identity of this satiety factor when they cloned the *ob* gene (9). The product, a 16kiloDalton secreted protein showed high homology between humans and rodents and was termed leptin, after the Greek "Leptos", meaning "thin". When recombinant leptin

was administered to *ob/ob* mice, their body weight and food intake decreased and glucose and insulin levels fell to normal (16-19). Conversely, when administered to *db/db* mice, no effect was observed, upholding the supposed lack of leptin in *ob/ob* mice and inability to respond in *db/db* mice (18).

1.2 Leptin production

In cloning the *obese* gene, Zhang *et al*. used Northern blot analysis of total RNA to demonstrate *ob* expression specific to white adipose tissue (WAT) (9). Consequently, in a series of transplantation experiments, Gavrilova *et al*. transplanted WAT from wildtype donors into lipodystrophic mice and observed improved glucose homeostasis in the recipient mice (20). They later used *ob/ob* donors and showed that WAT from *ob/ob* mice failed to have an effect on lipodystrophic recipients, confirming that leptin was a product of WAT and absent in *ob/ob* mice (21).

Subsequent research has confirmed WAT as the primary source of the leptin and additionally characterized the regulation of its release. Sinha *et al*. demonstrated that, in humans, leptin secretion exhibits diurnal variation with peaks during night (~1:00AM to ~1:30AM) and nadirs in the morning (~8:00AM) (22). The existence of high leptin levels in cord blood from full-term infants, as well as the surge in leptin levels in prepupertal boys and early postnatal rodents that is not associated with changes in body weight has been accepted as initial evidence for a supposed role for this hormone in development (23-25).

In addition to diurnal and developmental variation, serum leptin concentration is altered by a variety of long- and short-term physiological stimuli. Overfeeding, energy sources, insulin, glucocorticoids and estrogens are all associated with increases in serum leptin levels, while calorie restriction, androgens, thyroid hormones, catecholamines and inflammatory cytokines have been linked to decreases in leptin. Chronic changes in body weight and energy balance have been shown to cause changes in leptin at the transcriptional level, while acute alterations have been shown to regulate leptin at the level of translation, storage, release and degradation (26-29). In addition to estrogens and insulin, administration of other hormones produces changes in leptin levels (reviewed in 29). High-doses of prolactin increase leptin while IGF-1, high-dose growth hormone and a dopamine receptor agonist all decrease leptin. Dexamethasone causes a delayed increase in leptin while melatonin administration has variable effects on levels depending on time of day of administration (29). Thus leptin production and release is regulated by an array of stimuli, allowing leptin levels to reflect physiological alterations in the condition of the animal.

1.3 Leptin receptor isoforms

The leptin receptor gene, herein referred to as "*lepr*", encodes several isoforms of leptin receptors (LepRs). To date, five isoforms have been described due to alternative splicing at the C-terminus (LepRa, b, c, d, e), and can be divided into three categories based on protein size and signal transduction

capabilities: soluble short, membrane-bound short, and long forms (3,11,30). LepRe is the shortest at 805 amino acids in length. This isoform lacks a transmembrane domain and exists as a soluble short form. LepRa, c, and d at 894, 892 and 900 amino acids respectively retain a transmembrane region and are considered membrane-bound short forms. The final form, LepRb at 1162 amino acids is the only known long isoform. The short forms have variable tissue distributions and have been suggested to be involved in leptin transport and/or clearance, while LepRb mediates intracellular signaling and is thus crucial for leptin action (3,31-35). *Db/db* mice exhibit a mutation producing a premature stop codon, effectively resulting in shortening of LepRb to LepRa, thus removing all intracellular signaling function (12,30).

1.4 LepRb intracellular signaling

LepRb mediates the physiologic effects of leptin. This long isoform is a member of the class I cytokine receptor family, which lack intrinsic kinase activity, but mediate signaling via an associated Janus kinase-2 (JAK2) tyrosine kinase. The structure of LepRb consists of several domains which mediate intracellular signaling (Figure 1) (32,33). Upon leptin binding to LepRb, JAK2 non-covalently associates with the receptor at the JAK boxes, allowing JAK2 autophosphorylation on numerous residues and subsequent phosphorylation of LepRb at discrete sites, including tyrosines at positions 985, 1077 and 1138. The phosphorylation of tyrosine 985 (Tyr_{985}) recruits the tyrosine phosphatase, SH2-domain containing tyrosine phosphatase 2 (SHP-2), which thereby mediates a

portion of the activation of the canonical extracellular signal-regulated kinase (ERK) signaling pathway in cultured LepRb-expressing cells. Tyr_{985} also plays an important role in LepRb signal attenuation by binding the inhibitory suppressor of cytokine signaling-3 (SOCS3) (32,33).

Phosphorylation of Tyr_{1138} recruits the latent transcription factor, signal transducer and activator of transcription 3 (STAT3), to the LepRb/JAK2 complex, resulting in the tyrosine phosphorylation (pSTAT3) and nuclear translocation of STAT3 to effect its regulation of transcription (32,33). Among other genes, STAT3 activates the transcription of the neuropeptide, proopiomelanocortin (POMC), and the signaling inhibitor, SOCS3 (3). Tyr_{1077} and Tyr_{1138} on LepRb cooperate to mediate activation of STAT5. Finally, JAK2 tyrosine phosphorylation during LepRb stimulation mediates some signals independently of tyrosine phosphorylation sites on LepRb (e.g., a portion of ERK activation), but the exact nature and function of these signals is not yet fully understood (3).

The analysis of mice in which specific LepRb signals are perturbed has enabled investigation of the physiological function of these various LepRb signals. The role of LepRb→STAT3 signaling in energy balance has been clearly established by the study of rodents containing a homologous replacement of LepRb by a receptor mutant for Tyr_{1138}, the STAT3 binding site (s/s mice) (36-38). The s/s mice are obese and leptin resistant, similar to db/db mice (which lack all LepRb signaling), displaying increased food intake and decreased energy expenditure. Although normal growth, fertility, glycemic control, and immune

function are preserved in s/s mice and thus independent of Tyr_{1138}→STAT3 signaling, LepRb Tyr_{1138}-STAT3 signaling clearly plays a central role in energy homeostasis. In contrast, mutation of Tyr_{985} (the binding site for SHP-2 and SOCS3) yields animals (l/l mice) that display decreased feeding, body weight and adiposity, increased leptin sensitivity and normal fertility (39). In addition, l/l mice exhibit no evidence of any defects in leptin action. This suggests that the major role of Tyr_{985} involves feedback inhibition of LepRb signaling.

Roles for a number of intracellular signaling pathways have been examined in the regulation of energy balance. The pharmacological inhibition of phosphatidylinositol 3-kinase (PI3K) blocks the suppression of feeding by leptin, suggesting that PI3K signaling contributes to the regulation of energy balance by leptin (40). Indeed, activation of the PI3K-regulated Akt/protein kinase B pathway in the hypothalamus mediates anorexia (41-42). Although the deletion of SHP-2 or STAT3 from forebrain neurons results in overfeeding and obesity (43,44), it is not clear whether this obesity stems from perturbations in leptin signaling, per se, or is the less-specific consequence of the widespread deletion of these promiscuous signaling molecules.

1.5 Leptin access to the CNS

While the short isoforms of LepR are incapable of intracellular signaling, those that retain the transmembrane domain (LepRa, c, d) have been proposed to act as transporters, potentially providing a mechanism whereby leptin crosses the blood-brain-barrier (BBB) (35,44-47). Indeed using a general LepR probe,

which detects LepRa, -b, -c, -d and -e isoforms of the receptor, mRNA has been observed at choroid plexus, and this signal is absent when the LepRb isoform is exclusively targeted, indicating that it is the short forms which exist here (48). Furthermore, intravenous administration of peptides comprising leptin segments of varying lengths to rats, and subsequent measurement of the levels of those peptides in serum versus brain revealed regions required for significant brain uptake of the hormone (49). The correlation of these requisite regions with residues essential for receptor binding, suggest receptor-ligand interaction may play a role in CNS uptake of leptin.

Leptin has also been proposed to enter the CNS through “leaky” BBB areas such as the median eminence (50,51). The fact that cerebral spinal fluid (CSF) leptin levels are lower than serum levels might suggest the primary mechanism is through regulated, saturable transport, though the theory that LepR short forms act as primary transporters is challenged by the fact that CSF levels of leptin in lean controls are similar to those of Koletsky rats, which do not produce any LepR isoforms (52).

1.6 Physiological roles of leptin

1.6.1 Energy Homeostasis. The most apparent role of leptin lies in its ability to regulate body weight. Leptin signals the repletion of body energy stores to the brain, promoting anorexia (decreased appetite) and permitting the expenditure of metabolic energy by the neuroendocrine system (53-55). In mice, disruption of leptin (*ob/ob*), or its receptor (*db/db*), results in extreme obesity due to increased

food intake and decreased energy expenditure (53,54). The major cause of obesity in humans is not lack of leptin or its receptor; rather, their inappropriately small response to elevated serum levels of leptin, as well as the modest effect of leptin therapy, pointing to leptin resistance in most individuals (53,56). This leptin resistance may be secondary to alterations in leptin signaling or, alternatively, due to insensitivity of the neural pathways regulated by leptin.

1.6.2 Glucose homeostasis. The occurrence of diabetes and hyperglycemia in leptin deficient and leptin resistant obese humans and mice may arise indirectly as a result of obesity, however several lines of evidence suggest a more direct link between leptin and the regulation of glucose. While data suggesting leptin action on insulin-responsive peripheral tissues remains inconclusive, substantial colocalization of insulin receptor (IR) and LepRb can be found in the brain, and of particular interest in glucose-responsive neurons of the ARC, VMH and LHA (57,58). Here, the intracellular signaling pathways of IR and LepRb show significant overlap, providing potential points of crosstalk (59). In addition, transgenic overexpression of leptin in normal mice, as well as models of lipoatrophic diabetes, improves glucose metabolism and insulin sensitivity (60,61). The direct role of leptin in glucose homeostasis, as well as the specific contribution of ARC LepRb neurons, are indicated by data showing normalization of hyperglycemia in LepRb-deficient animals with ARC-specific reactivation of LepRb in the face of sustained obesity (62) Recently, Huo *et al*. further narrowed leptin regulation of glucose homeostasis to show that transgenic re-introduction

of LepRb in POMC neurons of *db/db* mice is sufficient to maintain euglycemia, once again in spite of obesity (63).

1.6.3 Immune function. Immune deficits and thymus atrophy have been reported in *ob/ob* and *db/db* mice (64). In addition, leptin has been shown to stimulate specific effectors of the cell-mediated immune response as well as T helper cells (65). Thus leptin represents a potential link between metabolic state and immune function.

1.6.4 Arousal. Frequent complaints reported to doctors by their obese patients are daytime fatigue and excessive sleepiness (66). While in many patients, this may be attributable to comorbidities such as sleep apnea or depression, evidence suggests that dysfunctional leptin signaling may have more direct ties to sleep and arousal. For example, decreased leptin has been associated with changes in the architecture of sleep, and with shorter duration of sleep (67). In rodents, chronic leptin deficiency has been shown to alter the synaptic connectivity of neurons containing arousal-associated neuropeptides such as orexin (68). It has been established that stimulation of orexin (OX) neurons promotes arousal, and feeding, while stimulation of neighboring melanin-concentrating hormone (MCH) neurons decreases metabolism and may promote sleep. Leptin has been shown to inhibit both orexin and MCH neurons in rodents, thus decreasing presumed feeding-directed arousal and metabolism (58).

1.6.5 Growth. Leptin deficient *ob/ob* mice are diminutive in linear length compared to their control littermates and show decreased serum levels of growth hormone (GH), which is reversible by administration of leptin (69-70). In normal rats, antibody-neutralization of leptin decreases plasma GH levels, however coadministration with growth hormone releasing hormone (GHRH) prevents this reduction, which may indicate leptin effects on GH occur at the level of the hypothalamus (71). In addition to analyses of GH, several groups have further proposed direct leptin action on chondrocytes at the growth plate indicative of effects on bone remodeling (72).

1.6.6 Neural Development. Leptin presence in fetal circulation as well as the responsiveness of the hormone to a variety of stimuli in the fetus is well documented (73,74). In rodents, LepRb mRNA has been observed as early as embryonic day 21 (E21) in the hypothalamus, and LepR mRNA at E18 in choroid plexus, although binding of radiolabeled leptin has not been shown at either of these ages (75).

Studies in *ob/ob* mice demonstrated a delay and overall decrease in the formation of neural projections comprising a hypothalamic circuit known to be involved in feeding behavior (ARC→PVN). Exogenous leptin treatment of early postnatal, but not adult, *ob/ob* mice rescues the formation of these projections, demonstrating the importance of leptin action in a precise developmental window on the formation of this circuit (76,77). Those connections that, in normal animals, develop before the described early postnatal leptin surge are unaltered, further supporting both a critical period of development, as well as a specific

contribution of leptin to discrete circuits (25). In addition, rats selectively bred for predisposition to diet-induced obesity display fewer ARC projections and a reduced responsiveness to leptin. Interestingly these rats show early leptin resistance even before the onset of obesity (78). The potential importance of these findings regarding leptin and development are underlined by the well-established importance of the early developmental environment in determining predisposition toward the metabolic syndrome.

In addition to those roles described above, research has linked leptin signaling to both hedonic reward and reproduction. In these systems, leptin has been linked to the "wanting" aspect of food reward as well as several aspects of reproduction including development and maintenance of reproductive competence. These important functions are discussed in detail in chapters 3 and 4 respectively.

1.7 Sites of leptin action

Many of the actions of leptin are attributable to effects in the CNS, particularly in the basomedial hypothalamus, including the ARC (58). A great deal of research has focused on two populations of leptin-responsive neurons in the ARC. The first population, which express neuropeptide Y (NPY) and Agouti-related peptide (AgRP), signal to increase food intake and decrease energy

expenditure; leptin inhibits these neurons. The second population, proopiomelanocortin (POMC)- and cocaine & amphetamine regulated transcript (CART)-expressing neurons, act to decrease food intake and increase energy expenditure and are activated by leptin (58).

ARC-specific expression of LepRb reduces appetite and decreases adiposity in rodents lacking LepRb suggesting the importance of ARC leptin action for energy balance (62). In addition, ARC LepRb expression restored serum glucose levels to normal, demonstrating that a substantial component of the adiposity-independent regulation of glucose metabolism by leptin is also mediated through the ARC. It is clear, however, that ARC leptin action represents only one component of leptin action on energy balance, because the deletion of LepRb from POMC neurons results in a relatively modest body weight phenotype, and the restoration of LepRb expression specifically in the arcuate nucleus of *db/db* mice reverses only a portion of the hyperphagia and obesity of these animals (62,79).

Whereas most attention has focused on the ARC LepRb neurons, many other populations of LepRb-expressing and leptin responsive neurons exist both within and outside the hypothalamus yet remain poorly characterized.

1.8 Summary

While other investigators have described the neuroanatomical locations of leptin-responsive or lepr mRNA-containing cells outside the ARC, or the effects of leptin on broad brain populations, we sought to first establish the sites of LepRb-expressing cells in the brain, and then to determine the specific role(s) of leptin action at discrete brain locations, specifically focusing on the LepRb cells in each region. In particular, we describe the mapping of LepRb cell populations in the brain using a novel LepRb-specific expression of the reporter enhanced green fluorescent protein (EGFP), followed by subsequent characterization of LepRb-expressing cells in two brain regions, the VTA and PMv.

The studies outlined in this thesis are designed to advance our knowledge of LepRb-mediated effects on cell populations beyond the canonically studied feeding circuits of the ARC. Our overall goal is to specifically characterize direct leptin action at discrete neuroanatomical sites and to link these sites to the known roles of leptin in physiology. In order to first identify LepRb-expressing cells we develop an inducible reporter line in which expression of a fluorescent protein is induced in LepRb cells (Chapter 2). We next identify two LepRb-expressing cells groups in the midbrain VTA andRLi, which we postulate lie within the mesolimbic dopamine system and may mediate aspects of hedonic reward (Chapter 3). Finally we characterize LepRb-expressing cells in the PMv, and link this population to regulation of reproduction using neuroanatomical tracing as well as LepRb deletion at this site (Chapters 4,5). Thus we propose that a portion of leptin's effects on food reward are mediated through direct action

at the midbrain, and that certain effects on reproductive competence are regulated by leptin action at the PMv.

Understanding the connectivity and regulation of LepRb-expressing neurons and circuits, as well as how these are altered in response to broader stimuli will advance our awareness of leptin regulation of physiology. Thus, these findings may provide new targets for the treatment of obesity and related conditions.

Chapter 2

Immunohistochemical Localization of LepRb-Expressing Cells in the CNS*

2.1 Introduction

Considerable advancements have been made in defining the physiological functions to which leptin signaling contributes however, frequently we are left with a list of leptin-associated processes, but an unknown mechanism linking the hormone to physiological or behavioral response. Anatomical location of cells within the CNS is often a useful tool in suggesting the system or overall function to which those cells contribute. For example, cells observed within the hippocampal formation will likely play roles in learning and memory, while those found in the cerebellum may function in coordination and motor control. In addition to determining specific brain nuclei within which the cell group of interest lies, mapping also provides details about the relative number and distribution of cells-of-interest within a region. Therefore, anatomical localization of a specific type of cell represents an important step in overall characterization and determination of function.

* Some work described here (Table 1, Figure 3) has been previously published (84). In these studies, Dr. H. Munzberg assisted with IF/IHC.

Anatomical mapping of sites of LepRs and leptin action in the brain has been previously performed utilizing various methods representing not only the technology available at the time, but also the specific systems interrogated. For example, Elmquist *et al*. sought to identify neurons in the rat in which intravenous (iv) or intraperitoneal (ip) leptin administration induced cFos immunoreactivity (Fos-IR) (80). While this approach revealed important populations of cells activated by leptin by the criteria of Fos-IR, the method was limited in routes of administration, time of stimulation as well as inability to identify cells in which leptin caused inhibition or no effect on membrane potential. In order to focus on energy homeostasis regulation, the study concentrated on hypothalamic cell populations. In addition, this technique does not exclude the possibility that Fos-IR was induced indirectly in a cell by leptin action on a neuron synaptically upstream.

In order to determine potential sites of direct leptin action throughout the brain, Elmquist went on to present a map of LepRb expression using *in situ* hybridization (ISH) in the rat (81). The publication additionally compared distribution of total LepR signal to that of LepRb with the most obvious difference lying in the hybridization of a non-isoform-specific LepR, but not LepRb probe, to the choroid plexus and meninges. The inclusion of non-hypothalamic sites of LepRb expression, such as hippocampus and cerebellum, importantly develops the potential for non-canonical leptin roles. While the data represent a significant

description of LepRb expression, the existence of mRNA does not absolutely guarantee presence of the functional protein.

Localization and characterization of leptin responsive cells progressed further in 2000 when Elias *et al*. combined leptin-induced Fos-IR with LepRb ISH, determining areas of overlap (82). The study highlighted the limitations of previous Fos-IR characterizations, observing leptin-induced Fos-IR in cells of the PVN, that did not consistently contain LepRb mRNA. In addition, they observed cells of the arcuate nucleus which contained LepRb mRNA, but no leptin-induced Fos-IR suggesting either leptin inhibition of these neurons, leptin action on these cell which resulted in no change in membrane potential, or lack of leptin action despite existence of LepRb mRNA. This investigation futher combined LepRb ISH or leptin-induced Fos-IR with labeling of other signaling proteins, such as cocaine- and amphetamine-regulated transcript (CART) and dynorphin, observing leptin-induced Fos-IR in CART cells of the ARC, PMv and DMH and in dynorphin cells of the ARC and VMH. While this study significantly advanced our knowledge of leptin responsive neurons, where they lie in the brain and what other neuropeptides they may contain, the study once again focused on the hypothalamus, and the constraints of leptin-induced Fos-IR were not fully overcome.

Very recent work demonstrated the technical advancement in methods to immunohistochemically detect LepRb-expressing cells (83). The group used a mouse strain with a cre-inducible reporter, yellow fluorescent protein (YFP)

combined with mice in which LepRb-expressing cells express cre in order to express YFP specifically in LepRb cells, thus permitting their immunohistochemical labeling. In comparing their YFP immunoreactive (YFP-IR) to ISH of LepRb, they confirmed the previous areas postulated to contain LepRb and identified several areas which contained ISH-labeled cells (LepRb mRNA), but YFP-IR. These included regions of cortex, hippocampus, thalamus, cerebellum and brainstem. They observed no regions containing YFP-IR, but not LepRb ISH.

Thus, while several assays detect LepRb expression within the CNS, each has limitations that prompted us (in parallel with others) to seek a more facile system for identifying LepRb-expressing neurons. Reliable detection of LepRb protein in the mouse brain using LepR-specific antibodies remains problematic, presumably because of the relatively low expression of LepRb even in neurons that express the receptor at functional levels as well as the cross-reactivity of these antibodies with non-signaling, short LepR isoforms. *In situ* hybridization (ISH) for LepRb is difficult when done in combination with immunohistochemistry (IHC) or immunofluorescence (IF) for other proteins. Functional assays for LepRb, immunohistological detection of leptin-induced STAT3 phosphorylation or Fos-IR, while robust, require prior treatment with leptin, limiting the use of this method in the absence of leptin or LepRb. Furthermore, neither ISH nor IHC/IF permit the identification of LepRb neurons before their electrophysiological examination.

To facilitate the detection and study of LepRb neurons throughout the brain, we thus generated mice expressing reporter molecules (enhanced green fluorescent protein (EGFP) or beta-gal (bgal)) in LepRb-expressing neurons ("LepRb^{EGFP}" and "LepRb^{bgal}" mice) by intercrossing *Lepr^{cre}*-containing mice with mice containing a cre-inducible reporter allele.

2.2 Methods

2.2.1 Materials. Chicken anti-EGFP was purchased from Abcam and goat anti-beta-galactosidase was from Biogenesis. Normal donkey serum (NDS) was purchased from Jackson ImmunoResearch. Alexa 488-conjugated goat anti-chicken, Alexa 488-conjugated donkey anti-goat were purchased from Invitrogen. Beta-galactosidase staining kit was purchased from Roche. All other immunohistochemical supplies were purchased from Sigma-Aldrich.

2.2.2 Animals. All mice were bred in our colony in the Unit for Laboratory Animal Medicine at the University of Michigan. All animals and procedures used were in accordance with the guidelines and approval of the University Committee on the Care and Use of Animals. B6;129S4-*Gt(ROSA)26Sor^{tm1Sho}* (*ROSA^{bgal}*), B6.Cg(D2)-Tg(xstpx-lacZ)32And/J (*beta-Actin^{bgal}*) and *Gt(ROSA)26Sor^{tm2Sho}* (*ROSA^{EGFP}*) mice were purchased from The Jackson Laboratory. Animals were given *ad libitum* access to food and water, and were housed in groups of 2–4.

In order to confer LepRb specificity to our analysis, we generated mice

that contain an internal ribosomal entry site (IRES)-driven second cistron encoding cre recombinase "knocked in" to the 3'-UTR of the LepRb-specific exon of *Lepr* (84). Hence, in *Lepr*^{cre} mice, the cre coding sequence is part of the LepRb-specific mRNA such that its expression is restricted to LepRb-expressing neurons. The LepRb coding region of these mice is fully intact, suggesting that energy homeostasis in these animals should be normal; indeed, we have not observed any body weight phenotype in *lepr*^{Cre} animals compared with control, even in homozygous mice (termed *Lepr*$^{cre/cre}$ animals; data not shown).

To identify LepRb-expressing neurons, we crossed the *Lepr*$^{cre/cre}$ mice with *Rosa*^{bgal}, *beta-Actin*^{bgal}, or *Rosa*^{EGFP} mice. These lines have been engineered such that cre-mediated deletion of a floxed transcription-blocking cassette results in the expression of beta-galactosidase (bgal) or enhanced green fluorescent protein (EGFP) from the neuronally expressed *chicken-beta-ACTIN* promoter, or the ubiquitously expressed *ROSA26* promoter or locus (85). Because IRES-mediated cre expression is modest, *Rosa*^{EGFP} mice were bred to homozygosity (*Lepr*$^{cre/cre}$;*Rosa*$^{EGFP/EGFP}$, also known as "LepRb^{EGFP}" mice) (Figure 2) to enhance the detection of LepRb neurons by EGFP expression.

Thus, in the LepRb$^{rosa\text{-}bgal}$, LepRb$^{actin\text{-}bgal}$, and LepRb^{EGFP} mice, excision of the transcription blocker results in beta-gal or EGFP expression in neurons that express LepRb mRNA and in which the promoter for the transgene operates strongly.

2.2.3 *Perfusion and immunolabeling.* Male mice ranging in age from 24 to 51

weeks, were perfused transcardially with phosphate-buffered saline (PBS, pH 7.4) followed by 4% paraformaldehyde. Brains were removed and postfixed as described (86). Brains were sectioned in 30 µm coronal sections, collected in four representative series, and stored at –20°C in cryoprotectant until use. For immunofluorescent (IF) labeling, free-floating brain sections were blocked in normal donkey serum (NDS) and then incubated with primary antibodies (anti-EGFP, 1:1000; anti-bgal, 1:3000). Sections were washed and incubated with Alexa-conjugated secondary antibodies (1:200). For labeling of beta-galactosidase, a Roche staining kit was used according to the instructions of the manufacturer and utilized with fixed tissue sections in culture wells at 37°C. Sections were mounted onto Superfrost Plus slides (Fisher Scientific) and coverslipped with ProLong Antifade mounting medium (Invitrogen).

2.2.4 Microscopy and image analysis. Microscopic images were obtained using an Olympus BX-51 brightfield microscope with DP30BW camera (Olympus). EGFP- or bgal-labeled neurons were counted using Adobe Photoshop software and qualitative estimates of relative densities of cells per region were recorded.

2.3 Results

The immunofluorescent detection of bgal in the brains of $LepRb^{rosa\text{-}bgal}$ and $LepRb^{actin\text{-}bgal}$ mice revealed positive cells in the ARC and VMH in both reporter strains. Specific to the $LepRb^{actin\text{-}bgal}$ mice, we observed abundant bgal-IR cells

in the hippocampus (Figure 3), as well as smaller numbers of cells in the pons. In LepRb$^{rosa\text{-}bgal}$ reporter animals, positive cells were abundant in the ARC, PMv, DMH, LHA, VMH and DR (Figure 3). The observed variation in sites of reporter labeling in the two strains may be due to the different modes of construction of the lines, LepRb$^{rosa\text{-}bgal}$ utilizing gene targeting of ROSA26 while LepRb$^{actin\text{-}bgal}$ used transgenic expression driven by chicken-beta-actin. No bgal-IR was detected in either strain in the absence of the *lepr*^{Cre} allele (data not shown). The distribution of bgal-IR in these reporter animals is consistent with previous reports of LepRb mRNA and with a potential functional role for leptin in these regions, though the degree of hippocampal labeling in LepRb$^{actin\text{-}bgal}$ animals is considerably greater and may be attributable to irregular beta-actin promoter activity in that population (80-83).

While immunofluorescent detection of bgal immunoreactivity (bgal-IR) revealed the presence of large numbers of LepRb-expressing cells in several hypothalamic regions, labeling in each bgal reporter line proved to grossly underrepresent the totality of LepRb-expressing neurons in intra- and extra-hypothalamic areas as compared to published reports as well as our LepRb^{EGFP} mice. Table 1 shows the relative density of labeled cells in LepRb$^{rosa\text{-}bgal}$ and LepRb$^{actin\text{-}bgal}$ reporter lines compared to EGFP immunoreactivity (EGFP-IR) in LepRb^{EGFP} mice at those sites. In addition to those detailed in Table1, LepRb^{EGFP} mice revealed EGFP-IR in a multitude of brain regions consistent with previous studies (Table 2). Those populations containing the greatest relative amounts of EGFP-IR cells are shown in Figure 4 and highlighted below.

Hypothalamus. The hypothalamus is the center for regulation of homeostasis, and leptin action in this area has been described (87). In our analysis of $LepRb^{EGFP}$ mice, we consistently observed copious EGFP-IR in ARC, PMv, LHA, VMH, DMH and POA. In the ARC, LHA and PMv, EGFP-IR cells were densely distributed throughout the brain region, with no apparent dominance of one subregion. In contrast, the VMH, DMH and POA populations showed patterns of labeling in which certain areas were spared. In the VMH, EGFP-IR was observed in the dorsomedial but not ventrolateral subregions. Previous studies have demonstrated that LepRb deletion in a subpopulation of VMH cells increases food intake and body weight (88). While the VMH has also been implicated in reproduction regulation, much of this role has been attributed to the ventrolateral VMH, where estrogen receptors, but not LepRb have been localized (89,90). In the DMH, the majority of EGFP-IR was localized to the dorsal and ventral regions with few in the compact region. The DMH has been ascribed roles in circadian rhythms, thermoregulation and arousal (91-93). The preoptic regions are a site of gonadotropin releasing hormone (GnRH) neurons in rodents and thus regulate the reproductive axis (189). In addition, the POA has been linked with thermoregulation and fever (94,95). The POA is a general term for the widespread collection of preoptic regions; we observed EGFP-IR throughout the medial subregions and a small number in lateral preoptic areas. While the LHA has been credited with roles in hunger and arousal, specific examination of LepRb action at this site is underway in the Myers Lab and others (87). Whereas reproductive and sensory-processing roles of the PMv as a whole have been

examined, our recent work analyzing LepRb neurons at this site is detailed in Chapters 4 and 5 of this thesis.

Brainstem. The brainstem is most associated with overall functions vital to life, such as respiration, cardiovascular control, sleep and pain perception. Here, we observed large numbers of LepRb-expressing cells in the VTA, SN, DR, PAG, PBN and DpMe. In the DR, labeled cells appeared proximal to the cerebral aqueduct, and extended ventrally. While the DR is closely associated with the large population of serotonin (5-HT) neurons within the region (96), we have not observed colocalization of EGFP-IR and 5-HT in $LepRb^{EGFP}$ mice (data not shown). The PAG is a center for pain processing and the proposed site of analgesia actions (97). Here we see EGFP-IR neurons sparsely distributed throughout. LepRb-expressing cells in the PBN localize specifically and densely in the lateral regions. The PBN is ascribed numerous roles, including cardiorespiratory control, taste aversion and ingestion (98,99). DpMe refers to a sizeable midbrain area, and EGFP-IR cells were found scattered throughout. This brain region is proposed to play roles in the “startle” response to fear as well as in nociception (100,101). The SN contained EGFP-IR cells specifically in the pars compacta region (SNC), an area associated with arousal and specifically affected in Parkinson’s disease (102,103). Finally, the occurrence of LepRb-expressing cells in the VTA points to a role for leptin in the mesolimbic reward circuit; further analysis of this population of LepRb-expressing cells continues in the subsequent chapter (Chapter 3).

Cortex. EGFP-IR cells were observed sporadically through several cortical regions including somatosensory cortex, auditory cortex, ectorhinal cortex and the dorsal endopiriform nucleus. In each of these areas, EGFP-IR cells were spread homogeneously throughout the regions, with no apparent clustering in discrete locations. The localization of LepRb in cortical brain centers provides a potential link between leptin regulation of unconscious processes and higher awareness, integrating peripheral information with sensory inputs and resulting in fine-tuning of synaptic connections. Here, leptin may act to adjust cognitive ability, effects observed in LepRb deficient mice (104,105).

2.4 Discussion

Within the hypothalamus, we and others have demonstrated the presence of large numbers of LepRb-expressing cell bodies in the ARC, VMH, DMH, LHA, PMV, among other places (80-83). Of these, the DMH, VMH, and LHA are areas known to be involved in the regulation of feeding and energy expenditure, while other sites may be most important for neuroendocrine actions of leptin distinct from feeding behavior and energy expenditure. The importance of identifying and analyzing these sites remains high: leptin action in these areas may contribute to the described roles of leptin other than energy homeostasis regulation, or to “side effects” of altered energy balance, such as sub-fertility.

In comparing our own data from each of the different reporter lines, we clearly find the $LepRb^{EGFP}$ mice to be far more consistent than either beta-gal line. In

the LepRb$^{rosa\text{-}bgal}$ mice, this may be due to the quality and nature of the antigens detected. While the EGFP-IR permeates the entire cell evenly, beta-gal labeling in LepRb$^{rosa\text{-}bgal}$ animals appears punctate and uneven, making discrimination from background more difficult. In the LepRb$^{actin\text{-}bgal}$ mice, beta-gal labeling is enhanced by a nuclear localization sequence, however, transgenic expression as well as the use of beta-actin promoter (as opposed to Rosa26) may limit or disproportionately alter spatial expression of the reporter.

We additionally compared our results to those obtained using similar methods by Scott *et al*. (83). We found a high degree of overlap in identified populations of LepRb-expressing cells, with only minor differences. There were three regions in which we identified consistent EGFP-IR ("+" or more), but in which they only observed mRNA: temporal association cortex, subparafascicular nucleus and supramammillary nucleus. We found only one area where we observed a significant population of EGFP-IR cells (+++), but which they do not list (commissure of the inferior colliculus), and, conversely one region where they describe significant numbers of positive cells, but we do not (retrochiasmatic area, RCh). In the latter case, we consciously grouped RCh with the ARC populations as this is a region adjacent to ARC and the boundaries are ill-defined. Smaller discrepancies between results may be due to unavoidable variations in neuroanatomical boundary definitions and may represent differences in representations of relative size, as both studies were qualitative.

The generation of this novel LepRb^{EGFP} reporter mouse will facilitate a myriad of future studies, many of which are currently underway in the Myers Lab.

LepRb^{EGFP} mice will be a valuable tool in dissecting each population of LepRb-expressing cells and further characterizing their response to leptin, co-expression of other signaling proteins as well as their putative roles in physiological processes. In addition, the manipulation of physiological parameters in these mice will allow immunohistological detection of alterations specifically within LepRb-expressing cells. For example, comparing basal or leptin-stimulated neuronal activity (Fos-IR) in LepRb^{EGFP} mice fed a normal chow diet versus mice consuming a high fat diet will allow examination of changes in the activities of populations in diet-induced obesity (DIO), as well as in their ability to respond to leptin.

Furthermore, the establishment of this mouse model in efficiently labeling LepRb-expressing cells will allow similar strategies to be employed. For example, using a farnesylated EGFP in place of the standard EGFP will allow the specific labeling of projections from LepRb-expressing cells in order to examine brain regions with which LepRb cells communicate.

In conclusion, we have used cre-inducible reporters to generate and analyze three mouse models which express bgal or EGFP in LepRb-expressing cells of the brain. In comparing the models to each other, as well as to similar published reports we have determined the efficient labeling of LepRb-expressing cells in our LepRb^{EGFP} mouse line. Future studies using this mouse will be crucial in understanding the mechanism of action of these novel populations of leptin-responsive neurons in mediating the physiological effects of leptin signaling.

Indeed we employ this mouse in subsequent chapters (Chapters 3,4) in order to study LepRb-expressing cells in two brain regions with relatively substantial numbers of EGFP-IR cells: the VTA and PMv.

CHAPTER 3

LepRb in Midbrain Neurons[‡]

3.1 Introduction

While a considerable amount of research has developed our knowledge of hypothalamic LepRb neuronal populations and their roles in the regulation of energy homeostasis based on physiological need, these studies do not incorporate a role for leptin in hedonic feeding. It is recognized, both experimentally and anecdotally, that when presented with an appetizing food, most animals will eat, regardless of physiological need for energy (106). In addition, after fasting or food restriction, food reward is increased and animals will often "binge" on palatable foods (107). This reward-motivated aspect of feeding is regulated by the same brain systems implicated in addiction to drugs of abuse, the mesocorticolimbic (ML) dopamine (DA) system, and crosstalk occurs between this system and satiety pathways (106,108). Administration of opioid receptor antagonists to rodents blunts the ability of AgRP to induce feeding (187), while opioid agonists increase palatable food intake (109,110).

The most obvious association between the MLDA system and feeding circuits is in the extensive connectivity between brain regions and cell types critical to each system. The MLDA circuit is composed of several interconnected

[‡] In these studies, G. Louis prepared our adenoviral construct described in 3.2.3, and Dr. C.J. Rhodes packaged the construct in adenovirus.

brain regions, including the VTA, nucleus accumbens (NAc), amygdala, prefrontal cortex (PFC), and hippocampus (111). The proposed role of DA in this circuit is in establishing the "wanting" of the food/drug and the motivation to seek it, or its incentive salience. In contrast, opioid transmission is implicated in "liking" of a stimulus, i.e. a food's palatability (112,113).

Leptin has previously been implicated in regulation of the MLDA circuit and associated behaviors. Central administration of leptin decreases sucrose preference, opioid-stimulated food intake and conditioned place preference by food (114-116). Central leptin infusion has also been shown to suppress DA release in the NAc, with an associated decrease in related feeding behaviors (117). More recently, two groups have specifically studied the action of leptin on VTA DA neurons. Hommel *et al.* found that leptin administered directly to the VTA induced pSTAT3 in DAergic neurons, decreased the firing rate of DA cells and decreased food intake in rats (118). In addition, viral-mediated knockdown of LepRb in VTA increased food intake (both chow and high fat diets), as well as increasing sucrose preference (118). While Fulton *et al.* similarly showed leptin-induced pSTAT3 in VTA DA cells, they then took a more generalized approach to leptin action within the MLDA system (119). Using retrograde tracing from the NAc, Fulton showed tracer accumulation in VTA cells with leptin-induced pSTAT3. In normal mice, administration of amphetamine causes an increase in locomotor activity. Repeated doses of amphetamine induces "sensitization", or successive increases in activity with consecutive administration (120). This response is mediated by cells of the MLDA system (121). Fulton *et al.*

demonstrated that while leptin deficient *ob/ob* mice *do* increase locomotor activity in response to amphetamine, they *do not* display sensitization upon repeated administration unless treated chronically with leptin (119). They further showed that *ob/ob* mice have lower basal levels of tyrosine hydroxylase (TH; the rate-limiting enzyme in DA production) in the NAc, however the levels can be restored to those of control mice with leptin treatment.

While the data by Hommel and Fulton seem to contradict one another, with Fulton showing lack of leptin decreasing MLDA function and Hommel observing leptin blocking DA neuronal activity, it is important to recognize the major distinctions between the two approaches. While Hommel studied the effects of acute leptin stimulation or knockdown, specifically focusing on the VTA, Fulton used a model of chronic systemic leptin deficiency. As previously described, the developmental changes in *ob/ob* mice may have resulted in compensatory changes not observed with adult deletion, nor in knockdown specific to one LepRb population.

It is clear that leptin regulates the incentive salience of food by modulating the MLDA system. The specific mechanism(s) by which leptin acts on this system have still not been clarified, however. In order to neuroanatomically place LepRb cells within the MLDA circuit, we have generated and utilized $LepRb^{EGFP}$ mice (as described in Chapter 2) to identify LepRb expression in midbrain neurons. We further reveal distinct projections of midbrain LepRb-expressing neurons, employing an adenoviral tract-tracer (Ad-iZ/EGFPf) in which cre recombinase induces the expression of a farnesylated EGFP that reveals axonal projections.

In addition, we used retrograde tracing to determine other leptin-responsive inputs to the midbrain that may additionally contribute to leptin regulation of the MLDA system. We show that LepRb VTA neurons represent a unique subclass of VTA neurons, distinct in their pattern of projection as well as in their expression of LepRb.

3.2 Methods

3.2.1 Materials. Fluorogold-equivalent, hydroxystilbamidine, was purchased from Biotium. Rabbit anti-Fluorogold was from Millipore Bioscience Research Reagents, chicken anti-EGFP was from Abcam, and mouse anti-tyrosine hydroxylase was from ImmunoStar. Normal donkey serum (NDS) and biotinylated donkey anti-rabbit were purchased from Jackson ImmunoResearch. Alexa 488-conjugated donkey anti-rabbit, Alexa 488-conjugated goat anti-chicken, and Alexa 568-conjugated goat anti-mouse were purchased from Invitrogen. ABC Vectastain Elite kit was purchased from Vector Laboratories. All other immunohistochemical supplies were purchased from Sigma-Aldrich.

3.2.2 Animals. All mice were bred in our colony in the Unit for Laboratory Animal Medicine at the University of Michigan. All animals and procedures used were in accordance with the guidelines and approval of the University Committee on the Care and Use of Animals. *Gt(ROSA)26Sor*^{tm2Sho} (*ROSA*^{EGFP}) mice were purchased from The Jackson Laboratory. Animals were given *ad libitum* access

to food and water, and were housed in groups of 2–4, except where indicated.

LepRb^{EGFP} mice. LepRb-Cre mice were crossed with Rosa26-EGFP reporter mice to produce offspring in which EGFP is expressed in LepRb cells as described in section 2.2.2.

3.2.3 Intracerebral injections. For the intracerebral administration of tracers, animals were anesthetized with isoflurane and placed in a stereotaxic frame (Kopf Instruments). The skull was exposed and coordinates for bregma were recorded. To these measures were added: -3.2 mm posterior (A/P) to bregma, -0.5 mm lateral to midline (M/L), -4.2 mm ventral to dura (D/V) for VTA/RLi; -1.2 mm A/P, -2.8 mm M/L, -4.8 mm D/V for CeA; and +1.0 mm A/P, -1.4 mm M/L, -4.8 mm D/V for NAc. A stainless steel guide cannula with dummy (Plastics One) was lowered to the appropriate depth. Immunohistological examination of aim sites using neuroanatomical landmarks confirmed correct targeting.

We modified the pShuttle vector (122) to generate an adenoviral transfer vector containing the CMV promoter upstream of a transcription-blocking cassette followed by sequences encoding farnesylated EGFP (EGFPf) to generate Ad-iZ/EGFPf (Figure 2), which mediates the expression of EGFPf only when transduced into cre-expressing cells. Adenoviral stocks were prepared as described previously (188). For injections of Ad-iZ/EGFPf to *Lepr$^{cre/cre}$* mice, cannulae were placed at VTA/RLi coordinates and 250 nl from a 5.1 x 10^{11} pfu/ml stock was injected over 5 minutes. After an additional 10 minutes, the injector was removed, the hole filled with bone wax (Ethicon) and skin closed with

sutures. Animals were allowed to recover on a heating pad and then single-housed in a biohazard containment room. Five days after injection, animals were perfused.

For injections of the retrograde tracer, Fluorogold-equivalent, hydroxystilbamidine (FG), cannulae were placed at CeA or NAc coordinates of $LepRb^{GFP}$ mice and 10 nl of a 2% FG solution was injected over 30 seconds. Ten minutes later, the injector was removed, the hole filled with bone wax and skin closed with sutures. Animals were allowed to recover on a heating pad and then single-housed in clean cages. Four days after injection, animals were perfused and brains were removed as described. For tracing from VTA, animals were treated for 2 h with leptin (5mg/kg, i.p.) in order to utilize leptin-induced phosphorylation of STAT3 (pSTAT3) as a marker of leptin-responsive cells.

3.2.4 Perfusion and immunolabeling. Mice were perfused transcardially and brains sectioned as described in section 2.2.3. For immunofluorescent (IF) labeling, free-floating brain sections were blocked in NDS and then incubated with primary antibodies (anti-EGFP, 1:1000; anti-Fluorogold, 1:3000; anti-TH, 1:5000; anti-pSTAT3, 1:1000). Sections were washed and incubated with Alexa-conjugated secondary antibodies (1:200). For immunohistochemical labeling (IHC) of pSTAT3, sections were pretreated sequentially in 1% H_2O_2/1% NaOH, 0.3% glycine, and 0.3% SDS, then blocked in NDS and incubated in primary antibodies (anti-pSTAT3, 1:500; anti-cFos, 1:40,000). Sections were washed, incubated in biotinylated donkey anti-rabbit (1:1000), followed by avidin-biotin-

complex labeling. Signals were developed with diaminobenzidine resulting in a brown precipitate. After washing, brains continued to IF for additional labeling. For both IF and IHC, sections were mounted were mounted onto Superfrost Plus slides (Fisher Scientific) and coverslipped with ProLong Antifade mounting medium (Invitrogen).

3.2.5 Microscopy and Image Analysis. Microscopic images were obtained using an Olympus BX-51 brightfield microscope with DP30BW camera (Olympus). For quantification of EGFP/TH or EGFP/FG double-labeled neurons, pictures of the identical areas were taken on channels for Alexa 488 (EGFP) or Alexa 568 (FG or TH). Using Adobe Photoshop software single- and double-labeled neurons were counted and recorded. Values are presented as mean ± SEM.

3.3 Results

3.3.1 LepRb expression in the midbrain. In addition to classic leptin responsive brain regions, GFP-immunoreactivity (GFP-IR) in brains of CCGG mice revealed populations of LepRb-expressing cells within the VTA and linear raphe (RLi). Of these, a significant portion (74.9% ± 3.9, n=3) express TH, a marker for DA neurons (Figure 5).

3.3.2 Projections from VTA and RLi LepRb cells. Since standard cytoplasmic EGFP in LepRb^{EGFP} mice is expressed in LepRb neurons throughout the entire brain and poorly labels long projections, we created a novel tract-tracing system

to interrogate the projections of specific LepRb populations. In this system, an adenovirus carrying a construct in which cre-mediated recombination induces a farnesylated, membrane-bound EGFP (EGFPf) is stereotaxically injected into the VTA and/or RLi of l*epr*^{cre} mice, resulting in the expression of EGFPf specifically in LepRb VTA and/or RLi neurons and permitting the visualization of their axonal projections. LepRb cells infected with virus (GFP-IR) were observed at the site of injection, in VTA and RLi (Figures 6, 7).

VTA LepRb neurons project rostrally to densely innervate several regions of the striatum, including the CeA and IPAC, but not the NAc (Figure 6). Projections from midline LepRb cells (including those in the RLi) were observed in CeA and IPAC, although these midline midbrain LepRb neurons also sent some projections to the core and lateral shell of the NAc (Figure 7). The observed projections from these populations of LepRb-expressing cells suggests that these neurons are a component of the MLDA system.

In order to confirm the LepRb VTA/RLi→amygdala and RLi→NAc circuits as well as to verify the scarcity of LepRb VTA→ NAc connections we performed retrograde tracing from CeA and NAc regions shown to receive LepRb inputs using our anterograde tracing method above. When the retrograde tracer Fluorogold (FG) was injected to CeA of LepRb^{EGFP} mice, we observed colocalization of FG and GFP in both VTA and RLi, validating the projection of LepRb midbrain neurons to CeA (Figure 8). An additional group of LepRb^{EGFP} mice, which received FG administered to NAc, showed abundant FG-IR cells throughout the midbrain, however, the bulk of tracer accumulation in GFP-IR

cells occurred in the RLi (Figure 8). Thus, LepRb VTA and RLi cells both project rostrally to CeA, while the vast majority of the modest number of LepRb projections to the NAc arise in LepRb RLi neurons.

3.3.3 LepRb-sensitive inputs to the VTA. In order to determine inputs to the midbrain from LepRb-responsive (leptin-induced pSTAT3 positive) cells outside the midbrain, we stereotaxically injected the retrograde tracer, Fluorogold (FG), into the VTA of C57Bl/6J mice treated systemically with leptin. FG-mediated retrograde labeling revealed that LHA, but not ARC, LepRb neurons comprise the major population of LepRb neurons that directly project to the VTA, suggesting the importance of these neuronal populations in the regulation of the MLDA system and food reward by leptin (58.9 +/- 2.2% of LHA leptin-responsive cells were FG-positive, n=7). (Figure 9).

3.4 Discussion

The complex regulation of feeding involves the processing of not only homeostatic need, but also social stimuli and hedonic drives (106). Indeed, when presented with appetizing food, even when physiological needs have been sated, most animals will partake. The rewarding nature of certain foods had evolutionary advantages to early ancestors and lower animals, as taste information usually correlated to nutrition wherein sweet and salty foods provided important nutrients and bitter or sour foods were often characteristics of toxins or

indications of rot. Therefore, hedonic incentives to choose nutrient-rich foods conferred an adaptive advantage. However, with the increased exposure of individuals in Western societies to palatable, high-calorie cuisine, in combination with the rewarding effects of such foods, the major cause of obesity becomes overfeeding beyond basic nutritional requirements.

Similar to addiction associated with drugs of abuse, the compulsion to ingest palatable foods involves the MLDA system (108-110). This circuit is well defined and includes defined brain regions including the VTA, NAc, amygdala, hippocampus and prefrontal cortex, with dopamine as the major signaling molecule. In order to provide a mechanism by which hedonic reward systems drive feeding, research has begun to examine the connection of the MLDA system with satiety hormones as well as energy homeostasis centers of the brain (116). Recent work has described the action of leptin within this network, examining the effects of both leptin administration as well as chronic and acute leptin deficiency (118,119). In both cases, actions of leptin on midbrain neurons have been shown in addition to downstream effects in target brain areas, though data identifying the actual circuitry of the LepRb-expressing subpopulation of midbrain neurons has remained somewhat lax owing to technical limitations in anatomically identifying LepRb cells in the midbrain.

Utilizing $LepRb^{EGFP}$ mice (which express EGFP specifically in LepRb-expressing cells), we confirmed the previously reported presence of LepRb in a subset of midbrain cells, including those of the VTA, RLi and SN. Consistent with

the colocalization of Lepr mRNA with TH in VTA by Hommel *et al*., we showed the colocalization of TH specifically in VTA EGFP-IR (LepRb-expressing) neurons, and that this comprises the majority of LepRb VTA neurons (118).

In order to determine the specific circuitry of LepRb midbrain neurons, we used a novel cre-inducible EGFPf-dependent tracing system to examine projections from LepRb VTA and RLi neurons. Previous tracing studies examining the overall population of VTA neurons demonstrated afferent projections to amygdala and striatal targets. In our investigation of EGFPf-containing projections using Ad-iZ/EGFPf-mediated tracing specifically from LepRb VTA and RLi neurons, we observed the specific projection of LepRb VTA neurons to the central (CeA) and CeA transition zone (IPAC), but scarce innervation of the NAc. In contrast, tracing of LepRb RLi neurons demonstrated a modest number of ascending projections to the NAC, in addition to projections to the CeA and IPAC. In addition, whereas retrograde tracer (FG) administer to the CeA accumulated in LepRb VTA and RLi neurons, NAc FG application to the NAc produced labeling in LepRb RLi neurons. These data are somewhat inconsistent with Fulton *et al*. who describe retrograde tracer from NAc accumulating in leptin-responsive cells of the VTA. This divergence may be due to the different techniques used to identify LepRb neurons in each method.

The finding of predominantly LepRb midbrain→amygdala projections, with only a small amount of LepRb midbrain→NAc innervation, further focuses the direct action of leptin on midbrain neurons to regulation of specific elements of

the reward circuit. A plethora of research has demonstrated amygdalar roles in the “wanting” aspects of reward, including regulation of incentive learning and aversive conditioning, more specifically stress- and gustatory associations (123,124). Subsequent analyses have further proposed the precise amygdala structures responsible: the basolateral amygdala (BLA) contributes to incentive learning and motivational conditioning associated with food stimuli (including taste), while the CeA mediates aversive conditioning and the stress/anxiety responses associated with the “wanting” of food reward (125). The specific localization of LepRb VTA afferents to the CeA, but not the BLA, points to leptin regulation of the latter aspect of food motivation through direct midbrain actions and is supported by studies linking leptin to the regulation of anxiety-like behaviors in rodents (126). The finding that innervation of the interstitial nucleus of the posterior limb of the anterior commissure (IPAC) originates from the same LepRb midbrain populations as those of the CeA corresponds with the IPAC as part of the amygdala transition zone; the IPAC’s connectivity and function have likewise been proposed to lie in the same sphere as those of the amygdala (127).

The NAc has been ascribed both “wanting” and “liking” functions (113,124) and mediates motivation associated with unconditioned and conditioned stimuli. A variety of studies have linked this region with the hedonic aspects of feeding as well as leptin actions, however LepRb-expressing cells are not found in this area and we observed only minor innervation of the NAc by midbrain LepRb neurons (128,129,118,119).

While leptin action directly at the midbrain is clearly positioned to mediate leptin effects on the hedonic reward of food, indirect actions through hypothalamic LepRb may also contribute to this regulation. We therefore applied FG to the VTA and explored the retrograde accumulation of the tracer in leptin-responsive cells outside the midbrain. Although FG immunoreactivity was observed throughout the hypothalamus, in several regions expressing LepRb, the most significant colocalization of FG with leptin-induced pSTAT3 was observed in the LHA, suggesting that leptin action at this site may influence the MLDA.

Thus, LepRb neurons are positioned to regulate the MLDA reward system through direct actions on midbrain VTA and RLi LepRb-expressing cells as well as indirectly through LHA innervation of the VTA (Figure 10). Future analyses of leptin's role in midbrain neurons and the MLDA system may include the use of transsynaptic tracing combined with midbrain leptin administration to determine the downstream effects on amygdala and accumbens target cells. In addition, a multitude of behavioral studies examining parameters of anxiety or addiction may be employed in concert with specific stimulation of midbrain LepRb neurons.

Chapter 4

LepRb in Neurons of the Ventral Premammillary Nucleus of the Hypothalamus[†]

4.1 Introduction

Appropriate energy balance governs reproductive competency: inadequate adiposity attenuates the activity of the reproductive axis, resulting in anovulation in females (130). Thus, a strong and precise signaling mechanism must link energy homeostasis with reproduction. The adipocyte-derived hormone, leptin, circulates in approximate proportion to fat stores to signal long-term energy status (2-7). In addition to attenuating feeding, leptin permits energy expenditure and activates the neuroendocrine reproductive axis: Adequate leptin levels enable the onset of puberty, whereas the lack of leptin in rodents or humans with genetic leptin deficiency or lipodystrophy results in hypothalamic amenorrhea that is reversible with leptin replacement (131-136). Similarly, food restriction, which decreases circulating leptin levels, inhibits the reproductive axis (131,137). Leptin

[†] Work described here has been previously published: Leshan RL, Louis GW, Jo YH, Rhodes CJ, Münzberg H, Myers MG Jr (2009) Direct innervation of GnRH neurons by metabolic- and sexual odorant-sensing leptin receptor neurons in the hypothalamic ventral premammillary nucleus. *J Neurosci* 29:3138-3147. In these studies, Dr. Y.H. Jo performed electrophysiology (Figure 13E), G. Louis generated the adenoviral construct, Dr. C.J. Rhodes packaged the construct inadenovirus, Dr. H Munzberg injected FG to POA and performed IHC/IF on these animals (Figure 18B,C), Dr. C. Patterson performed LepRb^{EGFPf} IHC/IF (Figure 16)

reverses much of this effect on food-restricted rodents, partially restoring testosterone (males) and luteinizing hormone (LH) levels and cyclicity (females) in mice (131). Leptin treatment additionally preserves LH pulse frequency, sexual maturation, estrus cycling, ovulation and sexual behaviors in a variety of rodent models (138-141). Thus, leptin represents a crucial metabolic signal to the reproductive axis.

Whereas GnRH neurons do not contain LepRb, intracerebroventricular leptin stimulates LH release and activates the reproductive axis, suggesting that leptin acts indirectly on the reproductive system, via neurons that synapse on GnRH neurons (139,142,143). While a considerable amount of attention has focused on the ARC LepRb neurons, the PMv exhibits substantial LepRb mRNA expression and responds to peripheral leptin administration (80-84). Although LepRb PMv neurons have not been specifically examined, a variety of data (described below) suggest a role in reproduction for at least some PMv neurons. The PMv is reciprocally connected with regions central to the regulation of reproduction, including the preoptic nuclei (POA) and anteroventral periventricular nucleus (AvPv), and with parts of the vomeronasal olfactory system, such as the bed nucleus of the stria terminalis (BST) and amygdala (144-149). Indeed, administration of estrogen or progesterone, or mating activates substantial numbers of PMv neurons, as does the exposure of rodents to bedding soiled by animals of the opposite sex (150-153). Unilateral lesions of the PMv in the male rat block the ability of ipsilateral medial amygdala (MeA) stimulation to elicit an increase in LH, placing the PMv between the MeA and the rostral

hypothalamic control of neuroendocrine reproductive function in a putative circuit beginning with sexual odorants and ending in rise of serum LH (154).

Given the placement of the PMv within this olfactory→reproductive circuit and the large population of LepRb neurons in this nucleus, we hypothesized that LepRb PMv neurons might sense both leptin and sexual odorant cues and communicate this information to the reproductive system by directly innervating rostral hypothalamic GnRH neurons. Indeed we show activation of LepRb PMv neurons by leptin as well as exposure to opposite-sex odors, and additionally use LepRb- and GnRH-specific tract-tracting tools to confirm the direct projection of LepRb PMv cells onto GnRH neurons of the POA.

4.2 Methods

4.2.1 Materials. Recombinant mouse leptin was obtained from the National Hormone and Peptide Program (Dr. A. F. Parlow). Fluorogold-equivalent, hydroxystilbamidine, was purchased from Biotium. Rabbit anti-pSTAT3 was from Cell Signaling Technologies, rabbit anti-cFos was from Calbiochem (EMD Biosciences/Merck), mouse anti-NeuN (clone A60) and rabbit anti-Fluorogold were from Millipore Bioscience Research Reagents, and rabbit anti-nNOS was from ImmunoStar. Rabbit anti-wheat germ agglutinin (WGA; used to detect barley lectin) was from Sigma-Aldrich, chicken anti-EGFP was from Abcam. Normal donkey serum (NDS) and biotinylated donkey anti-rabbit were purchased from

Jackson ImmunoResearch. Alexa 488-conjugated donkey anti-rabbit, Alexa 488-conjugated goat anti-chicken, and Alexa 568-conjugated goat anti-rabbit were purchased from Invitrogen. ABC Vectastain Elite kit was purchased from Vector Laboratories. All other immunohistochemical supplies were purchased from Sigma-Aldrich.

4.2.2 Animals. All mice were bred in our colony in the Unit for Laboratory Animal Medicine at the University of Michigan. All animals and procedures used were in accordance with the guidelines and approval of the University Committee on the Care and Use of Animals. C57Bl/6J and *Gt(ROSA)26Sor*^{tm2Sho} (*ROSA*^{EGFP}) mice were purchased from The Jackson Laboratory. Animals were given *ad libitum* access to food and water, and housed in groups of 2–4, except where indicated. *LepRb*^{EGFP} *mice.* LepRb-Cre mice were crossed with Rosa26-EGFP reporter mice to produce offspring in which EGFP is expressed in LepRb cells as described in section 2.2.2.

To generate the *Gt(ROSA)26Sor*^{EGFPf} (Rosa^{EGFPf}) animals, we obtained and used the pBigT/pROSA26PA targeting system from Dr. Frank Costantini (Columbia University) (155) and inserted the sequences for EGFPf in the targeting system for electroporation into R1 ES cells in the University of Michigan Transgenic Animal Model Core. Clones were initially screened by quantitative PCR functional loss of homozygosity assays, as described previously (156), and confirmed by Southern blotting. Positive clones were injected into C57 blastocysts for chimera generation and germline (brown) progeny from the chimeras were screened for the presence of EGFP. Germline progeny containing

the targeted allele were bred with LepRb^{cre} animals to generate *Lepr*$^{cre/+}$;*ROSA*^{EGFPf} (LepRb^{EGFPf}) animals (Figure 2).

The previously described "BIG" mice (157), which provide anterograde and retrograde tracing from GnRH cells, were generously provided by Drs. Linda Buck and Ulrich Boehm and were propagated in our colony.

4.2.3 Perfusion and Immunolabeling. Adult female (except as indicated) mice were injected intraperitoneally (i.p.) with leptin (5.0 mg/kg body weight) or equal volume vehicle (PBS, pH 7.4) where indicated, and were anesthetized 2–4 h later (as indicated) with i.p. sodium pentobarbital (150 mg/kg). In order to coincide with the normal active (dark) cycle, leptin and PBS administration was arranged such that all perfusions were performed during late afternoon, between 3:00 and 5:00 P.M., just before the onset of the dark cycle. Transcardiac perfusion and preparation of brain sections was completed as described in section 2.2.3. For immunofluorescent (IF) labeling, free-floating brain sections were blocked in NDS and then incubated with primary antibodies (anti-EGFP, 1:1000; anti-Fluorogold, 1:3000; anti-cFos, 1:40,000; anti-pSTAT3, 1:500; anti-NOS1, 1:1000). Sections were washed and incubated with Alexa-conjugated secondary antibodies (1:200). For immunohistochemical labeling (IHC) of pSTAT3 or Fos, sections were pretreated sequentially in 1% H_2O_2/1% NaOH, 0.3% glycine, and 0.3% SDS, then blocked in NDS and incubated in primary antibodies (anti-pSTAT3, 1:500; anti-cFos, 1:40,000). Sections were washed, incubated in biotinylated donkey anti-rabbit (1:1000), followed by avidin-biotin-complex labeling. Signals were

developed with diaminobenzidine resulting in a brown precipitate. After washes, brains were next subjected to additional IF labeling. For both IF and IHC, sections were mounted onto Superfrost Plus slides (Fisher Scientific) and coverslipped with ProLong Antifade mounting medium (Invitrogen).

4.2.4 Intracerebral injections. For the intracerebral administration of tracers, animals were anesthetized with isoflurane and placed in a stereotaxic frame (Kopf Instruments). The skull was exposed and coordinates for bregma were recorded. To these measures were added: –2.3 mm posterior (A/P) to bregma, –0.4 mm lateral to midline (M/L), –5.6 mm ventral to dura (D/V) for PMv; +0.4 mm A/P, –0.4 mm M/L, –4.45 mm D/V for POA; and –1.55 mm A/P, –1.85 mm M/L, –5.2 mm D/V for MeA. A stainless steel guide cannula with dummy (Plastics One) was lowered to the appropriate depth as determined by immunohistological examination using neuroanatomical landmarks or counterstaining.

We generated and delivered the adenovirally-delivered tracer, Ad-iZ/EGFPf as described in section 3.2.3, except in using the coordinates for PMv. Five days after injection, animals were perfused as described.

For injections of the retrograde tracer, Fluorogold-equivalent, hydroxystilbamidine (FG), cannulae were placed at POA coordinates of C57BL/6J mice, or MeA coordinates of $LepRb^{GFP}$ mice and 10 nl of a 2% FG solution was injected over 30 seconds. Ten minutes later, the injector was removed, the hole filled with bone wax and skin closed with sutures. Animals were allowed to recover on a heating pad and then single-housed in clean cages.

Four days after injection, animals were perfused and brains were removed as described. POA-injected C57BL/6J animals received 5 mg/kg i.p. leptin 2 hours before perfusion.

4.2.5 Electrophysiological slice preparation. Transverse brain slices were prepared from male and female $LepRb^{EGFP}$ mice at postnatal age 21–28 (prepubertal). Similar responses to leptin were observed in animals independent of age between 21 and 28 days. Animals were anesthetized with a mixture of ketamine and xylazine. After decapitation, the brain was transferred into a sucrose-based solution bubbled with 95% O_2-5% CO_2 and maintained at ~3°C. This solution contained the following (in mM): 248 sucrose, 2 KCl, 1 $MgCl_2$, 1.25 KH_2PO_4, 26 $NaHCO_3$, and 10 glucose. Transverse coronal brain slices (200 µM) were prepared using a Vibratome (Leica VT1000S). Slices were equilibrated with an oxygenated artificial cerebral spinal fluid (aCSF) for >1 h before transfer to the recording chamber. The slices were continuously superfused with aCSF at a rate of 2 ml/min containing the following (in mM): 113 NaCl, 3 KCl, 1 NaH_2PO_4, 26 $NaHCO_3$, 2.5 $CaCl_2$, 1 $MgCl_2$, and 5 glucose in 95% O_2/5% CO_2 at room temperature.

4.2.6 Electrophysiological recordings. Brain slices were placed on the stage of an upright, infrared-differential interference contrast microscope (Olympus BX50WI) mounted on a Gibraltar X-Y table (Burleigh) and visualized with a 40x water-immersion objective by infrared microscopy (DAGE MTI camera). Membrane potentials of EGFP-positive (LepRb-expressing) PMv neurons were recorded at

room temperature (25–26°C) to a PC after being filtered at 10 kHz by a Multiclamp 700B and analyzed using pClamp10 (Axon). The external solution contained the following (in mM): 113 NaCl, 3 KCl, 1 NaH_2PO_4, 26 $NaHCO_3$, 2.5 $CaCl_2$, 1 $MgCl_2$, and 5 glucose in 95% O_2/5% CO_2. CNQX (10 µM), DL-amino-phosphonovaleric acid (DL-AP-5, 50 µM), picrotoxin (100 µM) and strychnine (1 µM) were continuously present in the external solution to block synaptic inputs from glutamate, GABA and glycine. The internal solution contained the following (in mM): 115 K-acetate, 10 KCl, 2 $MgCl_2$, 10 EGTA, 10 HEPES, 2 Na_2ATP, 0.5 Na_2GTP, and 5 phosphocreatine. Pipette resistance ranged from 3 to 4 MΩ.

The effect of leptin (100nM) on membrane potential compared with control was analyzed using Student's *t* test (Origin 7.0). Responding neurons were divided from nonresponding neurons based on the criterion that the change in membrane potential induced by application of leptin was ±3 times the SD before treatment with leptin, as described in recent studies (118,158-160). Data were considered significantly different for $p < 0.05$. All statistical results are given as mean ± SEM.

4.2.7 Soiled bedding experiments. On day 0, adult (10-15 week old) male and female $LepRb^{GFP}$ mice were single-housed and designated to one of two groups: "fresh" bedding (n = 4 males, 3 females), or "soiled" bedding (n = 5 males, 3 females). On day 6, animals were brought to the lab to acclimate overnight. The following day, day 7, animals in the fresh group were moved to cages containing fresh bedding, whereas animals in the soiled group were moved to cages which

had previously individually housed a mouse of the opposite sex for 7 d. After 90 min of exposure, animals were perfused as described above. At the time of perfusion, estrus cycle stage was determined by vaginal histology (females), however all animals (regardless of stage) were used in analyses.

4.2.8 Microscopy and Image Analysis. Microscopic images were obtained using an Olympus BX-51 brightfield microscope with DP30BW camera (Olympus). For quantification of EGFP/pSTAT3-IR or EGFP/Fos-IR double-labeled neurons, pictures of the identical areas were taken on channels for Alexa 488 (EGFP), Alexa 568 (cFos), or brightfield (pSTAT3, cFos). Using Adobe Photoshop software (Adobe Systems), the brightfield channel was inverted (except in Figure 18) and false-colored red. Both channels (red and green) were merged in a red-green picture, and single- and double-labeled neurons were counted and recorded. [Immunolabeling of nitric oxide synthase-1 (NOS1) was used to define boundaries of the PMv for counting (Figure 11)]. Values are presented as mean ± SEM, and differences analyzed by Student's *t* test, or by one-way ANOVA followed by Tukey post-test, as indicated in the text. Differences were deemed significant for $p < 0.05$.

4.3 Results

4.3.1 Localization and Description of LepRb neurons in PMv.

Immunofluorescent detection of EGFP-IR in LepRb^{EGFP} mice revealed EGFP immunoreactivity (EGFP-IR) in a population of cells in the PMv, consistent with previous studies (81,83,84). Expression in other neighboring hypothalamic nuclei, such as VMH and DMH was observed, although distinct from the identified PMv subpopulation (Figure 4, Figure 11).

We found similar numbers of EGFP-IR cells in the PMv and the ARC (PMv: 4830 ± 200 per brain; *n* = 3; ARC: 4320 ± 330 per brain; *n* = 3). The well-known role of ARC LepRb neurons to leptin action and the similar size of the ARC and PMv LepRb populations suggest the importance of LepRb PMv neurons to leptin action (2-7). No gender-specific differences in cell number were observed for either of these nuclei (data not shown).

Colocalization of EGFP-IR in the PMv of LepRb^{EGFP} mice with the neuronal marker NeuN revealed that these LepRb PMv neurons comprise 44.6 ± 3.3% (*n* = 3) of the total number of PMv neurons (data not shown).

Activation of LepRb recruits STAT3 directly to the receptor to mediate STAT3 tyrosine phosphorylation (pSTAT3) (32,161). Although other growth factors and cytokines also regulate the phosphorylation of STAT3, the general level of immunohistochemically (IHC)-detectable pSTAT3 in the brain is low in the absence of leptin treatment, and the increase in pSTAT3-IR after leptin stimulation sensitively and reliably reveals cell-autonomous leptin action to identify neurons that express functional LepRb (86).

To confirm the expression of functional LepRb in the EGFP-containing PMv neurons in $LepRb^{EGFP}$ mice, we examined the colocalization of pSTAT3-IR with EGFP-IR in $LepRb^{EGFP}$ mice after treatment with vehicle or leptin. Only 1 ± 0.2% (*n* = 4) of EGFP-IR PMv cells contained IHC-detectable pSTAT3 in controls; 96 ± 0.2% (*n* = 3) of EGFP-IR neurons contained pSTAT3-IR in leptin-treated animals (Figure 12).

Thus, EGFP-containing PMv neurons in $LepRb^{EGFP}$ mice possess functional LepRb and these LepRb PMv neurons represent a subpopulation of the larger set of PMv neurons.

4.3.2 Direct Activation of PMv LepRb Neurons by Leptin

In order to understand whether leptin activates or inhibits LepRb PMv neurons, we used Fos-IR as an IHC marker of neuronal activity in EGFP-IR PMv neurons in *ad libitum*-fed $LepRb^{EGFP}$ mice treated for 4 h i.p. with leptin or vehicle, or with vehicle after a 24 h fast. Leptin stimulated the accumulation of Fos-IR in the majority of LepRb PMv neurons (Fed/PBS, 4 ± 2%; leptin, 69 ± 2%; *n* = 3 each condition; $p < 0.01$ by ANOVA followed by Tukey post-test) (Figure 13). In contrast to the ARC, in which fasting activates a population of EGFP-IR/LepRb neurons, fasting did not significantly alter PMv Fos-IR (Fasted, 2 ± 1%; *p* = n.s.) (Figure 14).

In order to rule out potential indirect actions of leptin on PMv LepRb neurons, such as via the regulation of classical neurotransmitter release from other LepRb neurons, we examined the activity of LepRb PMv cells in acute slice preparations from hypothalami of $LepRb^{EGFP}$ mice using whole-cell patch-clamp recordings from EGFP-identified neurons in the PMv. We measured the membrane potential of these cells in current clamp mode under conditions in which synaptic inputs from glutamate, GABA and glycine were blocked in order to eliminate indirect activation via these neurotransmitters.

Treatment with leptin depolarized ~67% of the LepRb PMv neurons tested (control: –65 ± 4 mV, plus leptin: –54 ± 5 mV; $p < 0.05$; $n = 8$ of 12 neurons) (Figure 13). The onset varied from ~60 to ~320 s after application of leptin (the mean onset time: 150 ± 35 s; $n = 8$), and the mean change in membrane potential was 11.1 ± 2 mV. Although some LepRb PMv neurons exhibited no significant response to leptin (control: n-69.6 ± 7 mV vs leptin: –69.7 ± 8 mV; $n = 4$), none were hyperpolarized by leptin. Thus, leptin acutely depolarizes LepRb PMv neurons independently of the presynaptic release of glutamate, GABA or glycine.

Given that a similar percentage of neurons were depolarized by leptin in electrophysiologic studies in slice preparations from prepubertal mice and by the criterion of Fos-IR *in vivo* in adult animals suggests that age and reproductive status do not affect the ability of leptin to activate LepRb PMv neurons, as well as suggesting the direct and physiologic activation of the majority of LepRb PMv

neurons by leptin. The uniformly high percentage of LepRb PMv neurons activated by leptin, and the absence of any leptin-stimulated hyperpolarization or fasting-mediated increased Fos-IR in these neurons further suggests that, in contrast to ARC LepRb neurons, LepRb PMv neurons represent a relatively uniform population of leptin-activated cells.

4.3.3 Activation of PMv LepRb Neurons by Sexual Odorants

Previous research describing activation of some PMv neurons after the presentation of sexual odorants suggested that LepRb PMv neurons might receive both odorant cues and leptin-mediated metabolic signals, thereby integrating this information in a single population of neurons (152,153). In order to determine whether the sexual odorant-responsive PMv neurons overlap with, or are distinct from the LepRb neurons in this region, we exposed $LepRb^{EGFP}$ animals to fresh bedding or bedding soiled by mice of the opposite sex and examined the activity of EGFP-containing LepRb PMv neurons by the criterion of Fos-IR. Exposure to soiled bedding from mice of the opposite sex increased the number of Fos-IR nuclei in the PMv of both males and females (females: fresh, 29 ± 11, n = 3; soiled, 296 ± 50, n = 3; p = 0.006) (males: fresh, 51 ± 29, n = 4; soiled, 156 ± 23, n = 5; p = 0.02). Fos-IR was not localized to any apparent subregion of the PMv, but appeared to be equally distributed throughout the area. Exposure to bedding soiled by a mouse of the same sex failed to elicit an increase in Fos-IR in the PMv (data not shown).

Similar to total PMv neurons, Fos-IR increased dramatically in the LepRb-expressing subpopulation of this region in odorant-exposed compared with fresh-bedding-exposed $LepRb^{EGFP}$ animals (females: fresh, 3 ± 2%, $n = 3$; soiled, 44 ± 2%, $n = 3$, $p = 0.0001$) (males: fresh, 4 ± 2%, $n = 4$; soiled, 18 ± 3%, $n = 5$; $p < 0.005$) (Figure 15).

Thus, LepRb PMv neurons are activated by metabolic cues via leptin and also by sexual odorant cues.

4.3.4 Projections of PMv LepRb Neurons

The overall connectivity of the PMv has been examined previously, however LepRb neurons comprise less than half of the total PMv neurons and therefore might exhibit restricted projection patterns compared with the entire PMv. Although using cytoplasmic EGFP expression in $LepRb^{EGFP}$ mice represents a reliable way to identify LepRb-expressing soma throughout the CNS, it poorly labels the distant projections of LepRb-expressing neurons.

We generated a novel targeted ROSA26 allele, *Gt(ROSA)26Sor*^{EGFPf}, in which cre recombinase-mediated excision of a transcription-blocking cassette induces the expression of a farnesylated EGFP (EGFPf); farnesylation drives EGFPf to the membrane, effectively labeling even very long axonal projections (162) (Figure 2). We crossed these *Gt(ROSA)26Sor*^{EGFPf} animals to

Lepr^{cre} mice to generate LepRb^{EGFPf} mice that express EGFPf in all LepRb neurons to facilitate the study of projections from these neurons.

We used brain sections from the LepRb^{EGFPf} mice to determine whether any LepRb-expressing cells innervated major projection targets of the PMv [the POA and the medial and posterior portions of the amygdala (144)], examining EGFP-IR (EGFPf-containing) projections from. This examination revealed copious diffuse EGFP-IR in the POA, consistent with the dense innervation of this region by LepRb neurons of an unknown neuroanatomical origin (Figure 16).

In contrast, whereas EGFP-IR projections from LepRb neurons were noted in the central nucleus of the amygdala (CeA) and in the nearby dentate gyrus (DG) of the hippocampus, little EGFP-IR was detectable in the medial and posterior portions of the amygdala of the LepRb^{EGFPf} mice, suggesting few LepRb neurons innervate this region (Figure 16). Although these data from LepRb^{EGFPf} mice reveal the general density of innervation of each region by LepRb neurons, this transgenic approach cannot distinguish the neuroanatomical source of any projections and thus cannot reveal projections specific to the PMv LepRb neurons.

To define projections from LepRb-expressing soma in specific brain regions, we used Ad-iZ/EGFPf, which merges the use of molecular tracers with the cre-inducible system (for LepRb-specificity) plus adenoviral stereotaxic injection (for anatomical specificity) (Figure 2). When transduced into cre-expressing cells, Ad-iZ/EGFPf mediates expression of EGFPf. Because this is a

replication-defective virus, only the neurons that initially take up this virus at the injection site will be infected. Hence, when Ad-iZ/EGFPf is injected into the PMv of *Lepr*^{cre} mice, EGFPf will be expressed only in LepRb neurons to mediate axonal tracing specifically from PMv LepRb neurons (avoiding tracing from non-LepRb neurons in the PMv).

After the injection of Ad-iZ/EGFPf into the PMv of *Lepr*^{cre} mice, injection sites displayed robust labeling of soma and local processes (Figure 17). No labeling was observed in control (non-cre-expressing) mice (data not shown). EGFPf-labeled fibers projected from the LepRb PMv neurons to the POA, including medial and lateral subregions, and AvPv. The appearance of bouton-like varicosities along labeled fibers in the POA and AvPv suggested the presence of synapses in these regions. Although some labeled fibers fell within the ventral border of the bed nucleus of the stria terminalis (BST), we did not detect significant projections from PMv LepRb neurons into the BST/ST or amygdala.

Thus, these results suggest that LepRb PMv neurons project primarily to the POA, and poorly innervate the amygdala.

Given the novelty of these EGFPf-based tracing systems, we used Fluorogold (FG) to perform retrograde tracing from the POA and MeA to confirm the LepRb PMv to POA circuitry as well as the paucity of LepRb PMv to MeA connections. We treated C57BL/6J mice with leptin for 2 hours before perfusion to examine the potential colocalization of pSTAT3 in LepRb PMv neurons with

the retrograde accumulation of FG from POA regions. Copious colocalization, visible as cytoplasmic FG around nuclear pSTAT3-IR was observed in the PMv of the animals examined, confirming the projection of LepRb PMv neurons into the POA (Figure 18).

We additionally injected LepRb^{EGFP} animals with FG into the MeA. FG-IR cells were observed in ipsilateral regions of the accessory olfactory bulb (data not shown), confirming that the targeted amygdala regions lie within the olfactory pathway. Although FG-labeled PMv cells were observed after the injection of FG into the MeA, these did not colocalize with EGFP-IR LepRb neurons (Figure 18).

Overall, these data confirm that LepRb PMv neurons project rostrally to innervate the POA, but poorly innervate other PMv projection targets, such as the MeA. LepRb PMv neurons densely innervate a subset of the regions innervated by the total population of PMv neurons, and the LepRb PMv neurons may mediate a specific subset of PMv functions.

4.3.5 PMv LepRb Neurons Synapse with GnRH Neurons

Although EGFPf- and FG-mediated tract tracing do not permit the identification of synaptic contacts, the projection of LepRb PMv neurons to brain regions containing GnRH neurons and the importance of the PMv for odorant-dependent LH release led us to hypothesize that LepRb PMV neurons directly

innervate GnRH neurons (154). We used a transgenic mouse line ("BIG") that expresses the trans-synaptic tracer, barley lectin, along with EGFP, in GnRH neurons, and which thus reveals the synaptic contacts of GnRH neurons by their accumulation of barley lectin [detected by immunoreactivity for the closely related lectin, wheat germ agglutinin (WGA)] (157).

The analysis of BIG mice revealed a large population of PMv neurons positive for WGA-IR and thus in synaptic contact with GnRH neurons (157). The absence of GnRH-IR axonal fibers in the PMv reveals that these WGA-IR PMv neurons lie afferent to (as opposed to efferent of) GnRH neurons (157) (data not shown).

To examine whether and which LepRb neurons might synapse directly onto GnRH neurons, we treated BIG mice with leptin (5 mg/kg i.p., 1 h) to determine the potential colocalization of cytoplasmic WGA-IR around pSTAT3-IR nuclei in the PMv. This analysis revealed that many WGA-IR PMv neurons in these animals express LepRb by the criterion of leptin-stimulated pSTAT3-IR, and conversely, that many pSTAT3-IR LepRb neurons in the PMv contain WGA-IR. No WGA-IR was detected in nontransgenic animals (Figure 19).

Thus, LepRb PMv neurons not only project to the POA/AvPv, but many LepRb PMv neurons synapse directly on GnRH neurons.

4.4 Discussion

Prioritization of physiological functions based on energy availability requires continuous processing of inputs as to the status of the body and environment. In 1974, Frisch and McArthur proposed the "critical weight hypothesis," linking energy stores to fertility by suggesting that a threshold level of body fat is required in order for females to achieve menarche and to maintain normal ovulatory cycles (163). Indeed, in normal weight women, a 10–15% decrease in body weight results in the interruption of normal ovulation and menstrual cycles due to decreased GnRH secretion by the hypothalamus (hence, "hypothalamic amenorrhea") (164-166). Since these early studies, much progress has been made in detailing mechanisms controlling the reproductive axis and energy balance individually, although the mechanisms by which these systems are integrated have remained unclear. Leptin acts via LepRb in the brain to regulate energy balance and reproduction, suggesting that LepRb-expressing neurons link fat mass and reproductive competence (36,131,133).

One substantial population of LepRb-expressing cells lies in the PMv, a region known to contain gonadal steroid receptors and to be activated by mating and sexual sensory inputs, as well as leptin, thus representing a potential site for the integration of reproductive and metabolic cues (150-153,167-170). Although the PMv as a whole has been investigated to some extent, the LepRb-expressing subpopulation of PMv neurons has remained little-studied.

Utilizing $LepRb^{EGFP}$ mice (which express EGFP specifically in LepRb-expressing cells) combined with leptin-stimulated pSTAT3-IR, we confirmed the

previously reported presence of functional LepRb in a subset of PMv cells. Although previous studies have also demonstrated increased Fos-IR in the PMv after leptin administration (82), the EGFP expression of LepRb neurons in the $LepRb^{EGFP}$ animals enabled us to examine the regulation of the LepRb PMv neurons specifically. We showed the colocalization of leptin-stimulated Fos-IR specifically in PMv LepRb neurons, and that leptin activates the majority of LepRb PMv neurons by this criterion. Direct electrophysiologic recordings from LepRb PMv neurons revealed the leptin-stimulated depolarization of a similarly high percentage of cells in acute slice preparations as was observed using Fos-IR to indirectly indicate activity *in vivo*. This leptin-stimulated depolarization was independent of transmission by the common amino acid neurotransmitters glutamate, GABA and glycine. Thus, these data demonstrate that leptin activates LepRb PMv neurons by direct action.

Previous studies of Fos-IR have revealed PMv activation after mating and estrogen or progesterone stimulation (with females responding to a greater degree) (151), as well as in response to odorant-containing bedding soiled by the opposite sex (152,153). These and other studies have placed the PMv behind both MeA and BST, but before the GnRH neurons in the POA in the sequence of stimulation beginning with sexual odorants and ending in rise of serum LH (152-154,171,172). Consistent with these previous reports in rats, Fos-IR increases in the PMv of both male and female mice exposed to opposite sex-derived odors in soiled bedding; this included a substantial population of LepRb PMv neurons, revealing the integration of odorant and metabolic (leptin) cues by these neurons

(Figure 20). Although we additionally observed soiled bedding-stimulated Fos-IR in other regions within the vomeronasal circuit, including the MeA, we did not detect the induction of Fos-IR in LepRb neurons elsewhere in the brain (data not shown), suggesting that LepRb PMv neurons represent the unique site for the integration of sexual odorant cues with leptin-mediated signals of energy balance.

To gain some insight into the potentially unique functions of the LepRb PMv neurons, we used two novel cre-inducible EGFPf-dependent tracing systems to examine projections from LepRb neurons into PMv projection targets. Previous tracing studies that examined the overall population of PMv neurons identified ascending projections to the POA and AvPv, and to the medial and posterior portions of the amygdala (144). EGFPf-containing projections from transgene-labeled LepRb neurons in $LepRb^{EGFPf}$ mice revealed dense projections into the POA/AvPv and a few regions of the amygdala [including the CeA, which is not innervated by the PMv (144)], but showed sparse innervation of the medial and posterior aspects of the amygdala that are targets of some PMv neurons. Indeed, Ad-iZ/EGFPf-mediated tracing specifically from LepRb PMv neurons revealed their projection to the preoptic region, including the POA and AvPv. In each of the regions with labeled processes, the appearance of varicosities/boutons suggested synapses at these locations. Although a few LepRb PMv neurons projected to the ventral BST, these neurons did not significantly innervate the amygdala. Similarly, whereas retrograde tracer applied to the POA accumulated in LepRb PMv neurons, these LepRb neurons did not accumulate retrograde tracer from the MeA.

Thus, LepRb PMv neurons contribute to a specific subset of the circuitry of the larger PMv, and LepRb PMv cells may thus participate in only a portion of PMv functions. The MeA processes sexual olfactory cues before relaying them to areas including the PMv, and the absence of projections from the LepRb PMv neurons to the MeA suggests that the LepRb PMv neurons receive odorant information, integrate it with metabolic information, and relay it forward to regions that govern reproduction, but do not contribute to the processing of pheromonal signals in the MeA itself. LepRb PMv neurons are thus well positioned to integrate sensory sexual and hormonal metabolic cues, and could function to regulate the reproductive axis based on availability of food and mates.

Indeed, our data using leptin-treated BIG mice demonstrate LepRb PMv cells lying upstream of GnRH neurons. Given the function of the PMv in integrating sexual odorant cues and the projection of LepRb PMv neurons to the POA, and specifically to GnRH neurons, along with the reported glutamatergic nature of the PMv (173), we hypothesize that these cells might function to integrate sexual cues with the leptin-mediated signal of energy status. Other mechanisms, including the regulation of kisspeptin-containing neurons by leptin (174,175), could also contribute to the metabolic regulation of reproduction. Future studies will be necessary to fully characterize the specific physiological roles of leptin in these circuits.

Chapter 5

LepRb deletion in cells expressing Nitric Oxide Synthase-1[††]

5.1 Introduction

Our aim to characterize the role of leptin action on PMv cells led us to pursue PMv-specific deletion of LepRb. While the majority of PMv-specific study of LepRb neurons has encompassed anatomical circuitry and processing of sexual odorants, a recent study by Donato *et al.* used bilateral excitotoxic lesioning of the PMv in adult female rats in order to assess reproductive and energy homeostasis parameters (176). This group concluded that leptin regulation of these processes involves at least partial anatomic separation, with the PMv mediating the majority of reproductive, but not energy homeostasis effects. The authors followed their PMv-lesioned animals to seven weeks post-surgery and observed in lesioned mice an acute disruption in estrus cycling (to 20 days post-surgery) with no overall alterations in body weight or food intake, except moderate differences in food intake during the proestrus→estrus transition. In addition, after surgery recovery, animals were euthanized during proestrus and found to have a decrease in activity of anteroventral periventricular and GnRH cells by the criterion of Fos-IR. While the effect on estrus cycling was

[††] Preparation of the Nos1-Cre construct as described in this chapter (section 5.2.2, Figure 22) was performed by Y. Gong

transient, ovarian histology revealed an overall decrease in the number of antral follicles in PMv-lesioned animals. Furthermore, lesions prevented normal leptin-stimulated increases in luteinizing hormone, suggesting leptin action at this site in regulating GnRH cells.

In order to fully examine the effects of chronic PMv LepRb deficiency, (as opposed to acute knockdown or deletion experiments), we sought candidate genes specifically colocalized in PMv LepRb cells which we could employ in cre-loxP mediated deletion of LepRb. In previous studies of the PMv, we habitually employed immunolabeling of nitric oxide synthase-1 (Nos1, nNOS; NOS1-IR) neurons as an anatomical marker defining the borders of the PMv (Figure 11). The nitric oxide synthases (NOS) appear in three known forms (177,178). NOS-1, is constitutively expressed and has been identified in neurons, astrocytes, neutrophils, skeletal muscle and testis. NOS-2, or inducible NOS (iNOS) is mostly found in immune cells and, as the name implies, expression is not constitutive. NOS-3, or endothelial NOS (eNOS) is constitutively expressed, found in endothelial cells and plays roles in vasodilation. The full-length human NOS-1 gene contains 29 exons, however there are several known splice variants, only 4 of which retain normal catalytic function (177,178). NOS-1 has been associated with regulation of the reproductive axis and, using both immunoreactivity as well as an assay of activity (NADPH diaphorase histochemistry), NOS1-expressing cells have been identified in the PMv of rats (179,180).

In the 1990s, Huang *et al.* created their first NOS-1 knockout mouse by deleting exon 2 of the NOS1 gene (181). It was subsequently discovered that by merely deleting exon2, this first knockout, (termed knockout 1, or KN1), only eliminate the NOS-1 alpha isoform, leaving several other isoforms with catalytic activity. The deletion produced mice with enlarged stomachs due to pyloric stenosis, and males exhibited increased aggression by several measures of aggressive behavior, both toward other males as well as females (181,182). No changes in serum testosterone were detected, as well as no deficits in general odor detection, alterations in strength, or anxiety.

Huang's group next generated the second NOS1 knockout, or KN2, deleting exon 6, resulting in removal of all NOS-1 isoforms (183). These mice displayed small gonads, fewer corpora lutea in the ovaries, and sexually dimorphic alterations in gonadotropins in addition to the pyloric stenosis also seen in KN1. In contrast to KN1 hyperaggressive males, which inappropriately mounted female mates, KN2 males mounted females at a decreased rate, and KN2 females showed less frequent litters upon mating with wildtype males.

NADPH diaphorase histochemistry on KN1 brain sections revealed loss of labeling in the PMv, indicating that Nos1 alpha is the predominant isoform in the PMv (184) (Figure 21). In order to determine whether NOS-1 was expressed in PMv LepRb cells, as well as its expression in other leptin-responsive populations, we treated C57BL/6J mice with leptin (5mg/kg i.p., 4 hours) and observed NOS1-IR in the majority of PMv cells with leptin-induced pSTAT3-IR

(93.8 +/- 1.1%, n=3) (Figure 21). More than 50% of PMv NOS-IR cells had pSTAT3-IR nuclei (62.8 +/-1.1%. n=3). We did not observe substantial colocalization of NOS1-IR and pSTAT3-IR in any other brain regions, suggesting that LepRb PMv neurons comprise the sole LepRb population with considerable expression of *Nos1*.

In order to examine the role of leptin action at the PMv, we generated a mouse line in which cre recombinase is expressed from the *Nos1* locus (Figure 22). We used these animals mated to mice in which a portion of exon 17 of the lepr gene is floxed in order to specifically delete LepRb in cells that express both LepRb and NOS1. Based on the known functions of the PMv as a whole, the effects of leptin on the reproductive axis, as well as our previous data demonstrating leptin activation of cells at this site, we hypothesized that removal of LepRb from the PMv would result in decreased fertility in these animals, evident as disrupted estrus cycling. However, based on the wealth of research pointing to the role of Kisspeptin (KiSS-1) neurons as mediators of leptin action on puberty onset, and the expression of KiSS-1 in the ARC and AvPv, but not PMv, we hypothesized that our *Nos1*^{cre};lepr$^{\Delta/flox}$ experimental animals would exhibit normal onset of puberty (174,175).

We observed a small, but consistent number of LepRb-expressing cells outside the PMv (e.g. DMH), which co-express NOS1-IR (data not shown). LepRb deletion in these cells may cause effects related to the known roles of

leptin at these sites, effects which are not attributable to PMv deletion; we therefore expect a mild increase in body weight.

While the characterization of these mice is in its infancy, and more detailed analysis is currently underway and/or anticipated (see Figure 24) our preliminary results reveal that compared to our control animals, *Nos1*^{cre};lepr$^{\Delta/flox}$ show normal vaginal opening (data not shown), however age at first estrus is delayed (Figure 27). *Nos1*^{cre};lepr$^{\Delta/flox}$ also show obesity, however this manifests later than is observed in mice with systemic deletion of leprb (*Nos1*^{cre};lepr$^{\Delta/\Delta}$) (Figure 25). In addition, whereas *Nos1*^{cre};lepr$^{\Delta/\Delta}$ mice are overtly diabetic, *Nos1*^{cre};lepr$^{\Delta/flox}$ are euglycemic (Figure 26).

5.2 Methods

5.2.1 Materials. Chicken anti-EGFP was purchased from Abcam, rabbit anti-NOS-1 was from ImmunoStar and rabbit anti-pSTAT3 was from Cell Signaling. Normal donkey serum (NDS) and biotinylated donkey anti-rabbit were purchased from Jackson ImmunoResearch. Alexa 488-conjugated goat anti-chicken and Alexa 568-conjugated donkey anti-rabbit were purchased from Invitrogen. ABC Vectastain Elite kit was purchased from Vector Laboratories. Nitroblue tetrazolium (NBT) was from Roche and beta-NADPH was from Calbiochem. All other immunohistochemical supplies were purchased from Sigma-Aldrich.

5.2.2 Animals. All mice were bred in our colony in the Unit for Laboratory Animal Medicine at the University of Michigan. All animals and procedures used were in accordance with the guidelines and approval of the University Committee on the Care and Use of Animals. *Gt(ROSA)26Sor*^{tm2Sho} (*ROSA*^{EGFP}), *B6;129S4-Nos1*^{tm1Plh}*/J* (KN1) and *C57BL/6J* mice were purchased from The Jackson Laboratory. Animals were given *ad libitum* access to food and water, and were housed in groups of 2–4 except where indicated. The previously described Lepr$^{flox/flox}$ mice were generously provided by Dr. Streamson Chua and were propagated in our colony (185).

Since transgenic strategies for cre expression often result in ectopic or poor overlap of expression with the endogenous gene in a significant percentage of founders/lines (even in the case of BAC transgenics), we opted to express cre from the *Nos1* locus by homologous targeting. In our targeting construct (Figure 22) we amplified genomic sequences derived from the 3'-end of *nos1* (including exon 25, the final exon of this gene) and inserted the IRES-Cre cassette from our *Lepr*^{cre} targeting vector between the STOP codon and polyadenylation site at the 3'-end of the final exon. The Neo selection cassette is flanked by FRT sites for Flp-mediated removal instead of being floxed for removal by Cre (since successful targeting of the cre recombinase could theoretically delete the neo cassette and prevent the selection of the cells).

We utilized PCR from R1 ES cell DNA and primers designed from the Nos1 locus (obtained from Genebank sequences) to generate a 6 kb fragment containing the mouse genomic sequence centered on the STOP codon in the

final (3') exon of Nos1. This fragment was TOPO cloned into pCR2.1. Quikchange mutagenesis was utilized to introduce an AscI site in place of a NotI site 60 bp 3' to the STOP codon, and an AscI fragment containing the sequences IRES-Cre-Frt-Neo-Frt was inserted into the new AscI site to generate pCRNos1-IRES-Cre-Frt-Neo-Frt. The entire insert was then excised using NotI and NheI and inserted into NotI/XbaI-cut pPNT backbone to generate pPNT-Nos1-IRES-Cre for targeting.

The construct was linearized with NotI, and we utilized the University of Michigan transgenic animal model facility for electroporation of the construct into ES cells and subsequent selection (http://www.med.umich.edu/tamc). For the initial screening, we used Taqman-based qPCR screening to identify correctly targeted clones, as we have recently done for other loci (156), followed by Southern blotting for final confirmation. Correctly targeted ES cells were then injected into blastocysts to generate chimeras, which were bred to C57Bl/6 animals to determine germline transmission. In order to anatomically compare cre expression with antibody detection of Nos1 cells, we bred our *Nos1*^{cre} mice with the previously described *ROSA*^{EGFP} animals to generate *Nos1*^{cre};*ROSA*^{EGFP} (Nos1^{EGFP}) animals.

Nos1^{cre} animals were further mated with Lepr$^{flox/flox}$ mice. Due to the periodic expression of cre during gametogenesis, *Nos1*^{cre};lepr$^{\Delta/+}$ (whole-body deficiency of one allele of lepr) mice were produced. We bred the *Nos1*^{cre};lepr$^{\Delta/+}$ animals to Lepr$^{flox/flox}$ mates in order to obtain experimental (*Nos1*^{cre};lepr$^{\Delta/flox}$) and

control (*Nos1*^{cre};lepr$^{+/+}$, lepr$^{\Delta/flox}$, *Nos1*^{cre};lepr$^{\Delta/\Delta}$) animals. Genotyping was performed by PCR as described in Balthasar *et al*. and in Figure 22 (185).

5.2.3 *Perfusion and immunolabeling.* Adult male and female mice were perfused and brains sectioned as described in section 2.2.3. IF/IHC was performed as detailed in section 3.2.4, using the following primary antibodies: anti-EGFP, 1:1000; anti-Nos1, 1:1000, anti-pSTAT3, 1:1000. Sections were mounted onto Superfrost Plus slides (Fisher Scientific) and coverslipped with ProLong Antifade mounting medium (Invitrogen).

For NADPH diaphorase histochemistry, fixed brain sections were washed in 0.2M PBS, pH 7.4, then incubated at 37°C overnight in 1mg/ml beta-NADPH and 0.2 mg/ml nitroblue tetrazolium prepared in dH_2O. The histochemical reaction was stopped using 100mM sulfuric acid and sections were mounted onto slides and coverslipped as described for IF/IHC.

5.2.4 Microscopy and image analysis. Microscopic images were obtained using an Olympus BX-51 brightfield microscope with DP30BW camera (Olympus). Cell counts were performed using Adobe Photoshop software and values are presented as mean ± SEM, with differences analyzed by one-way ANOVA followed by Tukey post-test. Differences were deemed significant for $p < 0.05$.

5.2.5 Phenotypic Studies. Female mice for study were housed individually from the time of weaning at 21 days old. Beginning at 28 days of age, body weight and chow (Purina Lab Diet #5001) weight were monitored weekly. Biweekly, blood was collected for serum via tail nicks, and blood glucose was measured with a glucometer. Mice were monitored daily for vaginal opening and then for vaginal estrus by cellular histology through three cycles, or until 12 weeks old. All data were collected between 14:00 and 16:00 and are reported as means +/- SEM, with differences analyzed by Students *t* test, or one-way ANOVA followed by Tukey post-test as indicated. Differences were deemed significant for $p < 0.05$. All phenotypic data described are exclusively from female animals.

5.3 Results

In order to determine the role of LepRb signaling in the PMv, we first generated mice in which cre recombinase was inserted into the Nos1 locus ($Nos1^{Cre}$ mice) by homologous recombination (Figure 22); thus cre expression is limited to cells expressing Nos1. In order to confirm cre activity and to compare expression to antibody labeling of Nos1 cells, we mated $Nos1^{Cre}$ animals to $ROSA^{EGFP}$ reporter mice (described in section 2.2.2) in order to induce EGFP expression in Nos1-expressing cells ($Nos1^{EGFP}$ mice). EGFP-IR overlapped with NOS1-IR in all regions examined, with labeling in $Nos1^{EGFP}$ mice revealing slightly more soma in most regions (Figure 23).

We additionally treated male and female Nos1^{EGFP} mice with leptin (5mg/kg ip, 2hours) in order to examine colocalization of leptin-induced pSTAT3 in cells with EGFP-IR both within the PMv as well as in other hypothalamic regions. Colocalization of EGFP-IR and pSTAT3 in the PMv of Nos1^{Cre} mice revealed that the majority of leptin-responsive PMv cells contain Nos1 (82.7 ±7.2% n=3 mice) compared to leptin-responsive cells of the ARC (5.7 ±1.1%, n=4), DMH (18.4 ±3.2%, n=3), VMH (9.4 ±0.4%, n=3) or LHA (12.3 ±1.8%, n=3) (Figure 23).

We next crossed our Nos1^{Cre} mice to lepr$^{flox/flox}$ mice in which a portion of exon 17 of the *lepr* gene is floxed in order to specifically inactivate LepRb in cells expressing both LepRb and NOS1 (Figure 22). The intermittent expression of cre during gametogenesis causes the occasional occurrence of *Nos1^{cre}*;lepr$^{\Delta/+}$ animals which produces systemic deficiency of one allele of lepr. We therefore bred *Nos1^{cre}*;lepr$^{\Delta/+}$ animals to Lepr$^{flox/flox}$ mates in order to obtain experimental (*Nos1^{cre}*;lepr$^{\Delta/flox}$) and control (*Nos1^{cre}*;lepr$^{+/+}$, lepr$^{\Delta/flox}$, *Nos1^{cre}*;lepr$^{\Delta/\Delta}$) animals. While future studies will utilize *Nos1^{cre}*;lepr$^{\Delta/+}$ control animals, at the time of the described studies these data were unavailable, therefore *Nos1^{cre}*;lepr$^{+/+}$ results were included in their place.

We initially formulated a study paradigm in which mice were weaned to single-housing at 21 days, with the data collection beginning the following week, at 4 weeks old, and continuing through 12 weeks of age (Figure 24). Our initial cohort of animals revealed a significantly increased body weight in

Nos1^{cre};lepr$^{\Delta/flox}$ females compared to controls, beginning at 6 weeks old (*Nos1*^{cre};lepr$^{\Delta/flox}$ 31.4 ±2.9 grams n=3, *Nos1*^{cre};lepr$^{+/+}$ 20.6 ±0.4 grams n=3, lepr$^{\Delta/flox}$ 23.8 ±0.8 grams n=7, *Nos1*^{cre};lepr$^{\Delta/\Delta}$ 36.4 ±1.5 grams n=4))($p<0.05$ *Nos1*^{cre};lepr$^{\Delta/flox}$ versus lepr$^{\Delta/flox}$) (Figure 25). The occurrence of significantly increased body weight was delayed in *Nos1*^{cre};lepr$^{\Delta/flox}$ females compared to controls with total LepRb deficiency (*Nos1*^{cre};lepr$^{\Delta/\Delta}$), becoming equivalent to *Nos1*^{cre};lepr$^{\Delta/\Delta}$ animals at 6 weeks old (Figure 25).

While food intake did not initially differ between *Nos1*^{cre}*;lepr*$^{\Delta/flox}$ and *lepr*$^{\Delta/flox}$, or *Nos1*^{cre}*;lepr*$^{+/+}$ control animals at the outset, weekly chow consumed by *Nos1*^{cre}*;lepr*$^{\Delta/flox}$ increased concomitant with the observed increase in body weight. Significant differences were measured beginning during the 5→6 week interval (*Nos1*^{cre}*;lepr*$^{\Delta/flox}$ 48.0 ±5.3 grams/week n=3, *Nos1*^{cre}*;lepr*$^{+/+}$ 28.8 ±2.2 grams/week n=3, *lepr*$^{\Delta/flox}$ 34.6 ±1.8 grams/week n=7, *Nos1*^{cre}*;lepr*$^{\Delta/\Delta}$ 92.1 ±5.9 grams/week n=4) ($p<0.05$ *Nos1*^{cre}*;lepr*$^{\Delta/flox}$ versus *lepr*$^{\Delta/flox}$) (Figure 25). However, *Nos1*^{cre}*;lepr*$^{\Delta/flox}$ mice consistently ate less each week than did *Nos1*^{cre}*;lepr*$^{\Delta/\Delta}$ animals.

Interestingly, whereas *Nos1*^{cre}*;lepr*$^{\Delta/flox}$ mice became obese, consuming more chow per week than control littermates, these mice did not display hyperglycemia, though the equally obese , all *Nos1*^{cre}*;lepr*$^{\Delta/\Delta}$ animals became hyperglycemic by 6 weeks of age (Figure 26).

With the proposed role for LepRb and the PMv in regulation of the reproductive axis, we assessed two parameters of reproductive development and

capability: vaginal opening (VO) and onset of vaginal estrus (VE). Day of vaginal opening did not differ between groups in this cohort (data not shown). Onset of estrus as assessed by cellular histology significantly differed between control and experimental animals, with *Nos1^{cre};lepr$^{\Delta/flox}$* mice showing a delayed onset (*Nos1^{cre};lepr$^{\Delta/flox}$* 64.3 ±10.3 days n=3, *Nos1^{cre};lepr$^{+/+}$* 41.8 ±1.7 days n=3, *lepr$^{\Delta/flox}$* 37.3 ±1.1 days n=7, no *Nos1^{cre};lepr$^{\Delta/\Delta}$* animals entered estrus n=4) (Figure 27).

These preliminary data demonstrate that deletion of LepRb from Nos1-expressing cells, the majority of which lie in the PMv, cause delayed-onset obesity, increased food intake and delayed estrus in female mice.

5.4 Discussion

Ob/ob and *db/db* mice first established the effect of deficiencies in leptin signaling on whole animal physiology, however animal models in which leptin action is specifically deleted from discrete populations of neurons are useful tools with which to elucidate the relative contribution of each population to the overall physiological and behavioral effects of leptin signaling.

By specifically deleting Lepr from NOS1-expressing cells in our *Nos1^{cre}*;lepr$^{\Delta/flox}$ animals, we reduce leptin deficiency to the PMv (in addition to some deletion in other hypothalamic regions), and allow specific inquiry as to whether leptin action at the PMv contributes to the reproductive defects observed in rodent and humans with deficient leptin signaling (133,138-141). While our results presented here are undoubtedly preliminary, with increases in animal

numbers and additional analyses yet to come, we can begin to presume a role for the LepRb PMv neurons in the regulation of the reproductive axis, as our *Nos1^{cre};lepr$^{\Delta/flox}$* mice exhibit delayed onset of estrus, as well as in the regulation of body weight.

In current and future studies, we will explore the reproductive capabilities of our *Nos1^{cre}*;lepr$^{\Delta/flox}$ animals by mating them to C57Bl/6 mice in order to determine ability to reproduce with normal frequency of litters as well as size of litters. We are currently collecting tissue and serum samples with which we will be able to examine gonad morphology and histology as well as serum for analyses of hormone levels. Furthermore, we will follow estrus cycling in our experimental animals in order to determine whether they display disruptions in normal estrus cycling in addition to estrus onset deficiencies.

While leptin regulation of the reproductive axis includes permissive actions on reproductive development, we did not expect, nor observe differences in time of vaginal opening (an indicator of onset of reproductive competence in rodents) in our animals (132). This agrees with recent data from Donato *et al.* in which PMv lesions resulted in no changes in KiSS-1 expression, a proposed modulator of puberty in rodents (174-176).

The delayed-onset obesity observed in our animals may be PMv-independent and caused by the deletion of *Lepr* from other hypothalamic areas. We will further assess metabolic parameters as these mice undergo body composition analysis as well as determination of oxygen consumption and locomotor activity using the Comprehensive Laboratory Animal Monitoring

System (CLAMS, Columbus Instruments). It is interesting to note that the body weight and food intake changes in this first cohort appears to occur around the time of normal onset of reproductive competence, suggesting the phenotype may perhaps be partly attributable to gonadal hormone imbalances. Future studies involving gonadectomy in these animals may reveal the vailidity of this hypothesis. Additionally, the deletion of *Lepr* in a portion in of DMH cells warrants careful examination of the stress axis in these animals.

Further experiments will additionally phenotypically examine male mice, though insufficient numbers of animals preclude this analysis at present. Moreover, we are currently crossing our *Nos1*^{cre};*lepr*$^{\Delta/flox}$ and control animals to the ROSA^{EGFP} background (described in section 2.2.2) in order to facilitate immunohistochemical examination of leptin-responsiveness in cre-expressing neurons of these animals.

Thus, our findings that deletion of *Lepr* from NOS1-expressing cells results in abnormal estrus and delayed-onset obesity are supportive of the proposed actions of leptin at the PMv, and potentially also attributable to additional deletion in extra-PMv LepRb neurons. Current and future studies of these animals will more completely elucidate the specific role of leptin in these cells.

Chapter 6

Summary and Conclusions

The physiological mechanisms underlying the regulation of energy homeostasis have been studied to varying degrees throughout history. The fact that this area of research is even now a dominant and growing field points to both its perpetual relevance, connection to modern health issues and overall complexity. While much progress has been made in understanding the mechanisms underlying hunger and satiety, an excess of unknowns and ensuing questions remain.

Research of the hormone leptin embodies a great deal of progress made in obesity research, and has also highlighted the tremendous complexity of body weight dysregulation. While leptin action does not comprise the totality of the pathways that regulate energy balance and associated processes, it represents a major component (2-7). It is therefore fundamentally necessary to define regions of leptin regulation and the physiological effects common or unique to leptin action at each site.

Although various studies have emerged demonstrating anatomical sites of leptin action, detection of LepRb-expressing cells was limited by the technology

available at the time, the relatively low expression of LepRb *in vivo* and the existence of non-signaling short *LepR* isoforms confounding results (80-84). We therefore generated a novel mouse model in which expression of the reporter EGFP is limited to cells expressing LepRb (LepRb^{EGFP} mice). These mice permit the complete mapping of sites of LepRb expression as well as the determination of leptin-responsiveness in the labeled cells. We used LepRb^{EGFP} mice to first generate a comprehensive map of sites of observed EGFP-IR and then to further determine leptin responsiveness, colocalization with other signaling proteins as well as anatomical circuitry of two sizeable populations of LepRb-expressing cells, those within the midbrain and PMv. Our initial characterization of EGFP-IR cell populations in LepRb^{EGFP} mice (Chapter 2) are by no means meant to serve as a quantitative report of LepRb population sizes, but rather a qualitative description of spatial distribution and relative abundance. Our designation of specific brain regions, while based on the widely-utilized Paxinos and Franklin atlas of the mouse brain (186), may be improved by the use of a counterstain in order to precisely define neuroanatomical boundaries.

The midbrain, and specifically the VTA and RLi have been broadly associated with drug reward and addiction and more recently with hedonic drives to feed, through their association with the mesolimbic dopamine (MLDA) reward system (106,111,116,118,119). In line with the identified general links to dopamine signaling and the MLDA, we demonstrated that a significant portion of

LepRb-expressing cells in the midbrain are dopaminergic. In addition, whereas previous reports have proposed the projection of LepRb VTA neurons to the NAc and amygdala (118,119), we show that the majority of LepRb afferents to the NAc arise in the RLi, though both LepRb VTA and RLi cells innervate the amygdala. In addition, we reveal LepRb projections originating in the lateral hypothalamus (LHA) that project to the VTA, providing a second means by which leptin may regulate the MLDA. Our studies described here are meant to focus on the circuitry and dopaminergic nature of midbrain LepRb neurons. Our analyses were able to show bouton-like varicosities in CeA, IPAC and NAc, suggesting synaptic terminals at these sites, however co-labeling using a synaptic marker, such as synaptophysin, or the use of a transsynaptic tracer would confirm synaptic contact at these regions.

These results are the first description of LepRb-specific VTA and RLi circuitry and will bring about future studies further characterizing leptin action on these midbrain populations as well as their molecular and behavioral downstream effects. As we have shown that the majority of VTA/RLi LepRb projections terminate in central and extended amygdalar regions (CeA, IPAC), it will be important to now determine the functionality of this circuit. These regions as a whole have been well-examined, and assigned roles in “wanting”-associated stress as well as aversive conditioning. Therefore, subsequent hypotheses and experiments may focus on midbrain leptin regulation of stress or conditioning associated with reward motivation. Specific activation or silencing of leptin

signaling at this site followed by analysis of anxiety-like behaviors or response to taste conditioning may reveal midbrain LepRb regulation.

Traditional notions of energy balance regulation by leptin have focused on central homeostatic pathways, wherein hunger is determined simply by the need for, or excess of peripheral energy stores. However, the brain is an integrating center, where an immense amount of information must be incorporated in order to determine the most appropriate response. In the case of energy balance, this includes not only physiological need, but also previous rewarding or aversive experiences associated with the food or situation. The preponderance of palatable foods in modern societies and the common occurrence of feeding in times of physiological satiety highlight the hedonic side of feeding. This drive closely parallels those associated with customarily taboo addictions, such as drugs, in both behavior and neural systems. Though it may largely account for the failure of most weight-loss diet plans, food reward and the hedonic drives to feed as areas of research have only recently become prevalent in discussions of weight control. Our investigation into leptin action within the known reward pathways, as well as the research of others in the field will provide important tools in a comprehensive understanding of feeding regulation in order to treat the hedonic components of excessive feeding.

Similar to the previously described midbrain cells, leptin action at the ventral premammillary nucleus of the hypothalamus (PMv) is not attributed to the

direct regulation of energy homeostasis, but rather to physiological responses to the status of the body's energy supply (176). The PMv as a whole is implicated in regulation of the reproductive axis as well as integration of sensory information, specifically from olfactory and stress systems (144,148-154,173,176). Notable research has also demonstrated leptin action at this site as well as the recent report that the PMv mediates leptin-induced changes in secretion of luteinizing hormone (82,176).

We sought to define leptin regulation of this site, first determining that leptin activates the majority of cells in this PMv population. We further demonstrated that opposite sex odorants also activated a smaller, but significant population of LepRb PMv cells. We localized the afferent projections of the POA, with selected direct innervation of GnRH neurons. In order to advance our studies to include the physiological ramification of LepRb deficiency at this site, we generated the $Nos1^{Cre}$ mice which, when crossed with $Lepr^{flox}$ animals resulted in deletion of *lepr* in cells expressing *Nos1* (the majority of which reside in the PMv). In agreement with our hypothesis, we found defects in normal estrus onset in our experimental animals. The delayed-onset obesity observed may be a direct result of lack of leptin signaling at the PMv, or may more likely be due to the sporadic deletion of *lepr* in cells in other hypothalamic regions. Future studies will aim to clarify the origins of each phenotype and provide additional information as to the extent of extra-PMv LepRb deletion. Specifically, leptin administration, and subsequent analysis of leptin-induced pSTAT3 will allow us to determine the extent to which leptin signaling is disrupted in various

populations. We will also explore the euglycemia in our experimental animals using more stringent assays of glucose handling, such as glucose tolerance test. While we have shown a delay in the onset of first estrus, it will be important to determine if subsequent estrus cycling is normal by continuing daily vaginal histological analyses through several cycles. In addition, we will determine complete reproductive competence by mating our experimental mice with control partners to ascertain ability to maintain a pregnancy and lactate (females) or to impregnate a mate (males). As the PMv is associated with reproductive behaviors (in addition to competence) we may assay social behaviors such as aggression and submission. Finally, as we have shown activation of PMv LepRb cells by opposite-sex odors, it will be important to determine whether this PMv activation, as well as the normally observed odorant-induced increase in LH, are preserved when leptin signaling is absent in Nos1 neurons.

The overlap of signals regulating energy status with those involved in reproductive competence represents an important evolutionary adaptation. The brain, as master regulator of the body, must ascertain the current state of body and environment in order to determine benefit or liability of nonessential physiological processes. For example when body energy stores are inadequate, the brain will prioritize energy expenditure on food-seeking, suspending energy-expensive axes such as reproduction. Halting the reproductive axis in this case ensures that mating and conception will not occur at times when ample energy is unavailable to support a pregnancy. Taking into consideration long-term survival of a species, this prioritization allows for population growth to recede in times of

food shortage in order to conserve resources. In our studies of PMv LepRb neurons described in this dissertation, we begin to unravel the complex mechanisms by which the brain perceives energy status and reproductive cues and thus regulates physiological output.

While our mapping of LepRb-expressing cells throughout the brain demonstrates the vast distribution of sites of potential leptin action and highlights the enormous amount yet unknown, we have significantly advanced our understanding of LepRb at two such sites, and can confidently attribute the contribution of LepRb midbrain and PMv neurons to leptin's actions on reward-motivated feeding and reproduction respectively. Restricting the specific sites of leptin action producing the observed physiological changes associated with leptin deficiency and leptin resistance will allow their further characterization as well as the identification of new therapeutic targets in the treatment of obesity and associated health conditions.

Tables

	LepRb^{EGFP}	**LepRb$^{rosa\text{-}bgal}$**	**LepRb$^{actin\text{-}bgal}$**
Dentate Gyrus	+	-	+++
CA1, CA2, CA3	+/-	-	+++
Arcuate Nucleus	++++	+++	+
Dorsomedial Hypothalamus	++++	+++	-
Lateral Hypothalamus	+++	+++	-
Premammillary nucleus, ventral	++++	+++	-
Ventromedial Hypothalamus	+++	+++	+
Dorsal Raphe	+++	+++	-
Reticulotegmental Nucleus of the Pons	-	-	+
Nucleus of the Solitary Tract	++	++	-

Table 1. Relative densities of labeled cells in LepRb$^{rosa\text{-}bgal}$ and LepRb$^{actin\text{-}bgal}$. Estimates of the numbers of labeled cells observed in each bgal reporter line is compared to the equivalent regional labeling in LepRb^{EGFP} reporter mice. *+/- <10 cells per one-fourth of the brain; + 10-50; ++ 50-100; +++ 100-500; ++++ >500 cells*.

FOREBRAIN

Claustrum	++
Insular Cortex	++
Temporal Cortex, Association Area	++
Somatosensory Cortex	+++
Auditory Cortex	+++
Visual Cortex	+
Perirhinal Cortex	+
Ectorhinal Cortex	+++
Dorsal Endopiriform Nucleus	+++
Ventral Endopiriform Nucleus	+/-
Dentate Gyrus	+
CA1, CA2, CA3	+/-
Lateral Septal Nucleus	++
Bed Nucleus of the Stria Terminalis	++
Central Amygdala	+
Substantia Innominata	+/-
Paraventricular Thalamic Nucleus	++
Parafascicular Thalamic Nucleus	+
Ventromedial Thalamic Nucleus	+
SubparafascicularThalamic Nucleus	+
Ventral Anterior Thalamic Nucleus	+
Paraventricular Thalamic Nucleus	+
Submedius Thalamic Nucleus	+/-
Reuniens Thalamic Nucleus	++
Reticular Thalamic Nucleus	+/-
Anteromedial Thalamic Nucleus	+
Central Medial Thalamic Nucleus	+/-
Anterior Hypothalamus	+
Preoptic Nuclei	+++
Parastrial Nucleus	+
Anteroventral Periventricular Nuc	+/-
Arcuate Nucleus	++++
Dorsomedial Hypothalamus	++++
Lateral Hypothalamus	+++
Paraventricular Nucleus	+
Premammillary nucleus, ventral	++++
Ventromedial Hypothalamus	+++
Posterior hypothalamus	+++
Supramammillary Nucleus	++
Perifornical area	++
Suprachiasmatic nucleus	+
Medial Tuberal Nucleus	+
Lateral Habenula	+/-
Zona Incerta	+
Medial Mammillary	+
ventral tuberomammillary nucleus	+/-

MIDBRAIN

nucleus of brachium of inferior colliculus	+/-
commissure of inferior colliculus	+++
layers of superior colliculus	++
intercollicular nucleus	+/-
intermed geniculate nuc/superior colliculus	+
Ventral Tegmental Area	+++
Substantia Nigra	+++
Edinger-Westphal Nucleus	++
Linear Raphe	++
Dorsal Raphe	+++
A8 Dopamine Cells	+
Median Raphe	+/-
Periaqueductal Gray	++++
Lateral Dorsal Tegmental Nucleus	+/-
red nucleus	+
raphe cap	+
Precommissural Nucleus	++
Cuneiform Nucleus	+
medial terminal nuc of acc optic tract	+/-
interfascicular nucleus	+
interpeduncular nucleus	+/-
Deep Mesencephalic Nucleus	+++
Supraoculomotor Cap	+
Supraoculomotor Central Gray	+
nucleus posterior commissure	+
parvocellular oculomotor nucleus	+/-

HINDBRAIN

Pontine Reticular Formation, Oral	++
Medullary Reticular Nucleus, dorsal	+
Nucleus of the Solitary Tract	++
Dorsal Motor Nucleus of Vagus Nerve	+
Hypoglossal Nucleus	+/-
Parabrachial Nucleus	+++
Parvicellular Reticular Nucleus	+
Spinal Trigeminal Nucleus	+/-
nucleus ambiguous	+/-
cuneate nucleus	+/-
Intermediate Reticular Nucleus	+
Subcoeruleus Nucleus, Dorsal Part	+/-
paralemniscal nucleus	+/-
nucleus intercalatus	+/-
rostroventrolateral reticular nucleus	+/-
prerubral field	+/-
prepositus hypoglossal nucleus	+

Table 2. Relative densities of labeled cells in LepRb^{EGFP} reporter mice.
+/- <10 cells per one-fourth of the brain; + 10-50; ++ 50-100; +++ 100-500; ++++ 500 cells.

		Abbreviation	Description/Use	Source	Figures
Cre Lines	Removes floxed sequences	Lepr^{cre}	Cre expressed exclusively in LepRb cells	Myers Lab	Tables1,2; Figures2-8,11-18
		Nos1^{cre}	Cre expressed exclusively in Nos1 cells	Myers Lab	Figures22,23,25-27
Inducible Reporter Lines	When combined with cre, removal of a floxed transcription block causes reporter expression	Rosa26^{bgal}	beta-gal reporter; ubiquitous expression from Rosa26 locus	Jackson Laboratory	Table1; Figures2,3
		Actin-bgal	beta-gal reporter; neural & skeletal muscle expression from chicken-beta-actin promoter; nuclear localization sequence	Jackson Laboratory	Table1; Figures2,3
		Rosa26^{EGFP}	egfp reporter; ubiquitous expression from Rosa26 locus	Jackson Laboratory	Tables1,2; Figures2-5,8,11-15,18,23
		Rosa26^{EGFPf}	farnesylated egfp reporter; ubiquitous expression from Rosa26 locus; farnesylation targets protein to membrane for visualizing projections	Myers Lab	Figures2,16
LepRb Reporters	Cre-inducible reporter crossed with LepRb^{cre}	LepRb$^{rosa-bgal}$	Lepr^{cre} x Rosa26^{bgal}; beta-gal expressed in LepRb cells	NA	Table1; Figures2,3
		LepRb$^{actin-bgal}$	Lepr^{cre} x Actin^{bgal}; beta-gal expressed in neural LepRb cells (nuclei)	NA	Table1; Figures2,3
		LepRb^{EGFP}	Lepr^{cre} x Rosa26^{EGFP}; EGFP expressed in LepRb cells	NA	Tables1,2; Figures2-5,8,11-15,18
		LepRb^{EGFPf}	Lepr^{cre} x Rosa26^{EGFPf}; EGFPf in projections from LepRb cells	NA	Figures2,16
Nos1^{cre}; lepr^{flox}	Lepr deletion in Nos1 cells	*Nos1^{cre}*;lepr$^{\Delta/flox}$	"Experimental" animals: Cre present; one lepr allele deleted in all lepr cells, one lepr allele deleted only in Nos1 cells	NA	Figures25-27
		Nos1^{cre};lepr$^{+/+}$	Control: Cre present; no floxed allele	NA	Figures25-27
		lepr$^{\Delta/flox}$	Control: No cre, one lepr allele deleted in all cells, one lepr allele floxed	NA	Figures25-27
		Nos1^{cre};lepr$^{\Delta/\Delta}$	Control: Cre, both lepr alleles deleted in all lepr cells (equivalent to db/db)	NA	Figures25-27
Other Lines		C57BL/6J	"wildtype"	Jackson Laboratory	Figures9,18,21
		Nos1^{EGFP}	Nos1^{cre} x Rosa26^{EGFP}; EGFP expressed in Nos1 cells	NA	Figures23
		BIG	Anterograde and retrograde transsynaptic tracing from GnRH cells; Barley lectin (in the absence of GnRH-positive fibers) denotes upstream cells	Linda Buck	Figures19
		Lepr^{flox}	Floxed lepr exon 17; When combined with cre, lepr deleted in cells expressing cre	Streamson Chua	Figures22,25-27
		KN1	Nos1-alpha knockout	Jackson Laboratory	Figure21

Table 3. Descriptions of utilized mouse lines.

Figures

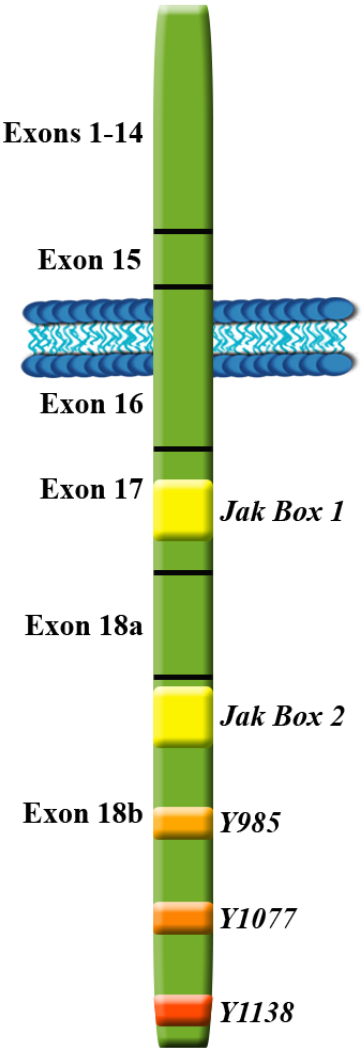

Figure 1. The leptin receptor gene, "*lepr*", encodes several isoforms of leptin receptors (LepRa, b, c, d, e). The structure of LepRb consists of several sites which mediate intracellular signaling. JAK2 non-covalently associates with the receptor at the JAK boxes, allowing JAK2 autophosphorylation on numerous residues and subsequent phosphorylation of LepRb at discrete sites, including tyrosines (Y) at positions 985, 1077 and 1138.

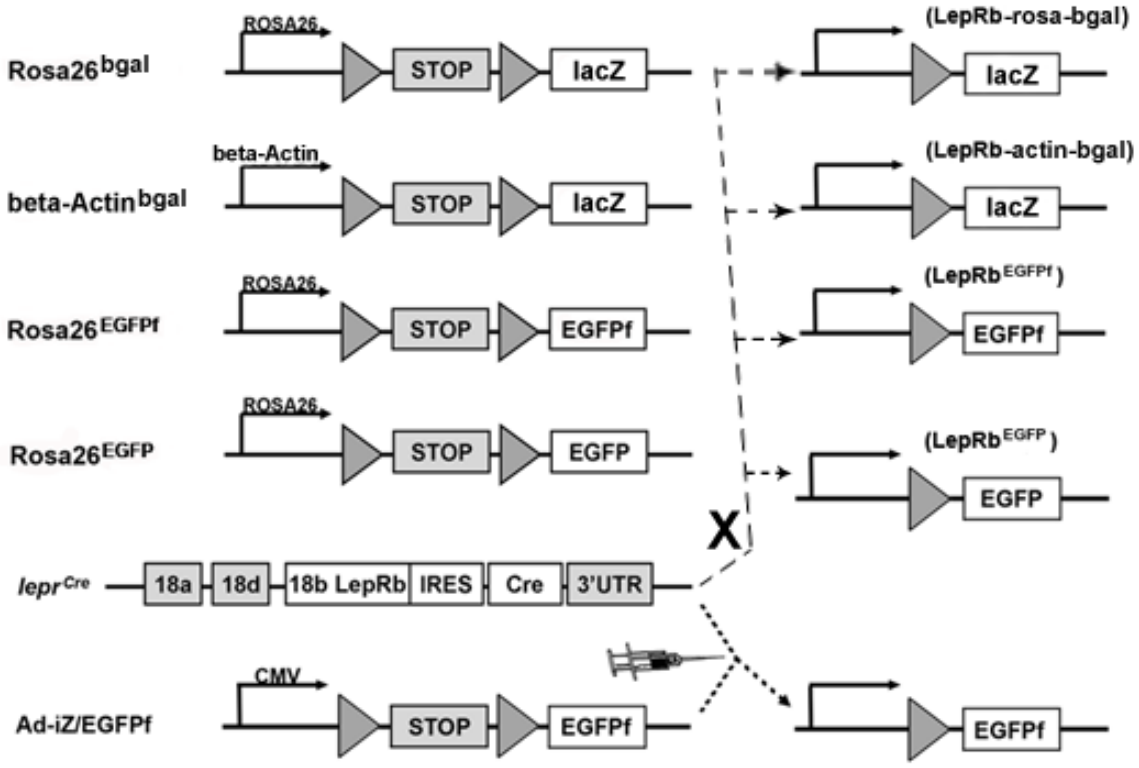

Figure 2. *Lepr*^{cre} mice and cre-inducible systems to interrogate LepRb neurons. The coding sequence of Cre recombinase was targeted into the LepRb-specific exon in the *lepr* gene (*lepr*^{cre} mice). *Lepr*^{cre} mice were mated with *beta-Actin*^{bgal}, *Rosa26*^{bgal}, *Rosa26*^{EGFP} mice, *Rosa26*^{EGFPf} mice, or injected with Ad-iZ/EGFPf. In each case a floxed transcription blocker precedes reporter gene sequences (lacZ, EGFP, or EGFPf) and cre-mediated excision of the transcription blocker results in bgal, EGFP or EGFPf expression in cells expressing cre/LepRb.

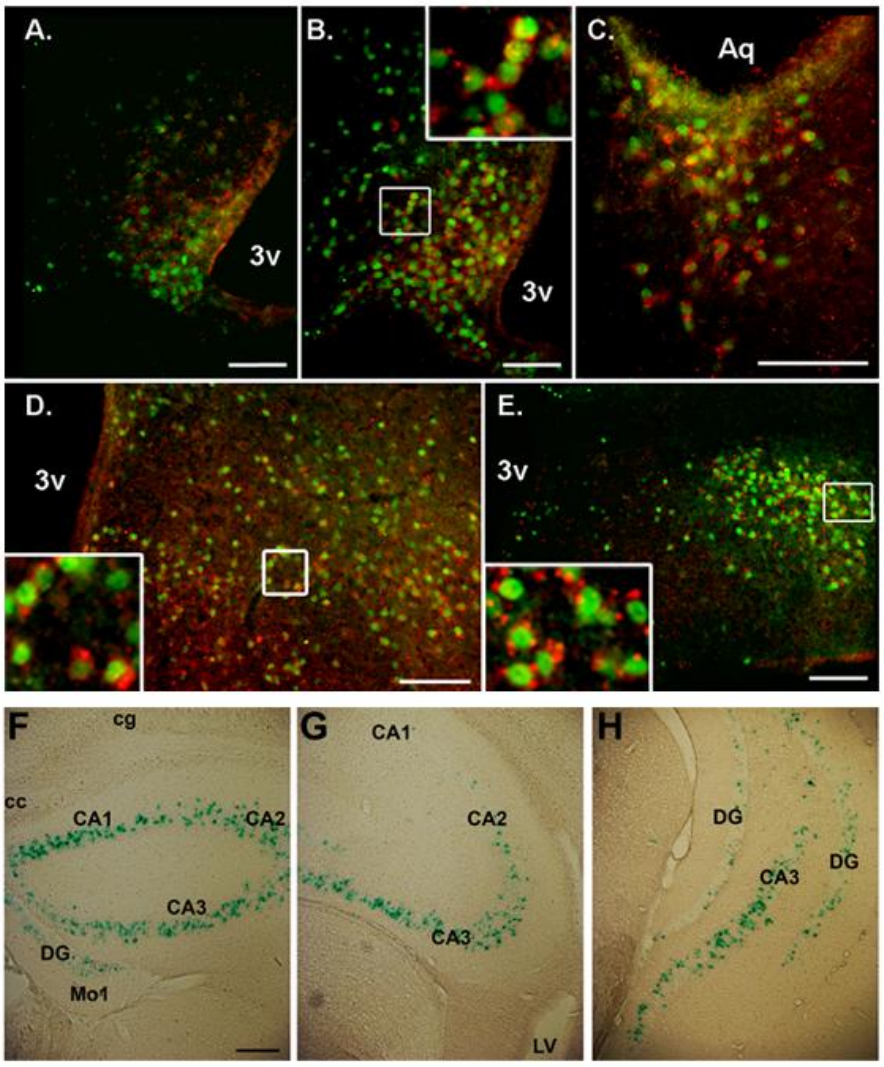

Figure 3. Beta-gal labeling in *Rosa26*^{bgal} and *beta-Actin*^{bgal} mice. Representative images from *Rosa26*^{bgal} mice show leptin-induced pSTAT3 immunoreactivity (green, nuclear) colocalized with beta-gal (red, cytoplasmic) in cells of the ARC (A, B), DR (C), DMH (D), and PMv (E). High magnification insets in B, D, E show colocalization. Histochemical staining of beta-gal (blue, nuclear) in *beta-Actin*^{bgal} mice reveals dense labeling in areas of the hippocampus (F-H), including CA1, CA2, CA3 and DG. *3v, third cerebral ventricle; Aq, cerebral aqueduct; scale bars, 100um.*

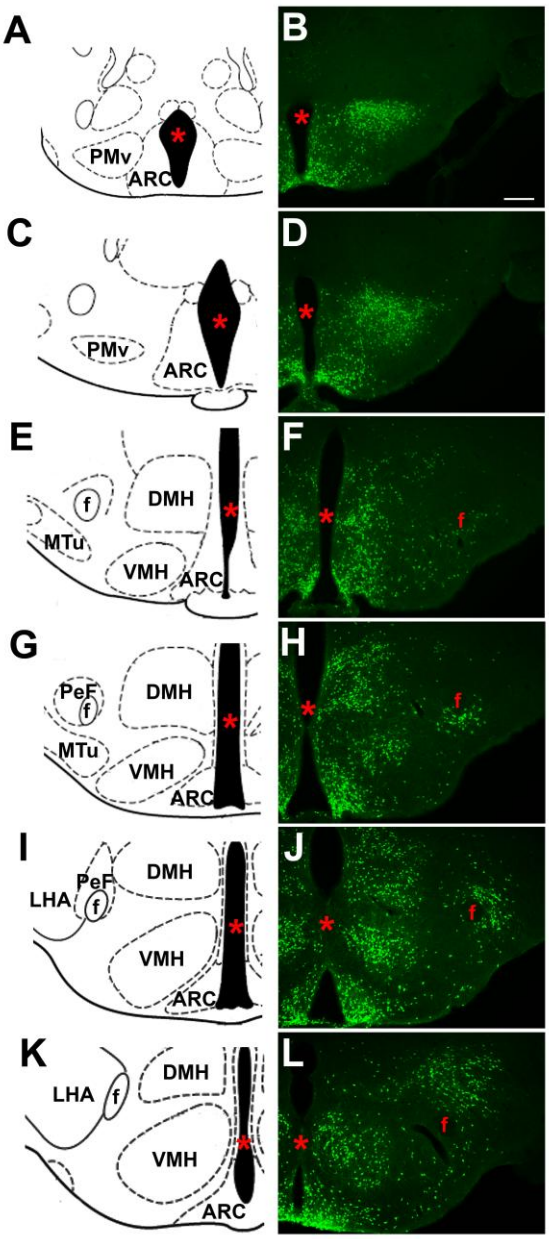

Figure 4. EGFP labelling in representative hypothalamic nuclei of LepRb^{EGFP} mice. EGFP immunoreactivity reveals LepRb-expressing cells in several caudal-to-rostral hypothalamic nuclei, including PMv (*B,D*), DMH (*F,H,J*), and VMH (*F,H,J,L*). Corresponding coronal diagrams label relative location of selected nuclei (A,C,E,G,I,K), adapted from Paxinos and Franklin (186). *scale bar: 200μm; asterisk labels third cerebral ventricle; Mtu, medial tuberal nucleus; f, fornix; PeF, perifornical nucleus.*

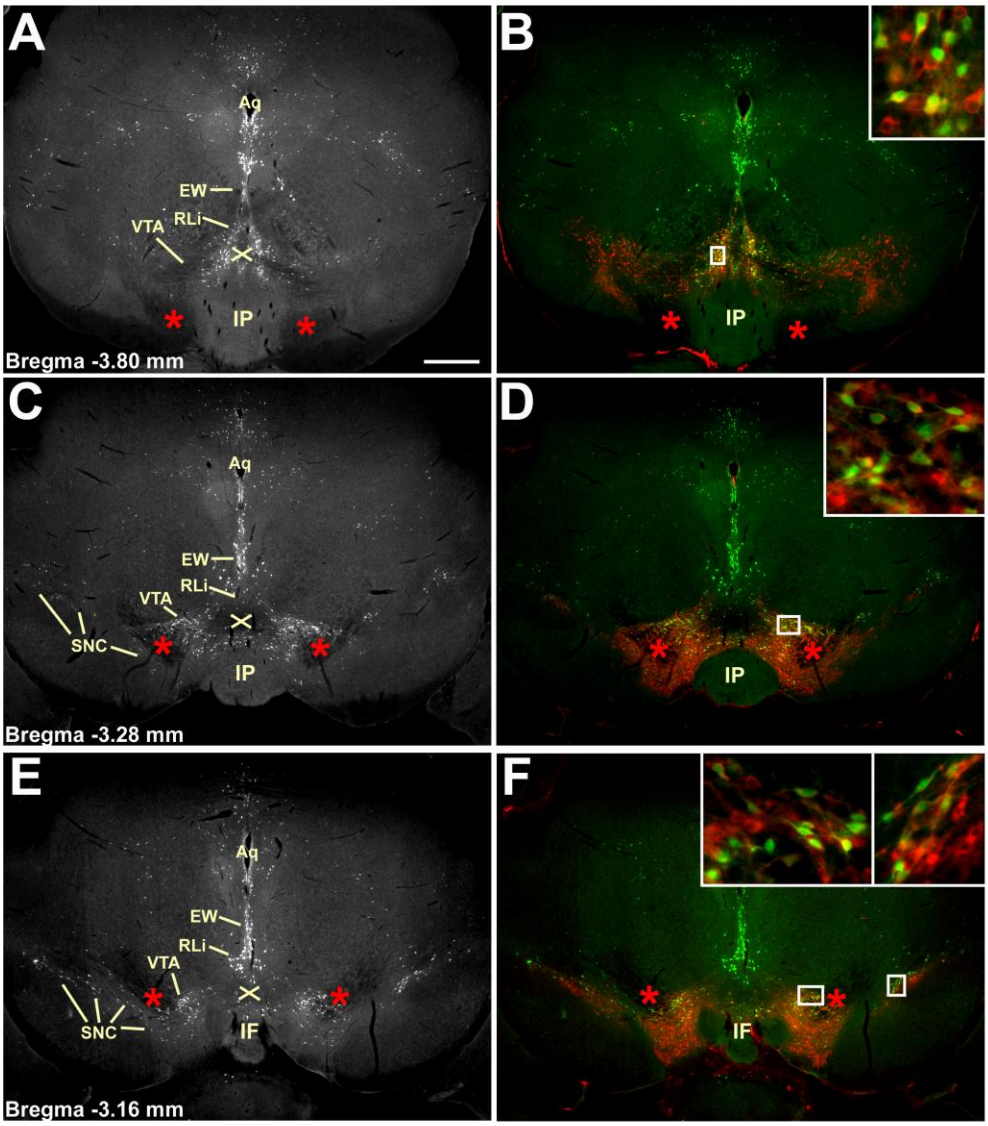

Figure 5. LepRb^{EGFP} mice show EGFP-IR (A,C,E white; B,D,F green) in midbrain cells through several caudal-to-rostral sections. The majority (74.9% ± 3.9, n=3) of EGFP-IR neurons express TH (B,D,F red). High magnification insets show colocalization of EGFP and TH in the indicated VTA and RLi regions. *IP, interpeduncular nucleus, IF,interfascicular nucleus EW, Edinger-Westphal nucleus, Aq, cerebral aqueduct ; asterisk labels medial lemniscus; "x" labels decussation of the superior cerebral peduncle; scale bar, 200um.*

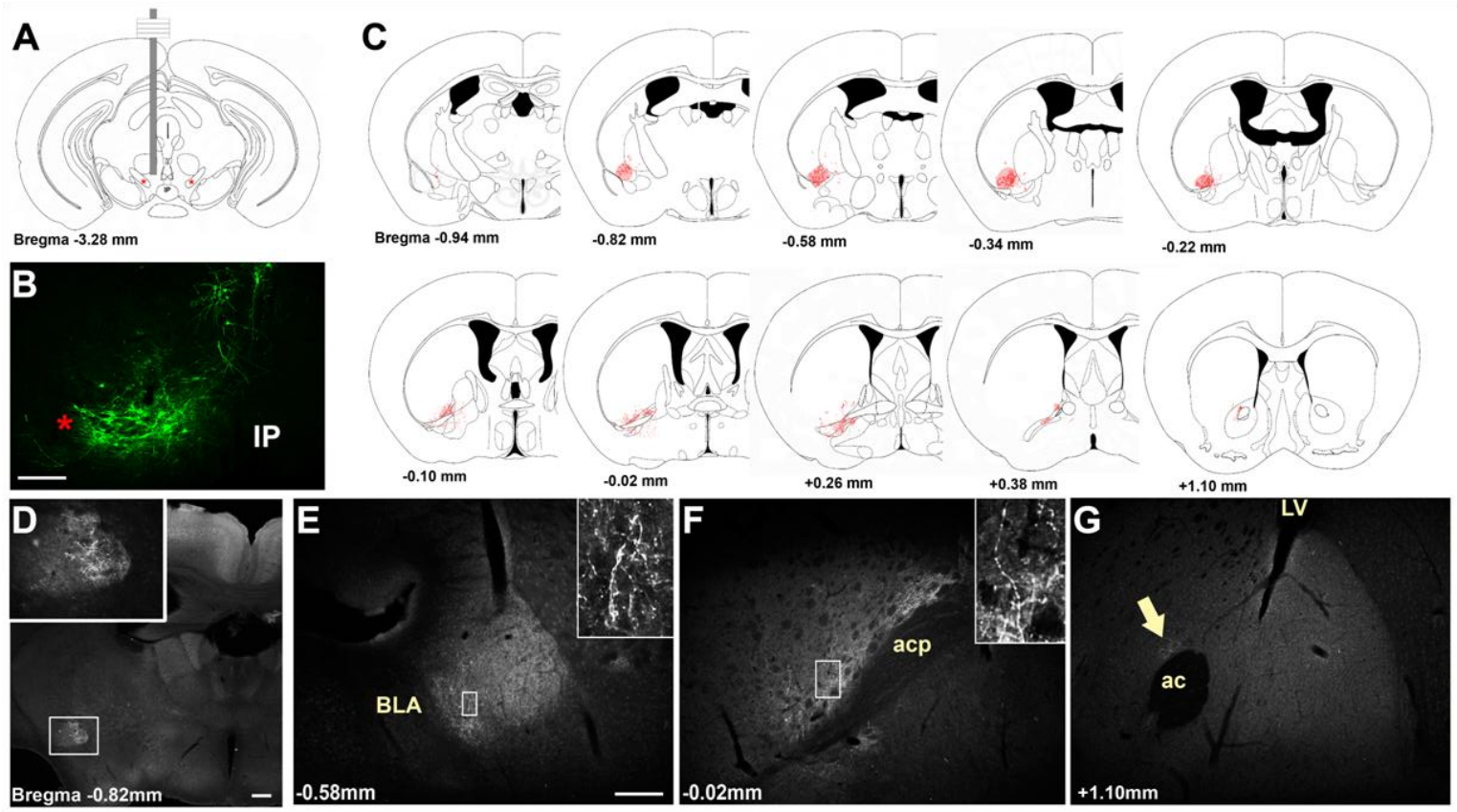

Figure 6. Anterograde tracing from LepRb VTA neurons. Following injection of Ad-iZ/EGFPf into the VTA of $Lepr^{Cre}$ homozygous mice, EGFP-IR cells were seen in VTA (B). EGFP-IR fibers were observed in throughout CeA (D) and IPAC (E,F). Fibers in NAc were rare (G). Diagrams adapted from Paxinos and Franklin (186) show aim site (A) as well as relative fiber densities (red) in VTA target regions (C). *IP, interpeduncular nucleus; acp, anterior commissure, posterior; ac, anterior commissure; BLA, basolateral amygdala nucleus, anterior; LV, lateral ventricle; asterisk denotes medial lemniscus in A and B. scale bars, 200um (B,D), 100um (E-G).*

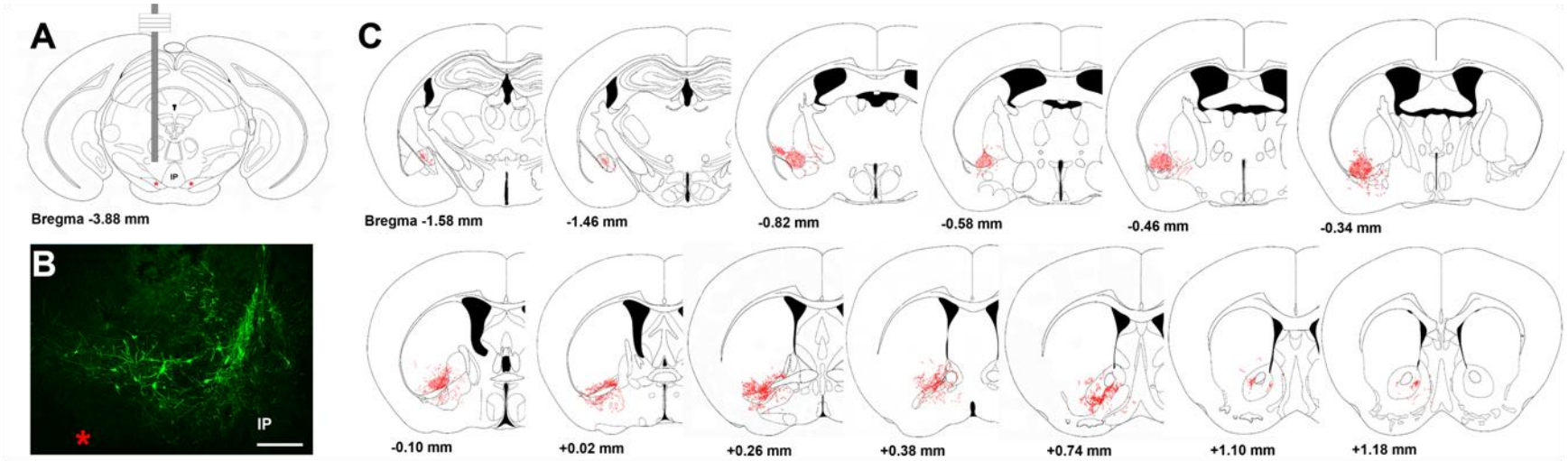

Figure 7. Anterograde tracing from LepRb VTA/RLi neurons. Following injection of Ad-iZ/EGFPf into the VTA/RLi of $Lepr^{Cre}$ homozygous mice, EGFP-IR cells were seen in VTA and midline cells (B). EGFP-IR fibers were observed in throughout CeA, IPAC and NAc (C). Diagrams adapted from Paxinos and Franklin (186) show aim site (A) as well as relative fiber densities (red) in VTA/RLi target regions (C). *IP, interpeduncular nucleus; asterisk denotes medial lemniscus in A and B. scale bar, 200um.*

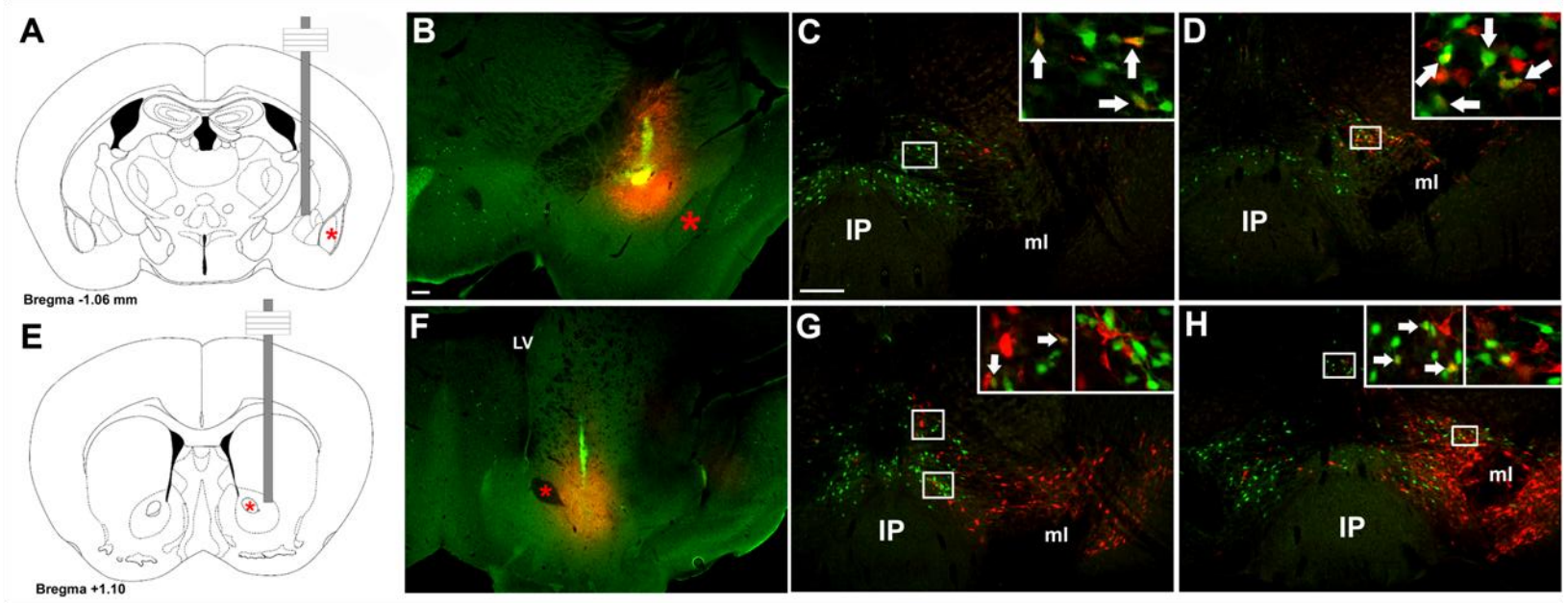

Figure 8. Retrograde tracing of inputs from LepRb VTA/RLi cells. Injection of FG-equivalent, Hydroxystilbamidine, into the CeA (B) or NAc (F) of $LepRb^{EGFP}$ mice revealed tracer plumes in the respective regions. Retrogradely traced, FG-positive cells (red) from CeA colocalized with EGFP-IR (green) in the VTA (C,D). Injection of FG into the NAc demonstrated EGFP-FG colocalization in RLi, but not VTA (G,H). Coronal diagrams adapted from Paxinos and Franklin (186) indicate CeA and NAc injection sites (A,E). Insets show high magnification with arrows pointing to EGFP-FG colocalization (where two insets in one panel: left insets, RLi regions; right insets, VTA regions). *asterisks label BLA (A,B) or anterior commissure (E,F); LV, lateral ventricle; ml, medial lemniscus; IP, interpeduncular nucleus; scale bars, 200um.*

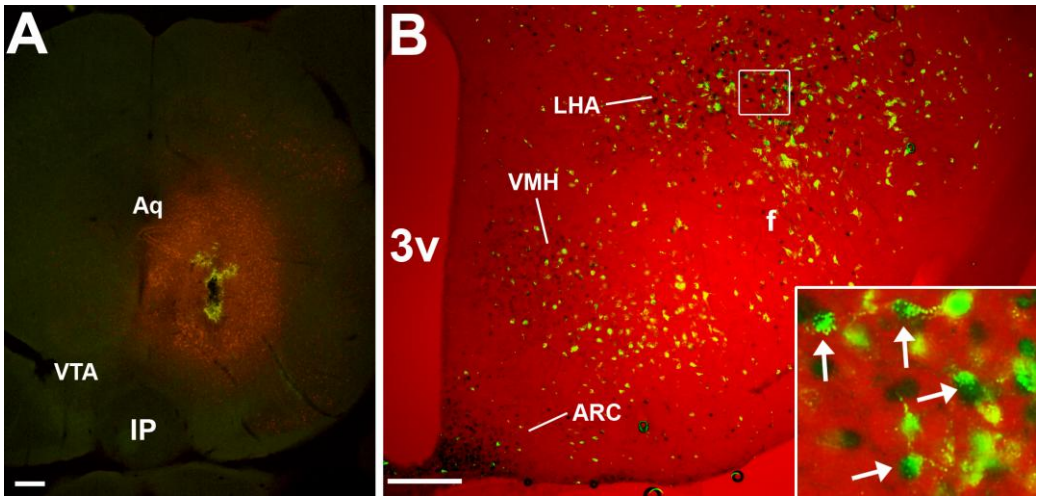

Figure 9. Retrograde tracing of leptin-responsive inputs to VTA. Injection of FG-equivalent, Hydroxystilbamidine, into the VTA (A) of leptin-treated C57BL/6 mice revealed a population of FG-labeled cells (green, cytoplasmic) in the hypothalamus (B), with a significant population in the LHA. Of the leptin-responsive (leptin-induced pSTAT3-immunoreactive) LHA cells, 58.9 +/- 2.2% (n=7) were FG-positive, while 39.9 +/- 2.3% of total FG-IR LHA cells showed leptin-induced pSTAT3-IR (black, nuclear). Few FG-pSTAT3 double-labeled celss were observed in ARC or VMH. Insets show high magnification with arrows pointing to pSTAT3-FG colocalization. Red plume in A shows FG labeling at the VTA injection site. *Aq, cerebral aqueduct, 3v, 3rd cerebral ventricle; IP, interpeduncular nucleus; scale bars, 200um.*

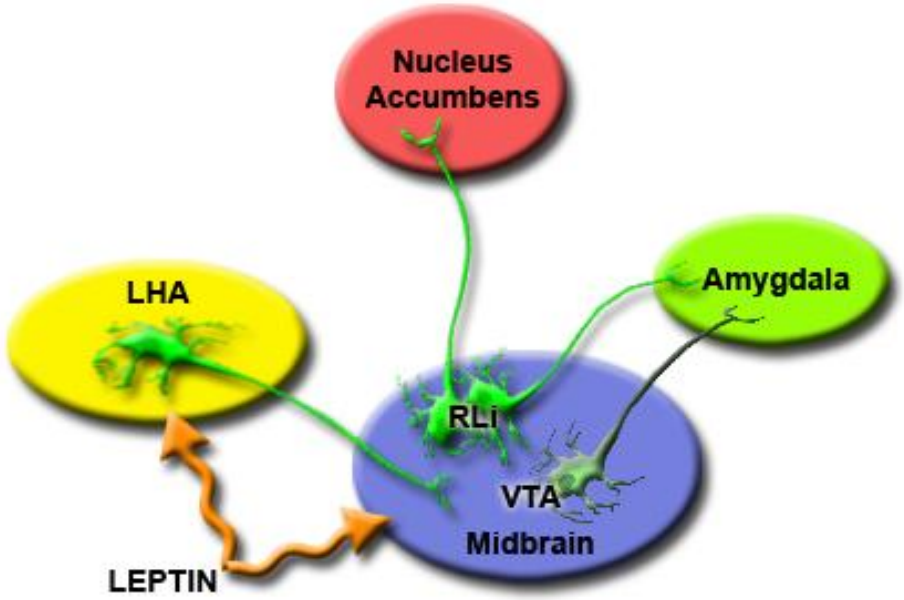

Figure 10. Summary of midbrain LepRb circuitry. The diagram depicts two populations of midbrain LepRb cells, those in the VTA and those midline in the RLi. LepRb VTA neurons project rostrally to innervate the CeA and IPAC (designated “amygdala”), with meager projections to NAc. LepRb RLi neurons also project to CeA and IPAC, as well as to NAc. In addition, leptin-responsive neurons in the LHA innervate the VTA. This circuit highlights the multiple potential points of leptin regulation of the mesolimbic dopamine (MLDA) reward system.

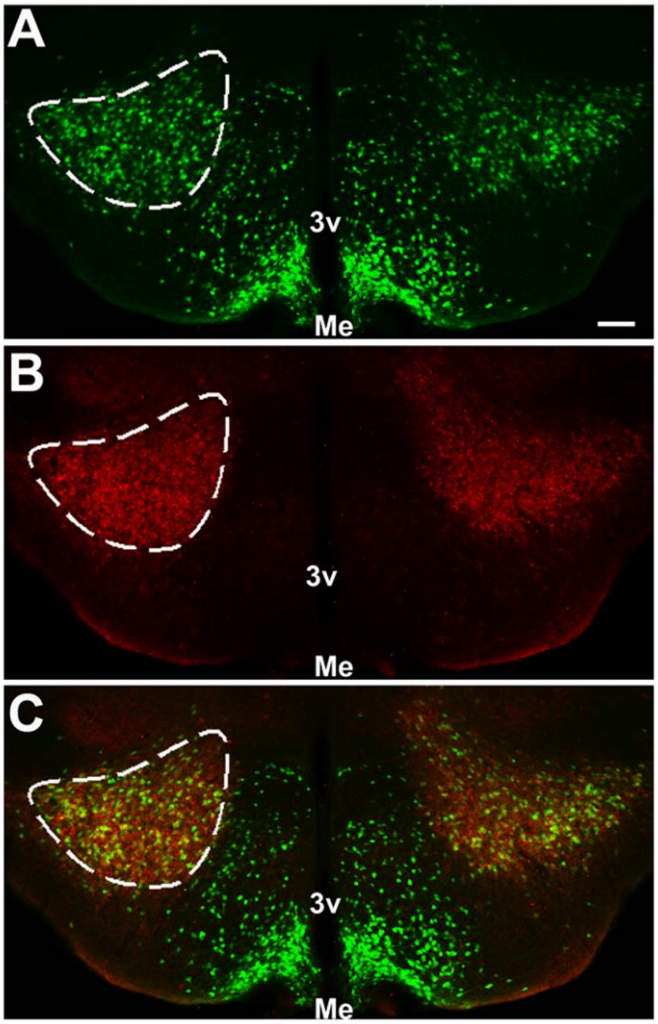

Figure 11. NOS1 immunoreactivity (NOS1-IR) defines PMv boundaries. Immunofluorescent labeling of NOS1 (*B*) was utilized to define the PMv in LepRb^{GFP} mouse brain slices. Representative images show EGFP-expressing LepRb cells (*A*) and merged NOS1-EGFP labeling (*C*) depicting determination of PMv boundaries (dashed lines). *3v, third cerebral ventricle; Me, median eminence; scale bar, 100um.*

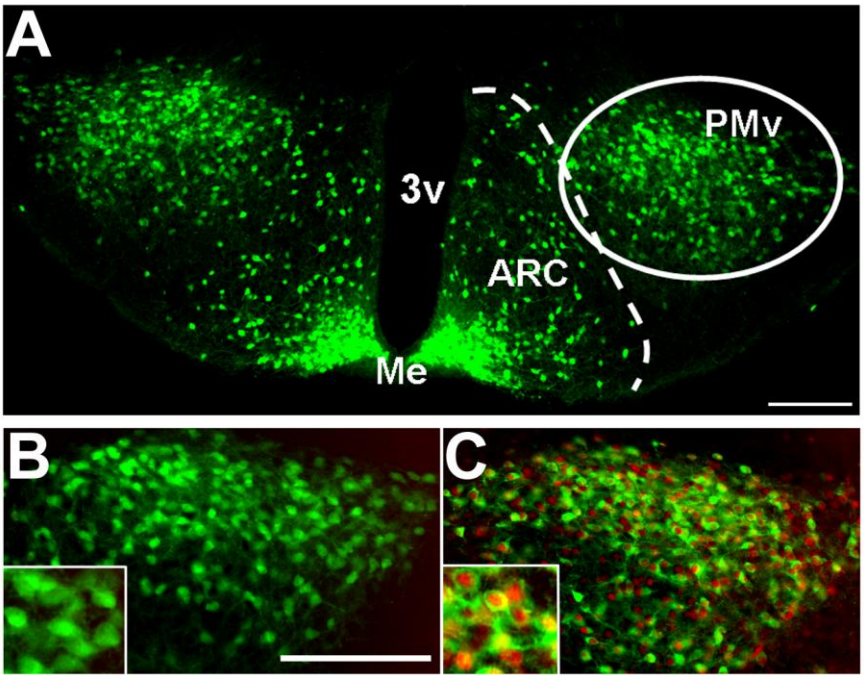

Figure 12. LepRb^{GFP} mice exhibit a substantial population of GFP-IR (green, cytoplasmic) cells in the PMv (A-C). Systemic leptin administration (5 mg/kg i.p., 2 hours) to LepRb^{GFP} mice induces phosphorylation of STAT3 (pSTAT3; red, nuclear) in 96±0.2% (n=3) of GFP-positive (LepRb) cells (C), compared to 0.6% ±0.2; n=4 in PBS treated animals (B). High magnification insets show colocalization of GFP and pSTAT3. *3v, third cerebral ventricle; PMv, ventral premammillary nucleus; Me, median eminence; ARC, arcuate nucleus; scale bars, 100um.*

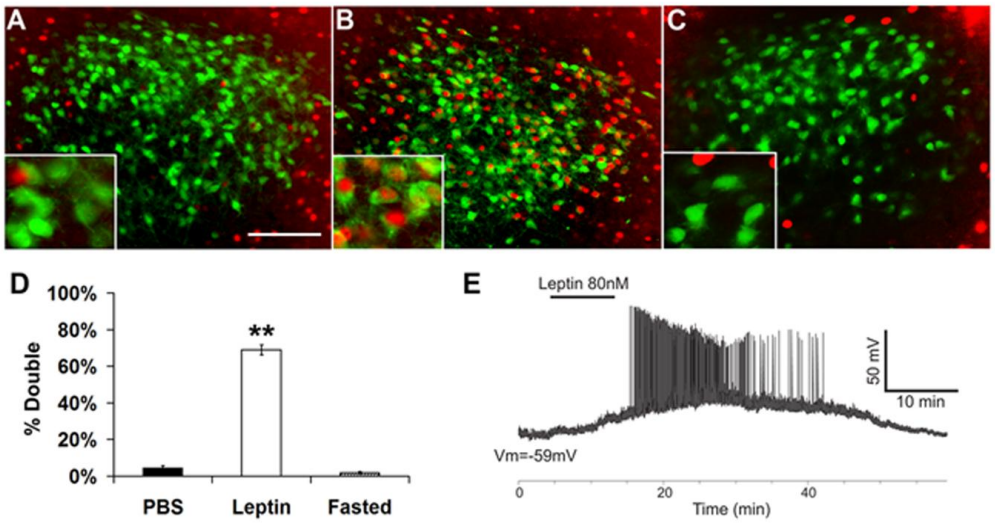

Figure 13. Regulation of LepRb PMv neuronal activity by leptin in LepRb^{GFP} mice. LepRb neurons showed increased cFos-immunoreactivity in response to leptin (B) (5 mg/kg i.p., 4 hours), but not PBS (A), or fasting (C), (PBS, 4±2%; leptin, 69±3%; fasted, 2±0.5%; n=3). High magnification insets show colocalization of GFP (green, cytoplasmic) and FosIR (red, nuclear). (D,E) Whole-cell patch-clamp recordings from LepRb PMv neurons in current clamp mode (synaptic inputs blocked). Treatment with leptin depolarized LepRb neurons in 67% of the neurons tested (control: −65 ±4 mV, plus leptin: −54 ±5 mV; n= 8 out of 12 neurons). *p<0.05, **p<0.0001 *scale bar: 100um*

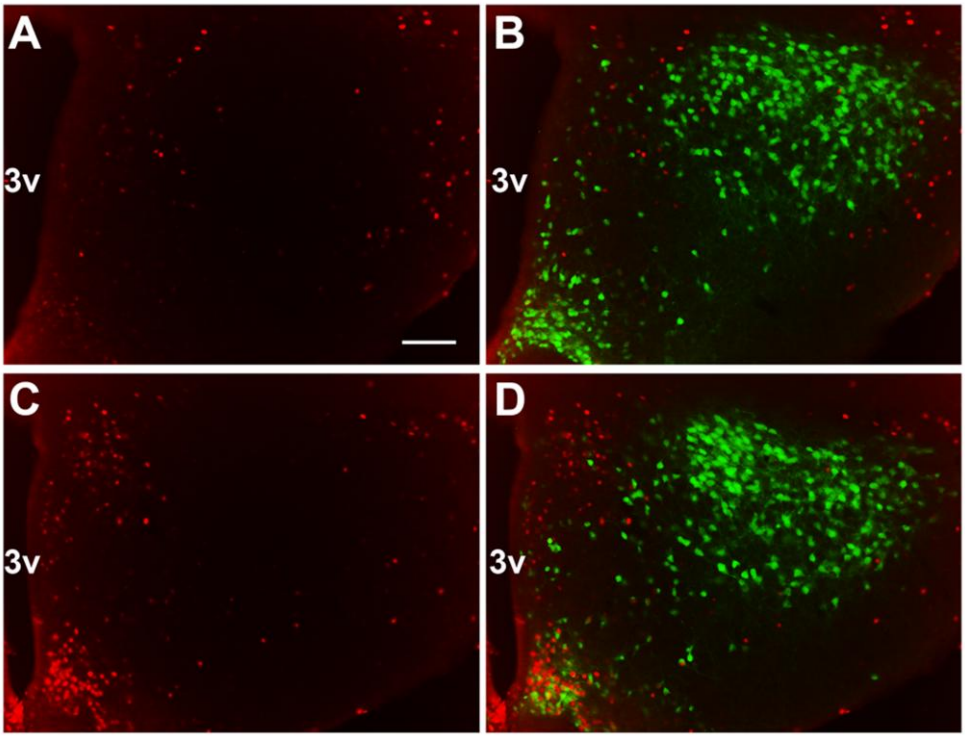

Figure 14. PMv LepRb neurons are not activated by fasting. Fos immunoreactivity (FosIR, red, nuclear) was used to designate activated cells in *ad lib* fed (A,B) or fasted (C,D) $LepRb^{GFP}$ mice. Simultaneous detection of LepRb cells using GFP (green, cytoplasmic) revealed fasting-activated LepRb cells in basomedial arcuate nucleus, but not PMv. *scale bar: 100um.*

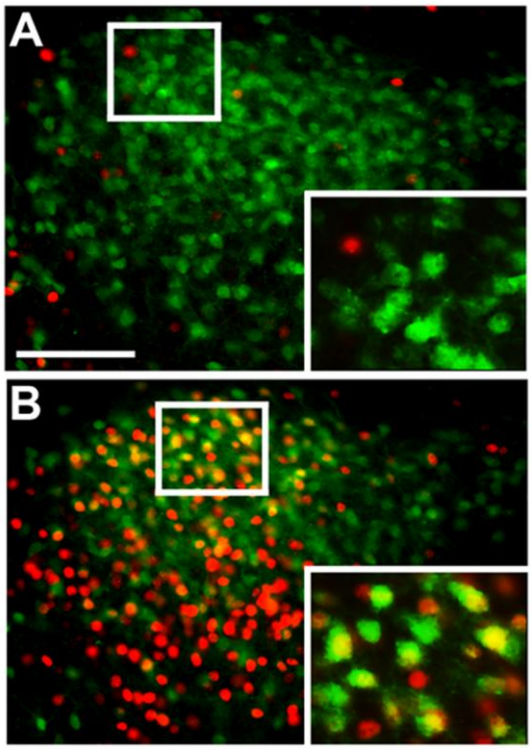

Figure 15. Male or female odors increase Fos-IR in LepRb PMv cells of the opposite sex. Representative images show increased Fos-IR (red, nuclear) in EGFP-IR PMv LepRb cells (green, cytoplasmic) of female $LepRb^{EGFP}$ mice exposed to opposite sex soiled bedding (B), compared with fresh bedding controls (A). Insets represent digital zooms of the indicated area. *scale bar: 100 µm.*

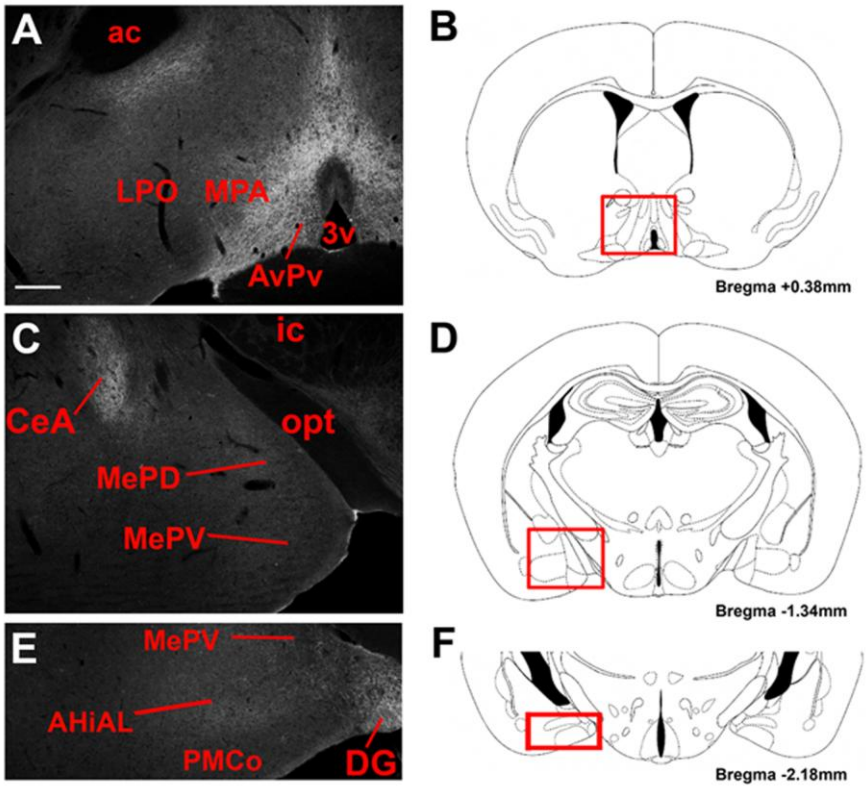

Figure 16. EGFP-IR projections from LepRb neurons to the POA and amygdala in LepRb^{EGFPf} mice. LepRb^{EGFPf} mice reveal EGFP-IR in POA and AvPv regions (A). Although labeling was observed in several amygdaloid regions (including CeA), and in the DG, no apparent labeling was observed in medial and posterior amygdaloid regions (C, E). Red boxes on reference diagrams (B, D, F) indicate comparable atlas sections for POA and amygdala images. *3v, Third cerebral ventricle; ox, optic chiasm; opt, optic tract; ac, anterior commissure; ic, internal capsule; MePV, medial amygdala, posteroventral part; AHiAL, amygdalohippocampal area, anterolateral part; PMCo, posteromedial cortical amygdaloid nucleus. Coronal diagrams adapted from Paxinos and Franklin (186); scale bar, 200um.*

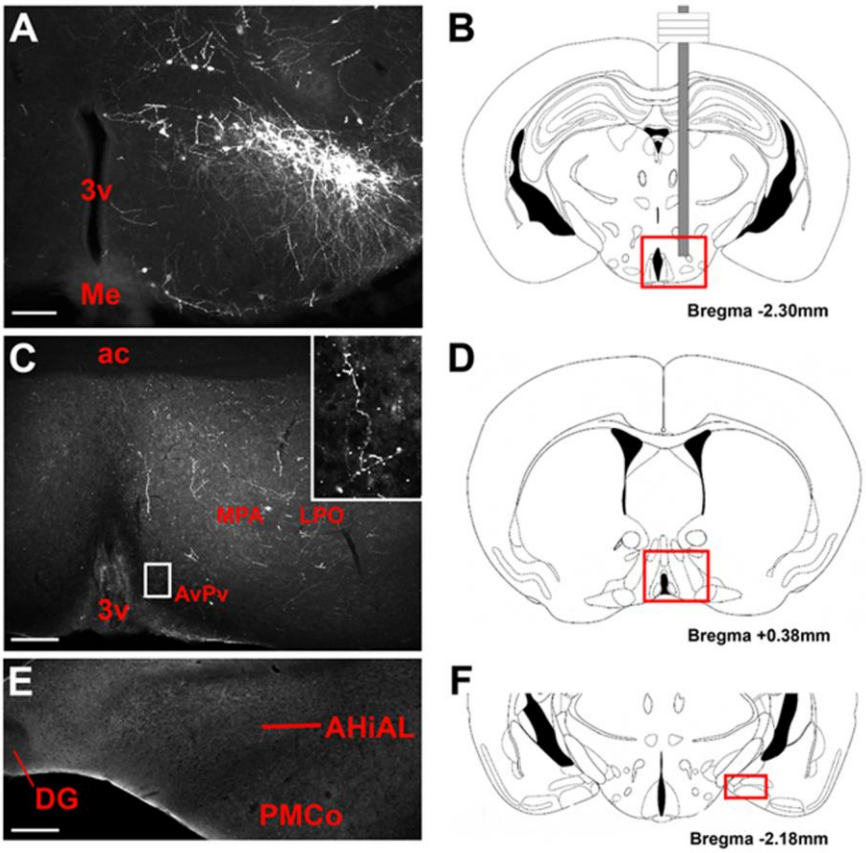

Figure 17. LepRb PMv projections in female mice. After administration of Ad-iZ/EGFPf to the PMv of female *lepr*$^{cre/cre}$ mice, EGFP-IR cells were observed at the injection site in the PMv (A). EGFP-IR projections were observed in lateral and medial preoptic areas and the anteroventral periventricular area (C). Inset shows high magnification of representative fibers with bouton-like varicosities in anteroventral periventricular nucleus. In contrast, little labeling was in medial and caudal amygdala regions (E). Red boxes on reference diagrams (B, D, F) indicate comparable atlas sections for PMv, POA and amygdala images respectively. *3v, third cerebral ventricle; ac, anterior commissure; AHiAL, amygdalohippocampal area, anterolateral part; PMCo, posteromedial cortical amygdaloid nucleus. Diagrams adapted from Paxinos and Franklin (186); scale bars, 100um.*

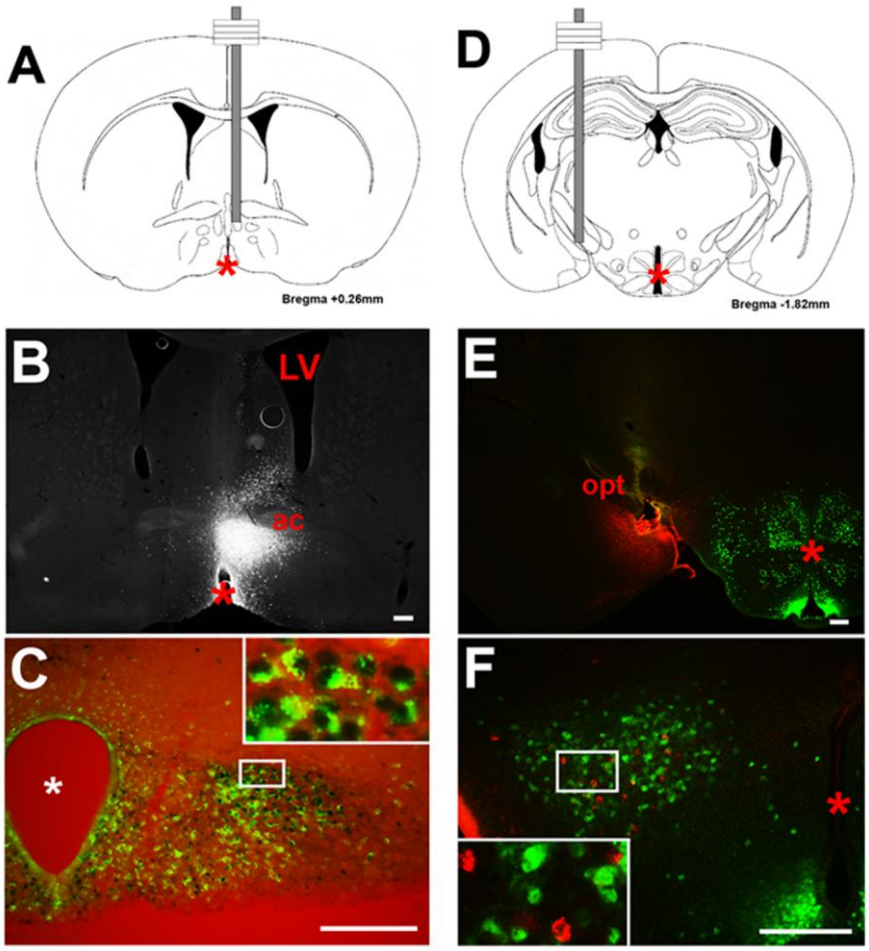

Figure 18. Retrograde tracing of inputs from LepRb PMv cells. Injection of FG into the POA of C57BL/6J mice revealed tracer plumes in the POA (B). Retrogradely traced, FG-IR (green, cytoplasmic) was detected around leptin-induced pSTAT3-IR (black, nuclear) in the PMv (C). Conversely, injection of FG into the MeA of $LepRb^{EGFP}$ mice revealed tracer plumes in MeA (E) (red), but no colocalization of PMv FG-IR cells (red) with EGFP-IR LepRb cells (green) (F). Coronal diagrams indicate POA and MeA injection sites (A, D). Insets show high magnification of colocalization. *Asterisks label 3rd cerebral ventricle. LV, Lateral ventricle; ac, anterior commissure; opt, optic tract. Diagrams adapted from Paxinos and Franklin (186); scale bars, 100um.*

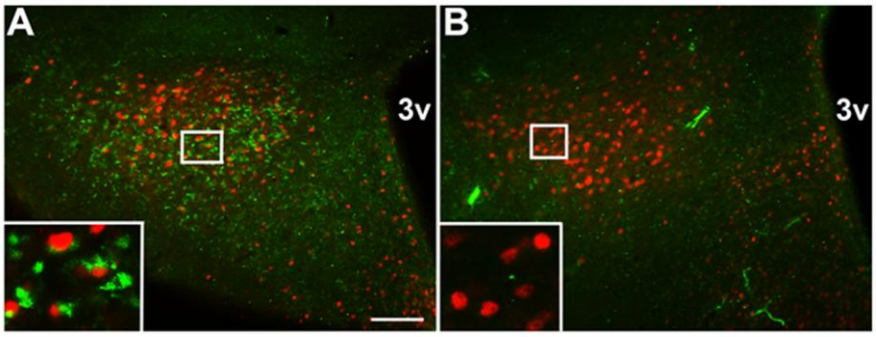

Figure 19. Retrograde tracing of inputs to GnRH neurons from leptin-responsive PMv cells in BIG mice. Female BIG mice were administered 5 mg/kg leptin i.p. for 1 hour. Representative images show colocalization of the transsynaptic tracer BL (WGA-IR, green, cytoplasmic) around leptin-induced pSTAT3-IR (red, nuclear) in the PMv of BIG mice (A). No WGA-IR was detected in leptin-treated control mice (B). Insets show high magnification of colocalized BL and pSTAT3. *3v, third cerebral ventricle; scale bar, 100um*

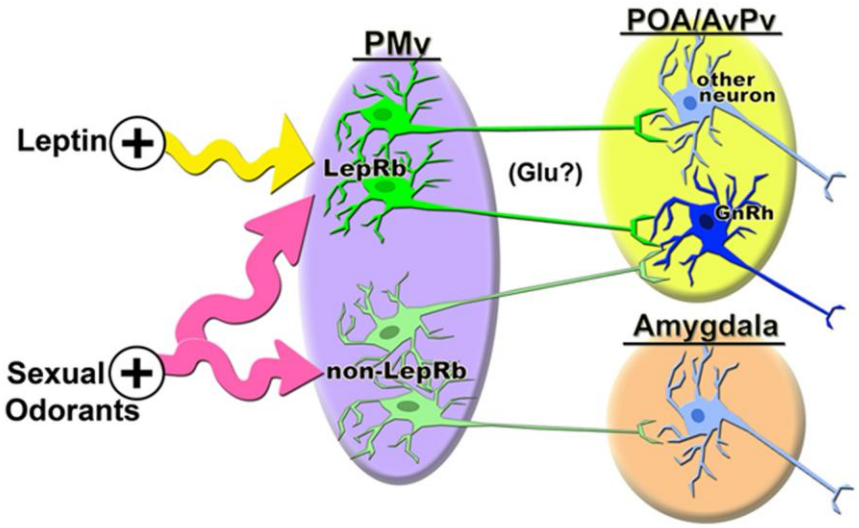

Figure 20. Integration of sexual odorant and leptin signaling pathways in PMv LepRb neurons. The diagram depicts a population of PMv LepRb cells that receive input from both leptin (directly) and sexual odorants (indirectly through MeA). LepRb PMv cells connect to POA/AvPv cells, including GnRH neurons, but do not significantly innervate the amygdala, as do other PMv neurons of undefined phenotype. This circuit integrates metabolic and sexual odorant signals within PMv LepRb cells for the presumably stimulatory glutamatergic (Glu?) innervation of GnRH neurons.

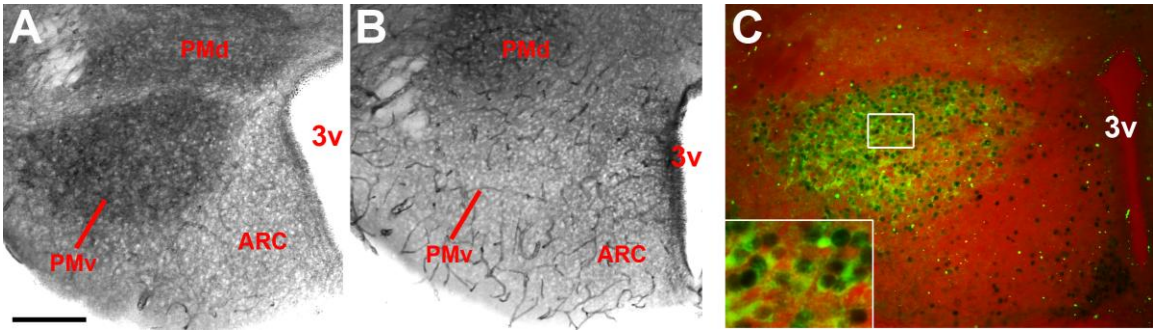

Figure 21. The PMv contains Nos-1 expressing cells. NADPH diaphorase histochemistry in C57BL/6J (A), but not KN1 (B), PMv indicates the Nos1-alpha isoform is present in PMv. NOS1-IR (green, cytoplasmic) exhibits significant colocalization with PMv pSTAT3-IR (black, nuclear) in leptin-treated (5mg/kg i.p., 4 hours) animals (C). Nearly all PMv pSTAT3-IR cells exhibited NOS1-IR (93.8 +/- 1.1%, n=3). More than 50% of PMv NOS-IR cells had pSTAT3-IR nuclei (62.8 +/-1.1%. n=3). *3v, 3rd cerebral ventricle; PMd, dorsal premammillary nucleus; scale bar, 200um*

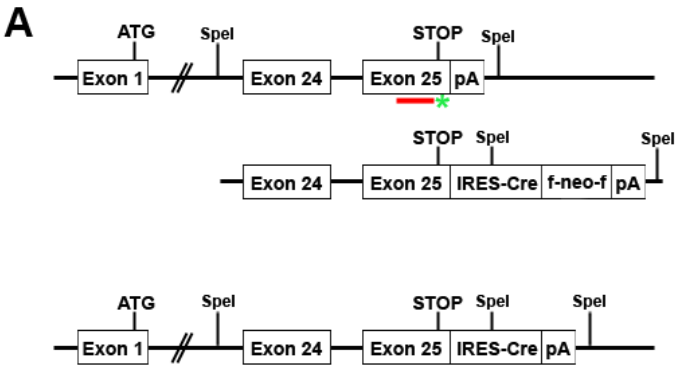

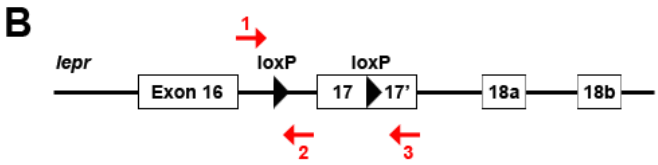

C

Genotype	Leprflox 1+2	Leprflox 1+3	Cre
Nos1^{Cre};*lepr*$^{\Delta/+}$	+ (198bp)	+	+
Nos1^{Cre};*lepr*$^{\Delta/\Delta}$	-	+	+
lepr$^{\Delta/flox}$	+ (249bp)	+	-
Nos1^{Cre};*lepr*$^{\Delta/flox}$	+ (249bp)	+	+

Figure 22. Generation of *Nos1*^{cre};*lepr*$^{\Delta/flox}$ mice to delete LepRb in Nos1-expressing neurons. A, The endogenous *nos1* locus is depicted above our targeting strategy, in which an IRES element-driven Cre coding region plus a FRT-flanked Neo selection cassette (f-neo-f) is inserted in the final *nos1* exon (exon 25) between the Stop codon and the polyadenylation (pA) site. Structure of the final targeted locus with neo removed is shown at bottom (A). The red line represents sequences used to prepare southern probes and the green asterisk denotes the insertion site, to which qPCR probes were targeted for rapid analysis of ES clones. *Nos1*^{cre} mice were mated with *lepr*$^{flox/flox}$ mice (B, provided by Dr. S. Chua) to generate *Nos1*^{Cre};*lepr*$^{\Delta/+}$, which were then mated to *lepr*$^{flox/flox}$ animals to produce *Nos1*^{cre};*lepr*$^{\Delta/flox}$ and control mice. Numbered red arrows (B) depict locations of primers used to distinguish genotypes (C).

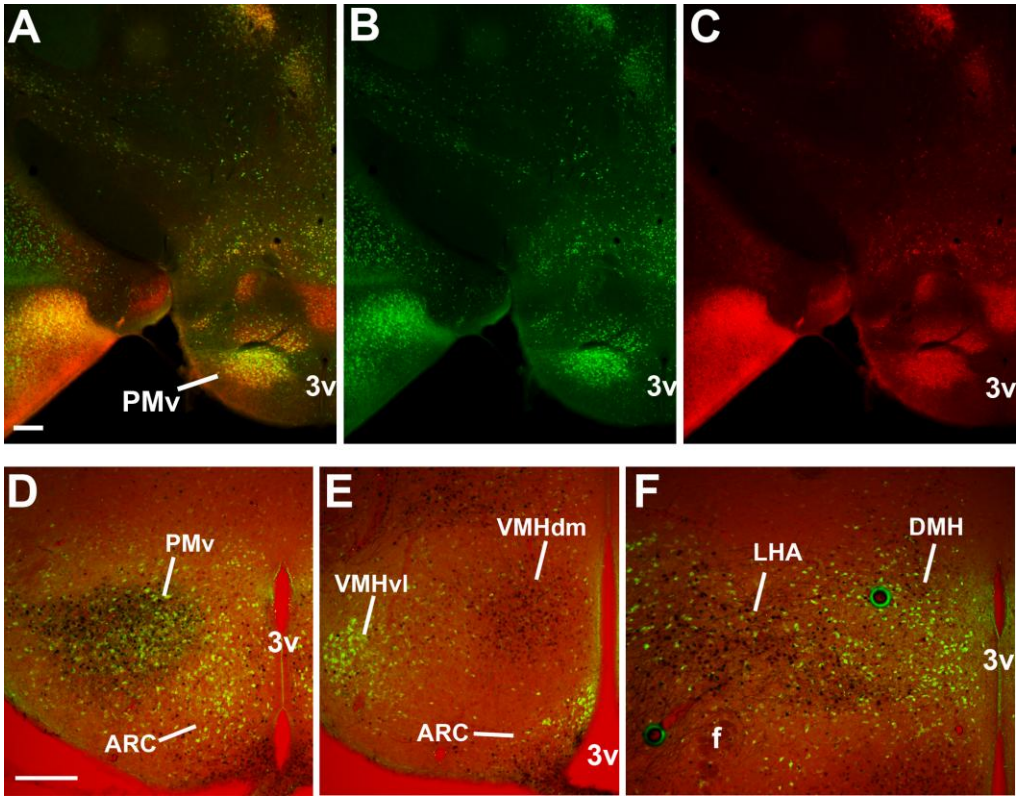

Figure 23. Nos1^{Cre} expression is comparable to NOS1-IR, and is efficiently expressed in leptin-responsive PMv cells. We mated Nos1^{Cre} animals to ROSA^{EGFP} reporter in order to induce EGFP expression in Nos1-expressing cells (Nos1^{EGFP} mice). EGFP-IR (B, green) overlapped with NOS1-IR (C, red) in all regions examined (Panel A shows B+C merged images). We administered leptin (5mg/kg i.p., 2 hours) to Nos1^{EGFP} mice and observed significant colocalization of EGFP-IR (green, cytoplasmic) and pSTAT3-IR (black, nuclear) in the PMv (D) of Nos1^{Cre} mice, with considerably fewer double-labeled cells in other hypothalamic nuclei (E,F) (PMv pSTAT3-IR with EGFP-IR, 82.7 ±7.2% n=3; ARC, 5.7 ±1.1%, n=4; DMH, 18.4 ±3.2%, n=3; VMH, 9.4 ±0.4%, n=3; LHA, 12.3 ±1.8%, n=3. *3v, 3rd cerebral ventricle; VMHdm, dorsomedial VMH; VMHvl, ventrolateral VMH; f, fornix; scale bars, 200um.*

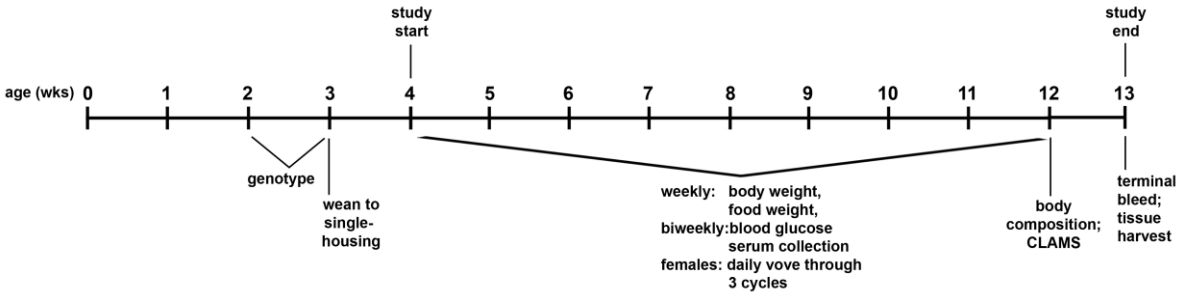

Figure 24. *Nos1*^{cre};lepr$^{\Delta/flox}$ study paradigm. Mice are genotyped between 14 and 21 days of age and animals with genotypes of interest are weaned to single-housing in static cages at age 21 days. Following a week of acclimation, mice begin weekly measurements of body weight and food intake. Biweekly, blood glucose is measured using a glucometer, and blood is collected from the tail vein for harvesting of serum. Females are additionally subjected to daily monitoring, first, for day of vaginal opening, and thereafter for vaginal estrus as determined by cellular histology. Vaginal estrus is monitoring through three cycles, or until the study is terminated. At 12 weeks of age, body composition is determined by Nuclear Magnetic Resonance (NMR) and mice are placed in CLAMS for monitoring of oxygen consumption and locomotor activity. At 13 weeks old, the study is terminated with tissues harvested and terminal blood collected for serum. *CLAMS, Comprehensive Laboratory Animal Monitoring System; vove, vaginal onset-vaginal estrus*

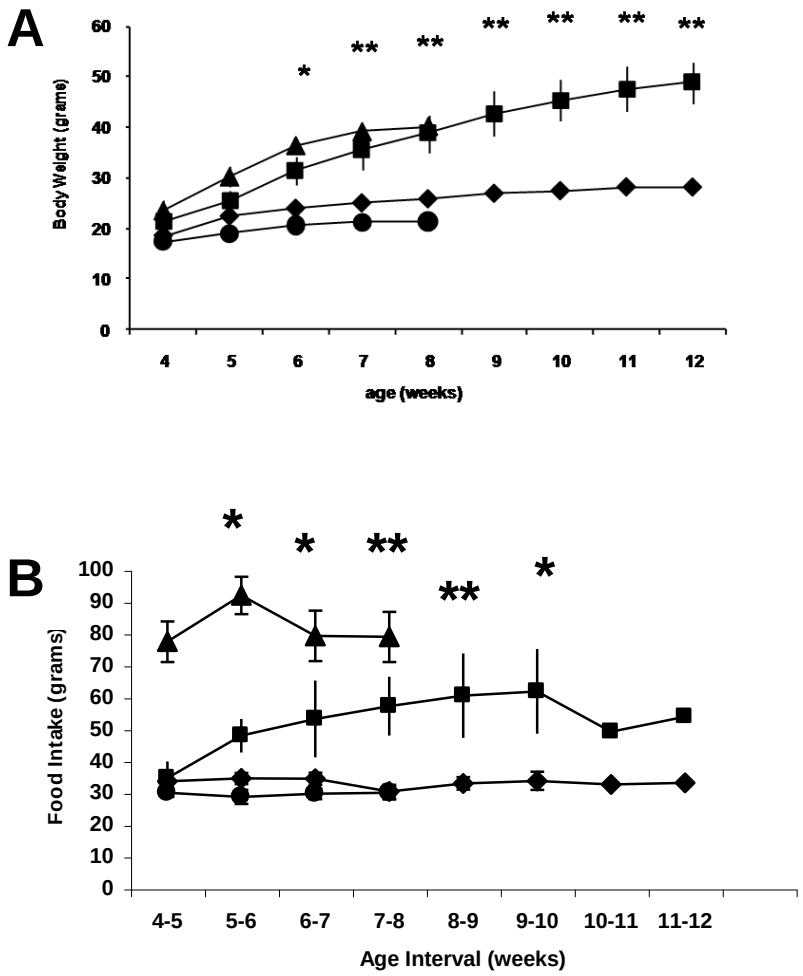

Figure 25. *Nos1*^{cre};lepr$^{\Delta/flox}$ females have altered energy regulation. *Nos1*^{cre};lepr$^{\Delta/flox}$ (■) females show an increased body weight (A) and food intake (B) compared to *Nos1*^{cre};lepr$^{+/+}$ (●) and lepr$^{\Delta/flox}$ (◆) controls. Compared to lepr-deficient *Nos1*^{cre};lepr$^{\Delta/\Delta}$ (▲) mice, *Nos1*^{cre};lepr$^{\Delta/flox}$ gain weight at a delayed rate, however by 6 weeks old, are equally obese (*Nos1*^{cre};lepr$^{\Delta/flox}$ 31.4 ±2.9 grams n=3, *Nos1*^{cre};lepr$^{+/+}$ 20.6 ±0.4 grams n=3, lepr$^{\Delta/flox}$ 23.8 ±0.8 grams n=7, *Nos1*^{cre};lepr$^{\Delta/\Delta}$ 36.4 ±1.5 grams n=4) ($p<0.05$ *Nos1*^{cre};lepr$^{\Delta/flox}$ versus lepr$^{\Delta/flox}$). Similarly, food intake became significantly greater in *Nos1*^{cre};lepr$^{\Delta/flox}$ animals during the 5-6 week period (*Nos1*^{cre};lepr$^{\Delta/flox}$ 48.0 ±5.3 grams/week n=3, *Nos1*^{cre};lepr$^{+/+}$ 28.8 ±2.2 grams/week n=3, lepr$^{\Delta/flox}$ 34.6 ±1.8 grams/week n=7, *Nos1*^{cre};lepr$^{\Delta/\Delta}$ 92.1 ±5.9 grams/week n=4) ($p<0.05$ *Nos1*^{cre};lepr$^{\Delta/flox}$ versus lepr$^{\Delta/flox}$). *Nos1*^{cre};lepr$^{\Delta/flox}$ mice consistently ate significantly less each week than did *Nos1*^{cre};lepr$^{\Delta/\Delta}$ animals. (*$p<0.05$ *Nos1*^{cre};lepr$^{\Delta/flox}$ versus lepr$^{\Delta/flox}$ by ANOVA; **$p<0.01$ *Nos1*^{cre};lepr$^{\Delta/flox}$ versus lepr$^{\Delta/flox}$ by ANOVA)

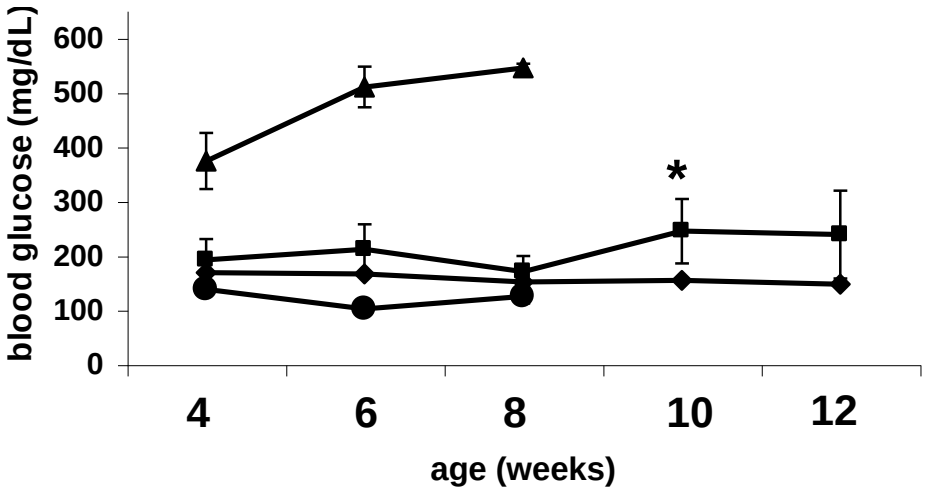

Figure 26. *Nos1*^{cre};lepr$^{\Delta/flox}$ females are euglycemic. *Nos1*^{cre};lepr$^{\Delta/flox}$ (■) females exhibit normoglycemia, not differing from *Nos1*^{cre};lepr$^{+/+}$ (●) and lepr$^{\Delta/flox}$ (◆) controls except at 10 weeks old (*Nos1*^{cre};lepr$^{\Delta/flox}$ 245.0 ±59.18 mg/dL n=3, lepr$^{\Delta/flox}$ 154.3 ±5.7 mg/dL n=7, p<0.03). *Nos1*^{cre};lepr$^{\Delta/\Delta}$ (▲); *p<0.03 *Nos1*^{cre};lepr$^{\Delta/flox}$ versus lepr$^{\Delta/flox}$ by students *t* test)

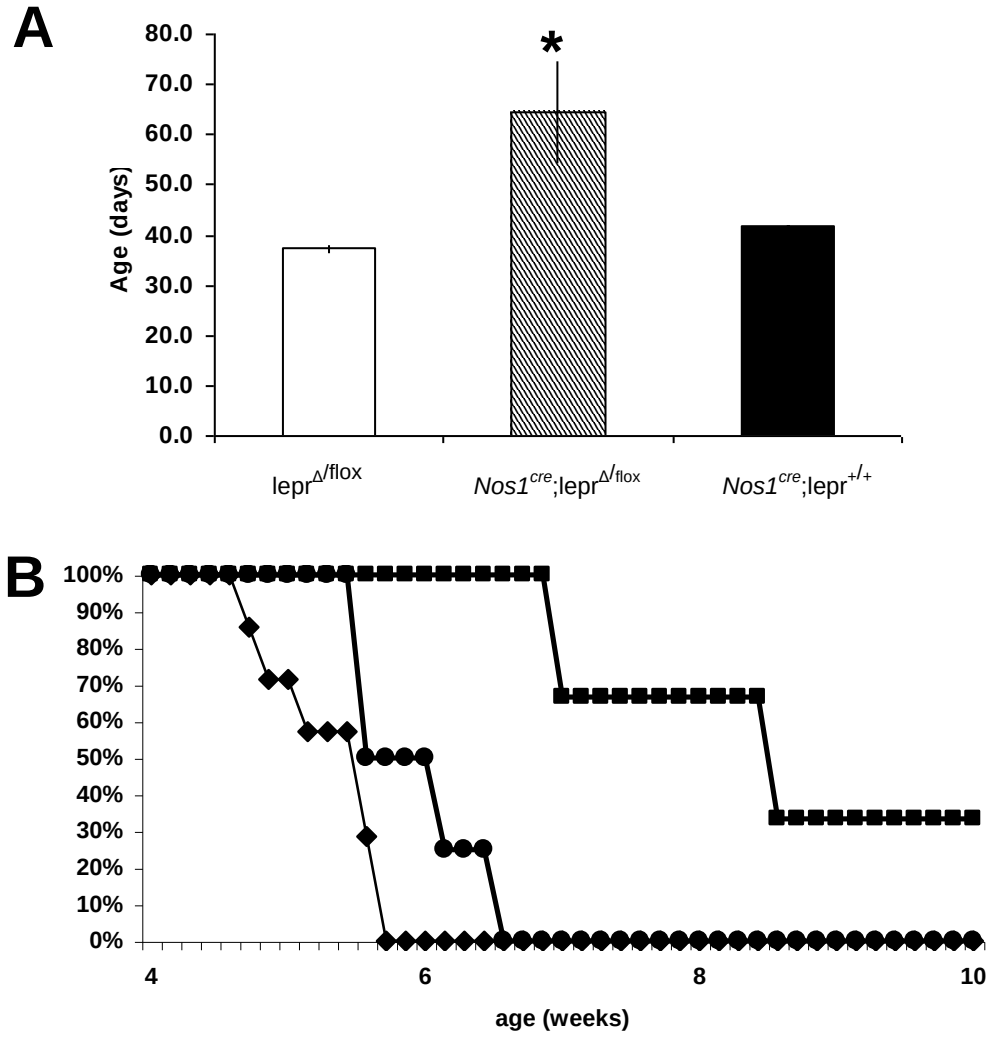

Figure 27. Onset of estrus is delayed in *Nos1*^{cre};lepr$^{\Delta/flox}$ females. *Nos1*^{cre};lepr$^{\Delta/flox}$ exhibit delayed estrus onset compared to controls (A) (*Nos1*^{cre};lepr$^{\Delta/flox}$ 64.3 ±10.3 days, n=3; lepr$^{\Delta/flox}$ 37.3 ±2.9 days, n=7; *Nos1*^{cre};lepr$^{\Delta/flox}$ 41.8 ±1.7 days, n=4; p<0.01). A survival curve (B) shows percent females in each group not yet in estrus (■ *Nos1*^{cre};lepr$^{\Delta/flox}$, ◆ lepr$^{\Delta/flox}$, ● *Nos1*^{cre};lepr$^{+/+}$. At 10 weeks, one *Nos1*^{cre};lepr$^{\Delta/flox}$ female had not yet entered estrus. *Nos1*^{cre};lepr$^{\Delta/\Delta}$ females do not cycle. (*p<0.01 by ANOVA).

References

1. Després JP, Lemieux I (2006) Abdominal obesity and metabolic syndrome. *Nature*. 444:881-887.

2. Friedman JM (2002) The function of leptin in nutrition, weight, and physiology. *Nutr Rev* 60:S1–S14.

3. Myers MG Jr (2004) Leptin receptor signaling and the regulation of mammalian physiology. *Recent Prog Horm Res* 59:287–304.

4. Elmquist JK, Coppari R, Balthasar N, Ichinose M, Lowell BB (2005) Identifying hypothalamic pathways controlling food intake, body weight, and glucose homeostasis. *J Comp Neurol* 493:63–71.

5. Morton GJ, Cummings DE, Baskin DG, Barsh GS, Schwartz MW (2006) Central nervous system control of food intake and body weight. *Nature* 443:289–295.

6. Berthoud HR (2007) Interactions between the "cognitive" and "metabolic" brain in the control of food intake. *Physiol Behav* 91:486–498.

7. Gao Q, Horvath TL (2007) Neurobiology of feeding and energy expenditure. *Annu Rev Neurosci* 30:367–398.

8. Ingalls AM, Dickie MM, Snell GD (1950) Obese, a new mutation in the house mouse. *J Hered* 41:317-318.

9. Zhang Y, Proenca R, Maffei M, Barone M, Leopold L, Friedman JM (1994) Positional cloning of the mouse obese gene and its human homologue. *Nature* 372:425-432.

10. Hummel KP, Dickie MM, Coleman DL (1966) Diabetes, a new mutation in the mouse. *Science* 153:1127-1128.

11. Tartaglia LA, Dembski M, Weng X, Deng N, Culpepper J, Devos R, Richards GJ, Campfield LA, Clark FT, Deeds J, Muir C, Sanker S, Moriarty A, Moore KJ, Smutko JS, Mays GG, Wool EA, Monroe CA, Tepper RI (1995) Identification and expression cloning of a leptin receptor, OB-R. *Cell* 83:1263-1271.

12. Chen H, Charlat O, Tartaglia LA, Woolf EA, Weng X, Ellis SJ, Lakey ND, Culpepper J, Moore KJ, Breitbart RE, Duyk GM, Tepper RI, Morgenstern JP (1996) Evidence that the diabetes gene encodes the leptin receptor: identification of a mutation in the leptin receptor gene in db/db mice. *Cell* 84: 491-495.

13. Finerty J (1952) Parabiosis in physiological studies. *Physiol Rev* 32:277–302.

14. Coleman DL, Hummel KP (1969) Effects of parabiosis of normal with genetically diabetic mice. *Am J Physiol* 217:1298–1304.

15. Coleman DL (1973) Effects of parabiosis of obese with diabetes and normal mice. *Diabetologia* 9:294–298.

16. Pelleymounter MA, Cullen MJ, Baker MB, Hecht R, Winters D, Boone T, Collins F (1995) Effects of the obese gene product on body weight regulation in ob/ob mice. *Science* 269:540–543.

17. Halaas JL, Gajiwala KS, Maffei M, Cohen SL, Chait BT, Rabinowitz D, Lallone RL, Burley SK, Friedman JM (1995) Weight-reducing effects of the plasma protein encoded by the obese gene. *Science* 269:543-546.

18. Campfield LA, Smith FJ, Guisez Y, Devos R, Burn P (1995) Recombinant mouse OB protein: evidence for a peripheral signal linking adiposity and central neural networks. *Science* 269:546-549.

19. Weigle DS, Bukowski TR, Foster DC, Holderman S, Kramer JM, Lasser G, Lofton-Day CE, Prunkard DE, Raymond C, Kuijper JL (1995) Recombinant ob protein reduces feeding and body weight in the ob/ob mouse*. J Clin Invest* 96:2065–2070.

20. Gavrilova O, Marcus-Samuels B, Graham D, Kim JK, Shulman GI, Castle AL, Vinson C, Eckhaus M, Reitman ML (2000) Surgical implantation of adipose tissue reverses diabetes in lipoatrophic mice. *J Clin Invest* 105 :271 –278.

21. Colombo C, Cutson JJ, Yamauchi T, Vinson C, Kadowaki T, Gavrilova O, Reitman ML (2002) Transplantation of adipose tissue lacking leptin is unable to reverse the metabolic abnormalities associated with lipoatrophy. *Diabetes* 51:2727-2733.

22. Sinha MK, Ohannesian JP, Heiman ML, Kriauciunas A, Stephens TW, Magosin S, Marco C, Caro JF (1996) Nocturnal rise of leptin in lean, obese, and non-insulin-dependent diabetes mellitus subjects. *J Clin Invest* 97:1344-1347.

23. Mantzoros CS, Flier JS, Rogol AD (1997) A longitudinal assessment of hormonal and physical alterations during normal puberty in boys. V. Rising leptin levels may signal the onset of puberty. *J Clin Endocrinol Metab*. 82:1066-1070.

24. Sivan E, Lin WM, Homko CJ, Reece EA, Boden G (1997) Leptin is present in human cord blood. *Diabetes* 46:917-919.

25. Ahima RS, Prabakaran D, Flier JS (1998) Postnatal leptin surge and regulation of circadian rhythm of leptin by feeding. Implications for energy homeostasis and neuroendocrine function. *J Clin Invest* 101:1020-1027.

26. MacDougald OA, Hwang CS, Fan H (1995) Regulated expression of the obese gene product (leptin) in white adipose tissue and 3T3–L1 adipocytes. *Proc Natl Acad Sci USA* 92:9034 –9037.

27. Saladin R, Staels B, Auwerx J, Briggs M (1996) Regulation of ob gene expression in rodents and humans. *Horm Metab Res* 28:638-641.

28. Lopez M, Tovar S, Vázquez MJ, Nogueiras R, Seoane LM, García M, Señarís RM, Diéguez C. (2007) Perinatal overfeeding in rats results in increased levels of plasma leptin but unchanged cerebrospinal leptin in adulthood. *Int J Obes* 2:371–377.

29. Lee MJ, Fried SK (2009) Integration of hormonal and nutrient signals that regulate leptin synthesis and secretion. *Am J Physiol Endocrinol Metab* 296:E1230-E1238.

30. Lee GH, Proenca R, Montez, JM, Carroll KM, Darishzadeh JG, Lee JI, Friedman JM (1996) Abnormal splicing of the leptin receptor in diabetic mice. *Nature* 379:632-635.

31. Fei H, Okano HJ, Li C, Lee GH, Zhao C, Darnell R, Friedman JM (1997) Anatomic localization of alternatively spliced leptin receptors (Ob-R) in mouse brain and other tissues. *Proc Natl Acad Sci USA* 94:7001-7005.

32. Banks AS, Davis SM, Bates SH, Myers MG Jr (2000) Activation of downstream signals by the long form of the leptin receptor*. J Biol Chem* 275:14563–14572

33. Fruhbeck G (2006) Intracellular signalling pathways activated by leptin. *Biochem* 1:7–20.

34. Bates SH, Kulkarni RN, Seifert M, Myers MG Jr (2005) Roles for leptin receptor/STAT3-dependent and -independent signals in the regulation of glucose homeostasis. *Cell Metab* 1:169-178.

35. Kastin AJ, PanW, Maness LM, Koletsky RJ, Ernsberger P (1999) Decreased transport of leptin across the blood-brain barrier in rats lacking the short form of the leptin receptor. *Peptides* 12:1449–1453.

36. Bates SH, Stearns WH, Dundon TA, Schubert M, Tso AW, Wang Y, Banks AS, Lavery HJ, Haq AK, Maratos-Flier E, Neel BG, Schwartz MW, Myers MG Jr (2003) STAT3 signalling is required for leptin regulation of energy balance but not reproduction. *Nature* 421:856-859.

37. Bates SH, Dundon TA, Seifert M, Carlson M, Maratos-Flier E, Myers MG Jr (2004) LRb-STAT3 signaling is required for the neuroendocrine regulation of energy expenditure by leptin. *Diabetes* 53:3067-3073.

38. Bates SH, Kulkarni RN, Seifert M, Myers MG Jr (2005) Roles for leptin receptor/STAT3-dependent and -independent signals in the regulation of glucose homeostasis. *Cell Metab* 1:169-178.

39. Björnholm M, Münzberg H, Leshan RL, Villanueva EC, Bates SH, Louis GW, Jones JC, Ishida-Takahashi R, Bjørbaek C, Myers MG Jr (2007) Mice lacking inhibitory leptin receptor signals are lean with normal endocrine function. *J Clin Invest* 117:1354-1360.

40. Niswender KD, Morton GJ, Stearns WH, Rhodes CJ, Myers MG Jr, Schwartz MW. (2001) Key enzyme in leptin-induced anorexia. *Nature* 413:795 –796.

41. Zhao AZ, Huan JN, Gupta S, Pal R, Sahu A (2002) A phosphatidylinositol 3-kinase phosphodiesterase 3B cyclic AMP pathway in hypothalamic action of leptin on feeding. *Nat Neurosci* 5:727 –728.

42. Xu AW, Kaelin CB, Takeda K, Akira S, Schwartz MW, Barsh GS (2005) PI3K integrates the action of insulin and leptin on hypothalamic neurons. *J. Clin. Invest.* 115**:**951–958.

43. Gao Q, Wolfgang MJ, Neschen S, Morino K, Horvath TL, Shulman GI, Fu XY (2004) Disruption of neural signal transducer and activator of transcription 3 causes obesity, diabetes, infertility, and thermal dysregulation. *Proc Natl Acad Sci USA* 101:4661–4666.

44. Burguera B, Couce ME, Curran GL, Jensen MD, Lloyd RV, Cleary MP, Poduslo JF (2000) Obesity is associated with a decreased leptin transport across the blood-brain barrier in rats. *Diabetes* 7:1219–1223

45. Burguera B, Couce ME (2001) Leptin access into the brain: a saturated transport mechanism in obesity. *Physiol Behav* 74:717-720.

46. Zhang EE, Chapeau E, Hagihara K, Feng GS (2004) Neuronal Shp2 tyrosine phosphatase controls energy balance and metabolism. *Proc Natl Acad Sci USA* 101:16064–16069.

47. Kurrimbux D, Gaffen Z, Farrell CL, Martin D, Thomas SA. The involvement of the blood-brain and the blood-cerebrospinal fluid barriers in the distribution of leptin into and out of the rat brain. *Neuroscience* 2004; 2: 527–536.

48. Mercer JG, Hoggard N, Williams LM, Lawrence CB, Hannah LT, Trayhurn P (1996) Localization of leptin receptor mRNA and the long form splice variant (Ob-Rb) in mouse hypothalamus and adjacent brain regions by in situ hybridization. *FEBS Lett* 387:113-116.

49. Barrett GL, Trieu J, Naim T (2009) The identification of leptin-derived peptides that are taken up by the brain*. Regul Pept* 155:55-61.

50. Peruzzo B, Pastor FE, Blazquez JL, Schobitz K, Pelaez B, Amat P, Rodriguez EM 2000 A second look at the barriers of the medial basal hypothalamus. *Exp Brain Res* 132:10–26

51. Faouzi M, Leshan R, Björnholm M, Hennessey T, Jones J, Münzberg H (2007) Differential accessibility of circulating leptin to individual hypothalamic sites. *Endocrinology* 148:5414-5423.

52. Banks WA, Niehoff ML, Martin D, Farrell CL (2002) Leptin transport across the blood-brain barrier of the Koletsky rat is not mediated by a product of the leptin receptor gene. *Brain Res* 950:130-136.

53. Friedman JM, Halaas JL (1998) Leptin and the regulation of body weight in mammals. *Nature* 395:763–770.

54. Elmquist JK, Elias CF, Saper CB (1999) From lesions to leptin: hypothalamic control of food intake and body weight. *Neuron* 22:221–232.

55. Bates SH, Myers MG Jr (2003) The role of leptin receptor signaling in feeding and neuroendocrine function. *Trends Endocrinol Metab* 14:447–452.

56. Considine RV, Sinha MK, Heiman ML, Kriauciunas A, Stephens TW, Nyce MR, Ohannesian JP, Marco CC, McKee LJ, Bauer TL, Caro JF (1996) Serum immunoreactive-leptin concentrations in normal-weight and obese humans. *N Engl J Med* 334:292-295.

57. Baskin DG, Wilcox BJ, Figlewicz DP, Dorsa DM (1988) Insulin and insulin-like growth factors in the CNS. *Trends Neurosci* 11:107-111.

58. Schwartz MW, Woods SC, Porte D Jr, Seeley RJ, Baskin DG (2000) Central nervous system control of food intake. *Nature* 404:661-671.

59. Niswender KD, Schwartz MW (2003) Insulin and leptin revisited: adiposity signals with overlapping physiological and intracellular signaling capabilities. *Front Neuroendocrinol* 24:1-10.

60. Ogawa Y, Masuzaki H, Hosoda K (1999) Increased glucose metabolism and insulin sensitivity in transgenic skinny mice overexpressing leptin. *Diabetes* 48:1822–1829.

61. Ebihara K, Ogawa Y, Masuzaki H (2001) Transgenic overexpression of leptin rescues insulin resistance and diabetes in a mouse model of lipoatrophic diabetes. *Diabetes* 50:1440–1448.

62. Coppari R, Ichinose M, Lee CE, Pullen AE, Kenny CD, McGovern RA, Tang V, Liu SM, Ludwig T, Chua SC Jr, Lowell BB, Elmquist JK (2005) The hypothalamic arcuate nucleus: a key site for mediating leptin's effects on glucose homeostasis and locomotor activity. *Cell Metab* 1:63-72.

63. Huo L, Gamber K, Greeley S, Silva J, Huntoon N, Leng XH, Bjørbaek C (2009) Leptin-dependent control of glucose balance and locomotor activity by POMC neurons. *Cell Metab* 9:537-457.

64. Lago R, Gómez R, Lago F, Gómez-Reino J, Gualillo O (2008) Leptin beyond body weight regulation--current concepts concerning its role in immune function and inflammation. *Cell Immunol* 252:139-145.

65. Matarese G, Moschos S, Mantzoros CS (2005) Leptin in immunology. *J Immunol* 174:3137-3142.

66. Vgontzas AN, Bixler EO, Chrousos GP (2006) Obesity-related sleepiness and fatigue: the role of the stress system and cytokines. *Ann N Y Acad Sci* 1083:329-344.

67. Adamantidis A, de Lecea L (2008) Sleep and metabolism: shared circuits, new connections. *Trends Endocrinol Metab* 19:362-370.

68. Horvath TL, Gao XB (2005) Input organization and plasticity of hypocretin neurons: possible clues to obesity's association with insomnia*. Cell Metab* 1:279-286.

69. Sinha YN, Baxter SR (1978) Concentrations and chromatographic profile of serum GH in old ob/ob mice. *Horm Metab Res* 10:454–455.

70. Luque RM, Huang ZH, Shah B, Mazzone T, Kineman RD (2007) Effects of leptin replacement on hypothalamic-pituitary growth hormone axis function

and circulating ghrelin levels in ob/ob mice. *Am J Physiol Endocrinol Metab* 292:E891-E899.

71. Gat-Yablonski G, Phillip M (2008) Leptin and regulation of linear growth. *Curr Opin Clin Nutr Metab Care* 11:303-308.

72. Nakajima R, Inada H, Koike T, Yamano T (2003) Effects of leptin to cultured growth plate chondrocytes. *Horm Res* 60:91-98.

73. Matsuda J, Yokota I, Iida M, Murakami T, Yamada M, Saijo T, Naito E, Ito M, Shima K, Kuroda Y (1999) Dynamic changes in serum leptin concentrations during the fetal and neonatal periods. *Pediatr Res* 45:71-75.

74. Forhead AJ, Fowden AL (2009) The hungry fetus? Role of leptin as a nutritional signal before birth. *J Physiol* 587:1145-1152.

75. Carlo AS, Meyerhof W, Williams LM (2007) Early developmental expression of leptin receptor gene and [125I]leptin binding in the rat forebrain. *J Chem Neuroanat* 33:155-163.

76. Bouret SG, Draper SJ, Simerly RB (2004) Trophic action of leptin on hypothalamic neurons that regulate feeding. *Science* 304:108-110.

77. Bouret SG, Simerly RB (2007) Development of leptin-sensitive circuits. *J Neuroendocrinol* 19:575-582.

78. Bouret SG, Gorski JN, Patterson CM, Chen S, Levin BE, Simerly RB (2008) Hypothalamic neural projections are permanently disrupted in diet-induced obese rats. *Cell Metab* 7:179-185.

79. van de Wall E, Leshan R, Xu AW, Balthasar N, Coppari R, Liu SM, Jo YH, MacKenzie RG, Allison DB, Dun NJ, Elmquist J, Lowell BB, Barsh GS, de Luca C, Myers MG Jr, Schwartz GJ, Chua SC Jr (2008) Collective and individual functions of leptin receptor modulated neurons controlling metabolism and ingestion. *Endocrinology* 149:1773-1785.

80. Elmquist JK, Ahima RS, Maratos-Flier E, Flier JS, Saper CB (1997) Leptin activates neurons in ventrobasal hypothalamus and brainstem. *Endocrinology* 138:839-842.

81. Elmquist JK, Bjørbaek C, Ahima RS, Flier JS, Saper CB (1998) Distributions of leptin receptor mRNA isoforms in the rat brain. *J Comp Neurol* 395:535-547.

82. Elias CF, Kelly JF, Lee CE, Ahima RS, Drucker DJ, Saper CB, Elmquist JK (2000) Chemical characterization of leptin-activated neurons in the rat brain. *J Comp Neurol* 423:261-281.

83. Scott MM, Lachey JL, Sternson SM, Lee CE, Elias CF, Friedman JM, Elmquist JK (2009) Leptin targets in the mouse brain. *J Comp Neurol* 514:518-532.

84. Leshan RL, Björnholm M, Münzberg H, Myers MG Jr (2006) Leptin receptor signaling and action in the central nervous system. *Obesity* 5:208S-212S.

85. Mao X, Fujiwara Y, Orkin SH (1999) Improved reporter strain for monitoring cre recombinase-mediated DNA excisions in mice. *Proc Natl Acad Sci USA* 96:5037–5042.

86. Münzberg H, Huo L, Nillni EA, Hollenberg AN, Bjørbaek C (2003) Role of signal transducer and activator of transcription 3 in regulation of hypothalamic proopiomelanocortin gene expression by leptin. *Endocrinology* 144:2121–2131.

87. Myers MG Jr, Münzberg H, Leinninger GM, Leshan RL (2009) The geometry of leptin action in the brain: more complicated than a simple ARC. *Cell Metab* 9:117-123.

88. Dhillon H, Zigman JM, Ye C, Lee CE, McGovern RA, Tang V, Kenny CD, Christiansen LM, White RD, Edelstein EA, Coppari R, Balthasar N, Cowley MA, Chua Jr S, Elmquist JK, Lowell BB (2006) Leptin directly activates SF1 neurons in the VMH, and this action by leptin is required for normal body-weight homeostasis. *Neuron* 49:191–203

89. Pfaff DW, Keiner M (1973) Atlas of estradiol-concentrating cells in the central nervous system of the female rat. *J Comp Neurol* 151: 121-158.

90. Calizo LH, Flanagan-Cato LM (2003) Hormonal-neural integration in the female rat ventromedial hypothalamus: triple labeling for estrogen receptor-alpha, retrograde tract tracing from the periaqueductal gray, and mating-induced fos expression. *Endocrinology* 144: 5430-5440.

91. Gooley JJ, Schomer A, Saper CB. (2006) The dorsomedial hypothalamic nucleus is critical for the expression of food-entrainable circadian rhythms. Nat Neurosci 9:398-407.

92. Chou TC, Scammell TE, Gooley JJ, Gaus SE, Saper CB, Lu J (2003) Critical role of dorsomedial hypothalamic nucleus in a wide range of behavioral circadian rhythms. *J Neurosci* 23:10691–10702.

93. Dimicco JA, Zaretsky DV (2007) The dorsomedial hypothalamus: a new player in thermoregulation. *Am J Physiol Regul Integr Comp Physiol* 292:R47-R63.

94. Clemens JA, Smalstig EB, Sawyer BD (1976) Studies on the role of the preoptic area in the control of reproductive function in the rat. *Endocrinology* 99:728-735.

95. Simon E, Pierau FK, and Taylor DC (1986) Central and peripheral thermal control of effectors in homeothermic temperature regulation. *Physiol Rev* 66: 235–300.

96. Molliver ME (1987) Serotonergic neuronal systems: what their anatomic organization tells us about function. *J Clin Psychopharmacol* 7:3S-23S.

97. Willis WD, Westlund KN (1997) Neuroanatomy of the pain system and of the pathways that modulate pain. *J Clin Neurophysiol* 14:2-31.

98. Chamberlin NL (2004) Functional organization of the parabrachial complex and intertrigeminal region in the control of breathing. *Respir Physiol Neurobiol* 143:115-25.

99. Reilly S (1999) The parabrachial nucleus and conditioned taste aversion. *Brain Res Bull* 48:239-254.

100. Zhao Z, Davis M (2004) Fear-potentiated startle in rats is mediated by neurons in the deep layers of the superior colliculus/deep mesencephalic nucleus of the rostral midbrain through the glutamate non-NMDA receptors. *J Neurosci*. 24:10326-10334.

101. Wang XM, Yuan B, Hou ZL (1992) Role of the deep mesencephalic nucleus in the antinociception induced by stimulation of the anterior pretectal nucleus in rats. *Brain Res* 577:321-325.

102. Condé H (1992) Organization and physiology of the substantia nigra. *Exp Brain Res* 88:233-248.

103. Gibb WR (1991) Neuropathology of the substantia nigra. *Eur Neurol* 31:48-59.

104. Li XL, Aou S, Oomura Y, Hori N, Fukunaga K, Hori T (2002) Impairment of long-term potentiation and spatial memory in leptin receptor–deficient rodents. *Neuroscience* 113:607–615.

105. Farr SA, Yamada KA, Butterfield DA, Abdul HM, Xu L, Miller NE, Banks WA, Morley JE (2008) Obesity and hypertriglyceridemia produce cognitive impairment, *Endocrinology* 149:2628–2636

106. Lutter M, Nestler EJ (2009) Homeostatic and hedonic signals interact in the regulation of food intake. *J Nutr* 139:629-632.

107. Berner LA, Avena NM, Hoebel BG (2008) Bingeing, self-restriction, and increased body weight in rats with limited access to a sweet-fat diet. *Obesity* 16:1998-2002.

108. Kelley AE, Bakshi VP, Haber SN, Steininger TL, Will MJ, Zhang M (2002) Opioid modulation of taste hedonics within the ventral striatum. *Physiol Behav* 76:365–377.

109. Hagan MM, Rushing P, Benoit SC, Woods SC, Seeley RJ (2001) Opioid receptor involvement in the effect of AgRP- (83-132) on food intake and food selection. *Am J Physiol Regul Integr Comp Physiol* 280:R814–R821

110. Zhang M and Kelley AE (2000) Enhanced intake of high-fat food following striatal mu-opioid stimulation: microinjection mapping and fos expression. *Neuroscience* 99:267–277.

111. Wise RA (2002) Brain reward circuitry: insights from unsensed incentives. *Neuron* 36:229-240.

112. Berridge KC, Robinson TE (1998) What is the role of dopamine in reward: hedonic impact, reward learning, or incentive salience? *Brain Res Brain Res Rev* 28:309-369.

113. Peciña S (2008) Opioid reward 'liking' and 'wanting' in the nucleus accumbens. *Physiol Behav* 94:675-680.

114. Figlewicz DP, Bennett JL, Naleid AM, Davis C, Grimm JW (2006) Intraventricular insulin and leptin decrease sucrose self-administration in rats. *Physiol Behav* 89:611-616.

115. Figlewicz DP, Bennett J, Evans SB, Kaiyala K, Sipols AJ, Benoit SC (2004) Intraventricular insulin and leptin reverse place preference conditioned with high fat diet in rats. *Behav Neurosci* 118:479–487.

116. Figlewicz DP, Naleid AM, Sipols AJ (2007) Modulation of food reward by adiposity signals. *Physiol Behav* 91:473–478.

117. Krügel U, Schraft T, Kittner H, Kiess W, Illes P (2003) Basal and feeding-evoked dopamine release in the rat nucleus accumbens is depressed by leptin. *Eur J Pharmacol* 482:185-187.

118. Hommel JD, Trinko R, Sears RM, Georgescu D, Liu ZW, Gao XB, Thurmon JJ, Marinelli M, DiLeone RJ (2006) Leptin receptor signaling in midbrain dopamine neurons regulates feeding. *Neuron* 51:801-810.

119. Fulton S, Pissios P, Manchon RP, Stiles L, Frank L, Pothos EN, Maratos-Flier E, Flier JS (2006) Leptin regulation of the mesoaccumbens dopamine pathway. *Neuron* 51:811-822.

120. Mendez IA, Williams MT, Bhavsar A, Lu AP, Bizon JL, Setlow B (2009) Long-lasting sensitization of reward-directed behavior by amphetamine. *Behav Brain Res* 201:74-79.

121. Heusner CL, Hnasko TS, Szczypka MS, Liu Y, During MJ, Palmiter RD. (2003) Viral restoration of dopamine to the nucleus accumbens is sufficient to induce a locomotor response to amphetamine. *Brain Res* 980:266–274.

122. He TC, Zhou S, da Costa LT, Yu J, Kinzler KW, Vogelstein B (1998) A simplified system for generating recombinant adenoviruses. *Proc Natl Acad Sci USA* 95:2509–2514.

123. Baxter MG, Murray EA (2002) The amygdala and reward. *Nat Rev Neurosci* 3:563-573.

124. Berridge KC, Robinson TE (2003) Parsing reward. *Trends Neurosci* 26:507-513.

125. Holland PC, Hatfield T, Gallagher M (2001) Rats with basolateral amygdala lesions show normal increases in conditioned stimulus processing but reduced conditioned potentiation of eating. *Behav Neurosci* 115:945-950.

126. Lu XY, Kim CS, Frazer A, Zhang W (2006) Leptin: a potential novel antidepressant. *Proc Natl Acad Sci USA 103:1593-1598.*

127. Shammah-Lagnado SJ, Alheid GF, Heimer L (1999) Afferent connections of the interstitial nucleus of the posterior limb of the anterior commissure and adjacent amygdalostriatal transition area in the rat. *Neuroscience* 94:1097-1123.

128. Cardinal RN, Parkinson JA, Hall J, Everitt BJ (2002) Emotion and motivation: the role of the amygdala, ventral striatum, and prefrontal cortex. *Neurosci Biobehav Rev* 26:321-352.

129. Kelley AE (2004) Ventral striatal control of appetitive motivation: role in ingestive behavior and reward-related learning. *Neurosci Biobehav Rev* 27:765-776.

130. De Souza MJ, Miller BE, Loucks AB, Luciano AA, Pescatello LS, Campbell CG, Lasley BL (1998) High frequency of luteal phase deficiency and anovulation in recreational women runners: blunted elevation in follicle-stimulating hormone observed during luteal-follicular transition. *J Clin Endocrinol Metab* 83:4220–4232.

131. Ahima RS, Prabakaran D, Mantzoros C, Qu D, Lowell B, Maratos-Flier E, Flier JS (1996) Role of leptin in the neuroendocrine response to fasting. *Nature* 382:250–252.

132. Ahima RS, Dushay J, Flier SN, Prabakaran D, Flier JS (1997) Leptin accelerates the onset of puberty in normal female mice. **J Clin Invest** 99:391–395.

133. Chehab FF, Lim ME, Lu R (1996) Correction of the sterility defect in homozygous obese female mice by treatment with the human recombinant leptin. *Nat Genet* 12:318–320.

134. Farooqi IS, Jebb SA, Langmack G, Lawrence E, Cheetham CH, Prentice AM, Hughes IA, McCamish MA, O'Rahilly S (1999) Effects of recombinant leptin therapy in a child with congenital leptin deficiency. *N Engl J Med* 341:879–884.

135. Shimomura I, Hammer RE, Ikemoto S, Brown MS, Goldstein JL (1999) Leptin reverses insulin resistance and diabetes mellitus in mice with congenital lipodystrophy. *Nature* 401:73–76.

136. Oral EA, Simha V, Ruiz E, Andewelt A, Premkumar A, Snell P, Wagner AJ, DePaoli AM, Reitman ML, Taylor SI, Gorden P, Garg A (2002) Leptin-replacement therapy for lipodystrophy. *N Engl J Med* 346:570–578.

137. Marsteller FA, Lynch CB (1987) Reproductive responses to variation in temperature and food supply by house mice. I. Mating and pregnancy. *Biol Reprod* 37:838–843.

138. Gruaz NM, Lalaoui M, Pierroz DD, Englaro P, Sizonenko PC, Blum WF, Aubert ML (1998) Chronic administration of leptin into the lateral ventricle induces sexual maturation in severely food-restricted female rats. *J Neuroendocrinol* 10:627–633.

139. Nagatani S, Guthikonda P, Thompson RC, Tsukamura H, Maeda KI, Foster DL (1998) Evidence for GnRH regulation by leptin: leptin administration prevents reduced pulsatile LH secretion during fasting. *Neuroendocrinology* 67:370–376.

140. Schneider JE, Goldman MD, Tang S, Bean B, Ji H, Friedman MI (1998) Leptin indirectly affects estrous cycles by increasing metabolic fuel oxidation. *Horm Behav* 33:217–228.

141. Sullivan SD, Howard LC, Clayton AH, Moenter SM (2002) Serotonergic activation rescues reproductive function in fasted mice: does serotonin mediate the metabolic effects of leptin on reproduction? *Biol Reprod* 66:1702–1706.

142. Gonzalez LC, Pinilla L, Tena-Sempere M, Aguilar E (1999) Leptin(116–130) stimulates prolactin and luteinizing hormone secretion in fasted adult male rats. *Neuroendocrinology* 70:213–220.

143. Burcelin R, Thorens B, Glauser M, Gaillard RC, Pralong FP (2003) Gonadotropin-releasing hormone secretion from hypothalamic neurons: stimulation by insulin and potentiation by leptin. *Endocrinology* 144:4484–4491.

144. Canteras NS, Simerly RB, Swanson LW (1992) Projections of the ventral premammillary nucleus. *J Comp Neurol* 324:195–212.

145. Canteras NS, Simerly RB, Swanson LW (1995) Organization of projections from the medial nucleus of the amygdala: a PHAL study in the rat. *J Comp Neurol* 360:213–245.

146. Li C, Vaughan J, Sawchenko PE, Vale WW (2002) Urocortin III-immunoreactive projections in rat brain: partial overlap with sites of type 2 corticotrophin-releasing factor receptor expression. *J Neurosci* 22:991–1001.

147. Rondini TA, Baddini SP, Sousa LF, Bittencourt JC, Elias CF (2004) Hypothalamic cocaine- and amphetamine-regulated transcript neurons project to areas expressing gonadotropin releasing hormone immunoreactivity and to the anteroventral periventricular nucleus in male and female rats. *Neuroscience* 125:735–748.

148. Cavalcante JC, Sita LV, Mascaro MB, Bittencourt JC, Elias CF (2006) Distribution of urocortin 3 neurons innervating the ventral premammillary nucleus in the rat brain. *Brain Res* 1089:116–125.

149. Hahn JD, Coen CW (2006) Comparative study of the sources of neuronal projections to the site of gonadotrophin-releasing hormone perikarya and to the anteroventral periventricular nucleus in female rats. *J Comp Neurol* 494:190–214.

150. Kollack-Walker S, Newman SW (1995) Mating and agonistic behavior produce different patterns of Fos immunolabeling in the male Syrian hamster brain. *Neuroscience* 66:721–736.

151. Coolen LM, Peters HJ, Veening JG (1996) Fos immunoreactivity in the rat brain following consummatory elements of sexual behavior: a sex comparison. *Brain Res* 738:67–82.

152. Yokosuka M, Matsuoka M, Ohtani-Kaneko R, Iigo M, Hara M, Hirata K, Ichikawa M (1999) Female-soiled bedding induced fos immunoreactivity in the ventral part of the premammillary nucleus (PMv) of the male mouse. *Physiol Behav* 68:257–261.

153. Cavalcante JC, Bittencourt JC, Elias CF (2006) Female odors stimulate CART neurons in the ventral premammillary nucleus of male rats. *Physiol Behav* 88:160–166.

154. Beltramino C, Taleisnik S (1985) Ventral premammillary nuclei mediate pheromonal-induced LH release stimuli in the rat. *Neuroendocrinology* 41:119–124.

155. Srinivas S, Watanabe T, Lin CS, William CM, Tanabe Y, Jessell TM, Costantini F (2001) Cre reporter strains produced by targeted insertion of EYFP and ECFP into the ROSA26 locus. *BMC Dev Biol* 1:4.

156. Soliman GA, Ishida-Takahashi R, Gong Y, Jones JC, Leshan RL, Saunders TL, Fingar DC, Myers MG Jr (2007) A simple qPCR-based method to detect correct insertion of homologous targeting vectors in murine ES cells. *Transgenic Res* 16:665–670.

157. Boehm U, Zou Z, Buck LB (2005) Feedback loops link odor and pheromone signaling with reproduction. *Cell* 123:683–695.

158. Cowley MA, Smart JL, Rubinstein M, Cerdán MG, Diano S, Horvath TL, Cone RD, Low MJ (2001) Leptin activates anorexigenic POMC neurons through a neural network in the arcuate nucleus. *Nature* 411:480–484.

159. Dhillon H, Zigman JM, Ye C, Lee CE, McGovern RA, Tang V, Kenny CD, Christiansen LM, White RD, Edelstein EA, Coppari R, Balthasar N, Cowley MA, Chua S Jr, Elmquist JK, Lowell BB (2006) Leptin directly activates SF1 neurons in the VMH, and this action by leptin is required for normal body-weight homeostasis. *Neuron* 49:191–203.

160. Smith MA, Hisadome K, Al-Qassab H, Heffron H, Withers DJ, Ashford ML (2007) Melanocortins and agouti-related protein modulate the excitability of two arcuate nucleus neuron populations by alteration of resting potassium conductances. *J Physiol* 578:425–438.

161. White DW, Kuropatwinski KK, Devos R, Baumann H, Tartaglia LA (1997) Leptin receptor (OB-R) signaling. *J Biol Chem* 272:4065–4071.

162. Zylka MJ, Rice FL, Anderson DJ (2005) Topographically distinct epidermal nociceptive circuits revealed by axonal tracers targeted to Mrgprd. Neuron 45:17–25.

163. Frisch RE, McArthur JW (1974) Menstrual cycles: fatness as a determinant of minimum weight for height necessary for their maintenance or onset. *Science* 185:949–951.

164. Pirke KM, Schweiger U, Lemmel W, Krieg JC, Berger M (1985) The influence of dieting on the menstrual cycle of healthy young women. *J Clin Endocrinol Metab* 60:1174–1179.

165. Bronson FH, Manning JM (1991) The energetic regulation of ovulation: a realistic role for body fat. Biol Reprod 44:945–950.

166. Loucks AB, Verdun M, Heath EM (1998) Low energy availability, not stress of exercise, alters LH pulsatility in exercising women. *J Appl Physiol* 84:37–46.

167. Simerly RB, Chang C, Muramatsu M, Swanson LW (1990) Distribution of androgen and estrogen receptor mRNA-containing cells in the rat brain: an in situ hybridization study. *J Comp Neurol* 294:76–95.

168. Pfaus JG, Kleopoulos SP, Mobbs CV, Gibbs RB, Pfaff DW (1993) Sexual stimulation activates c-fos within estrogen-concentrating regions of the female rat forebrain. *Brain Res* 624:253–267.

169. Osterlund M, Kuiper GG, Gustafsson JA, Hurd YL (1998) Differential distribution and regulation of estrogen receptor-alpha and -beta mRNA within the female rat brain. *Mol Brain Res* 54:175–180.

170. Veening JG, Coolen LM, de Jong TR, Joosten HW, de Boer SF, Koolhaas JM, Olivier B (2005) Do similar neural systems subserve aggressive and sexual behaviour in male rats? Insights from c-Fos and pharmacological studies. *Eur J Pharmacol* 526:226–239.

171. Yoon H, Enquist LW, Dulac C (2005) Olfactory inputs to hypothalamic neurons controlling reproduction and fertility. *Cell* 123:669–682.

172. Dulac C, Wagner S (2006) Genetic analysis of brain circuits underlying pheromone signaling. *Annu Rev Genet* 40:449–467.

173. Kocsis K, Kiss J, Csáki A, Halász B (2003) Location of putative glutamatergic neurons projecting to the medial preoptic area of the rat hypothalamus. *Brain Res Bull* 61:459–468.

174. Smith JT, Acohido BV, Clifton DK, Steiner RA (2006) KiSS-1 neurones are direct targets for leptin in the ob/ob mouse. *J Neuroendocrinol* 18:298–303.

175. Castellano JM, Roa J, Luque RM, Dieguez C, Aguilar E, Pinilla L, Tena-Sempere M (2009) KiSS-1/kisspeptins and the metabolic control of reproduction: physiologic roles and putative physiopathological implications. *Peptides* 30:139–145.

176. Donato J Jr, Silva RJ, Sita LV, Lee S, Lee C, Lacchini S, Bittencourt JC, Franci CR, Canteras NS, Elias CF (2009) The ventral premammillary nucleus links fasting-induced changes in leptin levels and coordinated luteinizing hormone secretion. *J Neurosci* 29:5240-5250.

177. Kavya R, Saluja R, Singh S, Dikshit M (2006) Nitric oxide synthase regulation and diversity: implications in Parkinson's disease. *Nitric Oxide* 15:280-294.

178. Rettori V, Fernandez-Solari J, Mohn C, Zorrilla Zubilete MA, de la Cal C, Prestifilippo JP, De Laurentiis A (2009) Nitric oxide at the crossroad of immunoneuroendocrine interactions. *Ann N Y Acad Sci* 1153:35-47.

179. Hadeishi Y, Wood RI (1996) Nitric oxide synthase in mating behavior circuitry of male Syrian hamster brain. *J Neurobiol* 30:480-492.

180. Yokosuka M, Prins GS, Hayashi S (1997) Co-localization of androgen receptor and nitric oxide synthase in the ventral premammillary nucleus of the newborn rat: an immunohistochemical study. *Brain Res Dev Brain Res* 99:226-233.

181. Huang PL, Dawson TM, Bredt DS, Snyder SH, Fishman MC (1993) Targeted disruption of the neuronal nitric oxide synthase gene. *Cell*. 1993 Dec 31;75(7):1273-86.

182. Nelson RJ, Demas GE, Huang PL, Fishman MC, Dawson VL, Dawson TM, Snyder SH (1995) Behavioural abnormalities in male mice lacking neuronal nitric oxide synthase. *Nature* 378:383-386.

183. Gyurko R, Leupen S, Huang PL (2002) Deletion of exon 6 of the neuronal nitric oxide synthase gene in mice results in hypogonadism and infertility. *Endocrinology* 143:2767-2774.

184. Scherer-Singler U, Vincent SR, Kimura H, McGeer EG (1983) Demonstration of a unique population of neurons with NADPH-diaphorase histochemistry. *J Neurosci Methods* 9:229-234

185. Balthasar N, Coppari R, McMinn J, Liu SM, Lee CE, Tang V, Kenny CD, McGovern RA, Chua SC Jr, Elmquist JK, Lowell BB (2004) Leptin receptor signaling in POMC neurons is required for normal body weight homeostasis. *Neuron* 42:983-991.

186. Paxinos G, Franklin KBJ (2001) *The mouse brain in stereotaxic coordinates*. San Diego: Academic Press.

187. Hagan MM, Rushing PA, Benoit SC, Woods SC, Seeley RJ (2001) Opioid receptor involvement in the effect of AgRP-(83–132) on food intake and food selection. Am J Physiol Regul Integr Comp Physiol 280:R814–R821.

188. Gelling RW, Morton GJ, Morrison CD, Niswender KD, Myers MG Jr, Rhodes CJ, Schwartz MW (2006) Insulin action in the brain contributes to glucose lowering during insulin treatment of diabetes. Cell Metab 3:67–73.

189. Silverman AJ, Livne I, Witkin JW (1994) The gonadotropin-releasing hormone (GnRH), neuronal systems: immunocytochemistry and in situ hybridization. In: J.D. Neill, Editor*, The Physiology of Reproduction*, New York: Raven Press. pp. 1683–1709.